VU VRIJE UNIVERSITEIT AMSTERDAM

VU Research Portal

Mathematical Modelling of Fungal Hyphae

Nolet, R.W.

2020

document version
Publisher's PDF, also known as Version of record

Link to publication in VU Research Portal

citation for published version (APA)
Nolet, R. W. (2020). *Mathematical Modelling of Fungal Hyphae*. [PhD-Thesis - Research and graduation internal, Vrije Universiteit Amsterdam].

General rights
Copyright and moral rights for the publications made accessible in the public portal are retained by the authors and/or other copyright owners and it is a condition of accessing publications that users recognise and abide by the legal requirements associated with these rights.

- Users may download and print one copy of any publication from the public portal for the purpose of private study or research.
- You may not further distribute the material or use it for any profit-making activity or commercial gain
- You may freely distribute the URL identifying the publication in the public portal ?

Take down policy
If you believe that this document breaches copyright please contact us providing details, and we will remove access to the work immediately and investigate your claim.

E-mail address:
vuresearchportal.ub@vu.nl

Download date: 05. May. 2023

VRIJE UNIVERSITEIT

Mathematical Modelling of Fungal Hyphae

ACADEMISCH PROEFSCHRIFT

ter verkrijging van de graad Doctor aan
de Vrije Universiteit Amsterdam,
op gezag van de rector magnificus
prof.dr. V. Subramaniam,
in het openbaar te verdedigen
ten overstaan van de promotiecommissie
van de Faculteit der Bètawetenschappen
op donderdag 7 mei 2020 om 11.45 uur
in de aula van de universiteit,
De Boelelaan 1105

door

Robert Willem Nolet

geboren te Utrecht

promotor:	prof.dr. J. Hulshof
copromotor:	dr. G. Prokert

Contents

Introduction **1**

1 Existence and Linear Stability of Solutions of the Ballistic VSC model **9**
1.1 Introduction . . . 9
1.2 The evolution equation . . . 11
1.3 Travelling waves . . . 13
1.3.1 Geometry . . . 13
1.4 Hyphoid solutions . . . 15
1.4.1 Existence and uniqueness . . . 16
1.4.2 Properties of the hyphoid solution . . . 18
1.5 Stability of the hyphoid solution . . . 21
1.5.1 The linearized evolution equation . . . 22
1.5.2 Divergence form . . . 22
1.5.3 Asymptotics . . . 23
1.5.4 Eigenvalues of $\tilde{L}$ . . . 24
1.5.5 Asymptotics of the eigenfunctions . . . 26
1.6 Numerical calculations . . . 27
1.7 Conclusions . . . 28

2 Asymptotics for the Ballistic VSC Model **29**
2.1 Introduction . . . 29
2.2 Asymptotics as $z \to -\infty$ . . . 30
2.2.1 Formal asymptotics as $z \to -\infty$ . . . 30
2.2.2 Asymptotic expansions for $r(z)$ as $z \to -\infty$ . . . 33
2.2.3 Asymptotics of $z(r)$ as $r \to 2$ . . . 39
2.3 Asymptotics in the tip . . . 43
2.3.1 Formal asymptotics as $r \to 0$ . . . 43
2.3.2 Asymptotic expansions as $r \to 0$ . . . 46
2.4 Linear stability of the hyphoid solution . . . 46
2.4.1 Eigenfunctions of $\tilde{L}[\phi]$ in 1D-divergence form . . . 47
2.4.2 Eigenfunctions for $\lambda \in \mathbb{C}$ . . . 48
2.4.3 Asymptotics of the eigenfunctions . . . 55
2.5 Eigenfunctions of $\tilde{L}[\phi]$ in 2D-divergence form . . . 55

2.5.1 Asymptotics of the eigenfunctions 57

3 Existence of solutions to the Diffusive VSC model 59
3.1 Introduction 59
3.1.1 Notation and conventions 61
3.2 The diffusive VSC model 62
3.2.1 The diffusive flux 62
3.2.2 Mass balance 62
3.2.3 Main result 63
3.2.4 Scaling 63
3.2.5 The unbounded travelling wave problem 64
3.2.6 The bounded travelling wave problem 65
3.3 The Schauder map 66
3.3.1 The domain of the Schauder map 66
3.3.2 Estimates on $r(s)$, $z(s)$ and distances 67
3.3.3 Exterior spheres 68
3.4 The Dirichlet problem 69
3.4.1 The domain Ω 70
3.4.2 Bounds on $F_\xi(s)$ 71
3.4.3 Bounds on $G_\xi(s)$ 73
3.4.4 Monotonicity of G_ξ in ξ 75
3.5 The travelling wave ODE 78
3.5.1 The forward solution 79
3.5.2 Determination of ξ_{min} and ξ_{max} 80
3.5.3 The backwards solution 80
3.5.4 Matching 81
3.6 Fixed point of the Schauder map 82
3.6.1 Determination of C 83
3.6.2 Determination of A 83
3.6.3 Hölder continuity 84
3.6.4 Continuity of $(r, z) \to G_\xi$ 84
3.6.5 Continuity of $G_\xi \to (\xi^*, r_{\xi^*}, z'_{\xi^*})$ 87
3.6.6 Fixed point 88
3.7 The limit as $s_{max} \to \infty$ 88
3.7.1 The limit profile r_∞, z_∞ 88
3.7.2 The cumulative flux G_∞ 89
3.7.3 The limit of G_n 90
3.7.4 Solution to the unbounded travelling wave problem 90
3.8 Conclusions 91

4 Asymptotics and other properties of the solution to the diffusive model 93
4.1 The $C^{1,\alpha}$ solution 93
4.1.1 The ODE and bounds on derivatives 94
4.1.2 Estimates in the tip 94
4.2 Attempts at C^2 regularity 95

4.2.1 The backward solution 96
4.2.2 The forward solution 98
4.2.3 Concavity 100
4.3 Asymptotic upper bounds away from the tip 100
4.3.1 Bounds on u and $u_{(a,b)}$ 100
4.3.2 Bounds on Du 101
4.3.3 Asymptotics of $G(s)$ as $s \to \infty$ 102
4.3.4 Asymptotics for r as $s \to \infty$ 103
4.3.5 Fourier-Bessel series expansion of $u(r, z)$ 104
4.3.6 Asymptotic bounds for the coefficients c_n 105
4.4 Asymptotic lower bounds away from the tip 113
4.4.1 A lower bound for $c_1(z)$ 113
4.4.2 A lower bound for the flux 115
4.5 The $C^{2,\alpha}$ Schauder map 117

5 Numerical simulations of the Diffusive VSC model 119
5.1 Initial condition and two dimensional formulation of the dynamics 119
5.2 Grids and finite differences 120
5.3 Level set formulation 121
5.4 Finite element method 121
5.4.1 Triangulation 121
5.4.2 Weak formulation of the Dirichlet problem 123
5.5 Numerical simulation of the dynamics of the VSC model 124
5.6 Results 125

6 Modifications to VSC type models 129
6.1 Introduction 129
6.2 Geometry 130
6.3 Minimization of kinetic energy 131
6.4 Travelling waves 131

Summary 137

Acknowledgements 139

Introduction

Fungi: The largest organisms on Earth

Fungal colonies form networks of thread-like hypha in the soil, known as a mycelium. This mycelium absorbs water and nutrients from the surrounding soil and can grow to tremendous size. In 1993 Smith *et al.* discovered a single organism of *Armillaria bulbosa* in a northern Michigan hardwood forest whose mycelium covered a region of 15 hectares and was estimated to be more than 1500 years old [21]. At the time this was reported to be one of the largest and oldest living organisms known to man. Ten years later, this record was broken. In 2003 Ferguson *et al.* reported a single organism of *Armillaria ostoyae* in a mixed-conifer forest in northeast Oregon. This fungus' mycelium was estimated to cover an area of 963 hectare and its age was estimated to be between 1900 and 8650 years old [8].

Obviously, the size of these fungi caused biologists to express interest in the mechanism by which these organisms grow. The mycelium is a network of branching hyphae – threadlike, tubular structures. By placing ink markers on the cell wall of these hypha, it was observed that the hypha grow from their tips. Ink markers stayed roughly in place, moving only orthogonally to the cell wall, while new wall surface was created at the tip. A cellular body called the *Spitzenkörper* (see Figure 1) near the tip is suspected to play a role in this growth. These observations form the basis for many mathematical models for the growth of hyphae.

Surfaces expanding my insertion of a flux of surface area.

Cells, either fungal hyphae or other types, absorb water and nutrients from their surroundings through the the boundary of their cells. When mathematically modelling the growth of such cells, this implies that modelling mass or volume uptake by the cell requires that we model various transport processes across the cell wall and membranes, distribution of various substances within the cell, as well as the mechanics of actually expanding the cell. Such models can be found, for example, in Bessonov *et al.* [3] where a one dimensional model for plant

growth is given, describing the concentrations of nutrients $C(x,t)$ and growth factors $R(x,t)$ on a time dependant interval $x \in [0, L(t)]$. Such models assume the wall is extended by turgor pressure and new wall materials are added to maintain a constant wall thickness [20].

The boundary of cells consists of a flexible lipid bilayer membrane. Aside from the cell membrane, plants, fungi and various prokaryotic cells have a cell wall, usually made of cellulose in the case of plants, or chitin in the case of fungi. In contrast to water, the main component of the volume of a cell, the components of the cell wall and membrane are produced inside the cells and not as readily available from the surroundings. As such, it might make more sense to model the growth of the surface area of the boundary of the cell, instead of the length or volume of the cell itself. This motivates the study of surfaces, or geometric manifolds, which evolve by a prescribed rate of increase of surface area. The two models studied in this thesis are examples of such manifolds.

While in reality the cell wall and cell membrane are separate and the distance between wall and membrane may not be insignificant when compared to the overall dimensions of the cell, we will treat the combined wall and membrane as a mathematically flat, single surface. We model this as a geometric embedded manifold $M(t) \subset \mathbb{R}^3$. This manifold is evolving through a velocity field $\vec{u}(\vec{x},t)$ defined in a neighbourhood of $M(t)$. The physical interpretation of this velocity field is the velocity of particles of, or ink markers attached to, the cell wall. In contrast to general geometric flows, where the manifold can be continually reparametrized such that the velocity field is always normal to the surface, this cannot be done in our models. Such a reparametrization would destroy the interpretation of $\vec{u}$ as the velocity of a physical particle, and any material inserted between particles could no longer be expressed in terms of $\vec{u}$.

If a flux of surface materials F is continually arriving and being absorbed by the cell wall, this implies that when $\Gamma \subset M(t)$ is an arbitrary bounded subset of $M(t)$ with surface area $A(t)$, then

$$\frac{\mathrm{d}A}{\mathrm{d}t} = \int_\Gamma F \mathrm{d}A. \tag{0.0.1}$$

This can be related to the velocity $\vec{u}$ of the cell wall through Gauss' formula for the first variation of area,

$$\frac{\mathrm{d}A}{\mathrm{d}t} = -\int_\Gamma H(\hat{n}\cdot u)\mathrm{d}A + \oint_{\partial\Gamma} (\hat{m}\cdot u)\mathrm{d}l, \tag{0.0.2}$$

where H is the mean curvature, $\hat{n}$ is the outward pointing normal to $M(t)$ and $\hat{m}$ is the outward pointing normal to $\partial\Gamma$ tangent to $M(t)$.

If we now assume that the velocity field is normal to the surface, $\vec{u} = u_n\hat{n}$, then the integral over $\partial\Gamma$ vanishes. Since the subsurface Γ was chosen arbitrarily, the integrands must be equal. This gives us a relation between the normal velocity u_n and the local increase of surface area F,

$$u_n = -\frac{F}{H}. \tag{0.0.3}$$

The assumption of normal velocity is mathematically convenient, and justified by observations, however it is not without its problems. Some objections to this assumption will be discussed in chapter 6.

Various well known geometric flows can now be reformulated in terms of local increase of area under the assumption of normal velocity. For example the well known mean curvature flow $u_n = -H$ corresponds to the case where the local decrease of surface area is proportional to the square of the mean curvature, or $F = -H^2$. Similarly, the inverse mean curvature flow, studied by Gerhardt [10], Huisken [14], [15], Urbas [25] and many others, corresponds to a constant flux $F = 1$.

Aside from geometric flows, some models of fungal hypha also have a flux which is purely described by the geometry of this manifold. For example, Goriely *et al.* [13] describe a model where the flux is a function of the curvature, similar to the geometric flows described above.

VSC type models

In this thesis we will study two models, the ballistic VSC model and the diffusive VSC model, for the growth of fungal hyphae. These models correspond to two different choices for the flux F as described above. These models were first proposed by Bartnicki-Garcia *et al.* [2], [1], and later expanded upon by Eggen [6], [7] and Tindemans [23]. For an overview of these, and many other similar models see De Keijzer *et al.* [5].

Both models assume that all material for the cell wall is produced at a point source inside the cell called the *vesicle supply center* (VSC). Physically, the VSC coincides with the Spitzenkörper at the tip of the fungal hypha. The VSC produces a total of P units of area per unit of time, and is moving along the z axis at a velocity of c. A physical mechanism for this movement might be that the Spitzenkörper is attached to the tip of the hypha and thus its movement is generated by the growth of the hypha, however for modelling purposes we will assume it's velocity is simply a given constant. After rescaling of units it is possible to choose $P = 4\pi$ and $c = 1$. The cell wall material produced by the VSC is then transported to the cell wall by vesicles, a cellular transport method where nutrients and/or other materials are packed in spherical membranes which are transported to their desired location. These vesicles are transported by one of two methods:

- **The Ballistic VSC model** – The vesicles produced by the VSC are distributed equally in all directions. This results in a flux $F(\vec{x}, t)$ of material being absorbed at a point $\vec{x}$ on the cell wall which is proportional to the inverse square of the distance to the VSC, and the cosine of the angle between the normal vector and the ray from the VSC to $\vec{x}$. So

$$F(\vec{x}, t) = \frac{P}{4\pi} \frac{\hat{n} \cdot (\vec{x} - ct\hat{e}_z)}{|\vec{x} - ct\hat{e}_z|^3}. \tag{0.0.4}$$

In chapter 1 we discuss the existence and stability of travelling waves in the ballistic model, as published in [17]. In chapter 2 we show some additional calculations for this article, mainly concerning the asymptotics of these solutions.

- **The Diffusive VSC model** – The vesicles produced by the VSC diffuse outwards. The density u of cell wall material is assumed to be in equilibrium at all times. This results in a partial differential equation for the density u of these vesicles in the interior Ω of the cell,

$$\begin{aligned} \Delta u &= -P\delta(\vec{x} - ct\hat{e}_z) && \text{in } \Omega, \\ u &= 0 && \text{on } \partial\Omega. \end{aligned} \tag{0.0.5}$$

The flux of material at the cell wall is now given by the normal derivative of u at $\partial\Omega$

$$F = -\frac{\partial u}{\partial \hat{n}}. \tag{0.0.6}$$

In chapter 3 we discuss the existence of travelling wave solutions in the diffusive model, as published in [16]. In chapter 4 we show some additional calculations for the diffusive model, some asymptotics and properties of the solution if it were possible to show it is $C^{2,\alpha}$ Hölder continuous. In chapter 5 we show some numerical results for the evolution of the diffusive model.

For a spherical cell of radius $R(t)$ with a stationary ($c = 0$) VSC in the center, these two models would be equivalent. If $P = 4\pi$ then $F = 1/R(t)^2$ and $H = 2/R(t)$ and we get a differential equation for $R(t)$,

$$\frac{\mathrm{d}R}{\mathrm{d}t} = \frac{1}{2R(t)}, \tag{0.0.7}$$

which can be solved to yield $R(t) = \sqrt{R(0)^2 + t}$. We are however not interested in such solutions, instead we are looking for solutions with a cylindrical symmetry where the VSC is moving with a constant, non-zero, velocity.

Travelling waves with cylindrical symmetry

The goal of both the ballistic and the diffusive VSC model, as well of any future modifications of these models, is to reproduce the observed behaviour of fungal hyphae. These fungal hyphae appear to have a cylindrical symmetry and are moving along with the VSC while keeping the same shape. In other words, in a coordinate system moving at a speed c in the z direction, both the VSC and the cell surface $M(t)$ appear stationary.

In order to derive equations for the shape of the travelling wave profile, we start again with Gauss' formula for the first variation of area (0.0.2). In this moving frame of reference, $\vec{u}$ is replaced by $\vec{u} - c\hat{e}_z$.

$$\int_\Gamma F\mathrm{d}A = -\int_\Gamma H\hat{n}\cdot(\vec{u} - c\hat{e}_z)\mathrm{d}A + \oint_{\partial\Gamma} \hat{m}\cdot(\vec{u} - c\hat{e}_z)\mathrm{d}l. \tag{0.0.8}$$

Now since the manifold is stationary, $\vec{u} - c\hat{e}_z$ must lie tangent to $M(t)$ and the integral over Γ on the right hand side vanishes. Furthermore, since the original velocity $\vec{u}$ was assumed to be normal to the surface, the term $\hat{m} \cdot \vec{u}$ vanishes, resulting in

$$\int_{\Gamma} F \mathrm{d}A = -\oint_{\partial\Gamma} (\hat{m} \cdot \hat{e}_z) \mathrm{d}l. \tag{0.0.9}$$

This equation relates the cumulative flux over Γ to the slope $\hat{m}$ of the manifold on $\partial\Gamma$.

If we now look for cylindrically symmetric solutions, we can choose Γ to have the same symmetry. Specifically we choose Γ to be that part of $M(t)$ which lies to the right of some plane $z = z^*$. As a result, $\partial\Gamma$ is a circle in the plane $z = z^*$ with radius r^* and the tangent unit vector $\hat{m}$ has only radial and z components. Moreover, $\hat{m} \cdot \hat{e}_z$ is constant over $\partial\Gamma$ and the integral on the right hand side is equal to the value of $-\hat{m} \cdot \hat{e}_z$ at $z = z^*$ times the circumference of $M(t)$ at $z = z^*$. We denote the integral on the left hand side as $2\pi G^*$ to obtain

$$2\pi G^* = -2\pi r^* (\hat{m} \cdot \hat{e}_z). \tag{0.0.10}$$

After a suitable choice of parametrization, this results in an ordinary differential equation for the shape of travelling wave solutions.

- **The Ballistic Model** – For the ballistic VSC model we parametrize by the z coordinate, the cell surface is the graph of some function $r(z)$ rotated around the z axis. In this parametrization,

  $$\hat{m}(z) = \frac{r'(z)\hat{e}_r - \hat{e}_z}{\sqrt{1 + r'(z)^2}} \tag{0.0.11}$$

  and if we write $G^* = G(z)$ we obtain the ODE

  $$G(z) = \frac{r(z)}{\sqrt{1 + r'(z)^2}}, \qquad \text{or} \qquad r'(z) = -\sqrt{\left(\frac{r(z)}{G(z)}\right)^2 - 1}. \tag{0.0.12}$$

- **The Diffusive Model** – For the diffusive VSC model we parametrize by the pathlength s from the tip of the hypha, along the cell surface, to the plane $z = z^*$. The cell surface is now the parametrized curve $(r(s), z(s))$ for $s \geq 0$, rotated around the z axis. In this parametrization,

  $$\hat{m}(s) = r'(s)\hat{e}_r + z'(s)\hat{e}_z, \tag{0.0.13}$$

  and if we write $G^* = G(s)$ we obtain $G(s) = -z'(s)r(s)$. Combining this with the pathlength requirement that $r'(s)^2 + z'(s)^2 = 1$ gives an ODE for $r(s)$,

  $$r'(s) = \sqrt{1 - \left(\frac{G(s)}{r(s)}\right)^2}. \tag{0.0.14}$$

Note that in both models, the full dynamics of the model, as given by (0.0.6) is a second order equation, as the normal velocity u_n depends on the mean curvature H. However, for a travelling wave solution the curvature term vanishes and we are left with a first order ODE.

In chapter 1 we obtain the same result through a more classical approach. From the evolution equation we make an equilibrium assumption in co-moving coordinates to obtain a second order ODE for the tip shape. We then find an integrating factor to transform this to a first order ODE equivalent to the one described above. The above calculations show that this is not happenstance. Whatever the choice of flux, if one makes the assumption of a normal velocity, such an integrating factor is a necessary result from Gauss' first variation of area, and can always be found.

Solving the travelling wave equation

The differential equations, (0.0.12) for the ballistic model, and (0.0.14) for the diffusive model illustrate the central dilemma of this thesis. In order to solve the ODE for the tip shape, we need to know the cumulative flux G. However the flux depends on the tip shape. How do we resolve this 'chicken and egg' problem?

- **The Ballistic Model** – For the ballistic model, the cumulative flux is proportional to the spatial angle of the cone with an apex at the VSC, height z and radius $r(z)$. This allows us to express the cumulative flux G explicitly in terms of the function describing the tip shape, resulting in

$$G = 1 - \frac{z}{d}, \qquad \text{with} \qquad d^2 = r(z)^2 + z^2, \tag{0.0.15}$$

  and so

$$r'(z) = -\sqrt{r(z)^2 \left(1 - \frac{z}{d}\right)^{-2} - 1}. \tag{0.0.16}$$

  In chapter one we use various ODE techniques to show the existence and uniqueness of a suitable solution to this equation. We then show the linear stability of this solution.

- **The Diffusive Model** – For the diffusive model we cannot derive an explicit formula for G. Instead, in chapter 3, we start with a 'guess' of the tip shape, calculate the properties of the cumulative flux for such a tip, then solve (0.0.14) to obtain a new tip shape. This sets up a map from tip shapes to tip shapes, proof of a travelling wave solution then follows from Schauder's fixed point theorem. The difficulty in this approach lies in choosing the right function space for the function r describing the tip shape, and choosing suitable bounds on r. Chapter 3 gives an existence proof for a $C^{1,\alpha}$ Hölder continuous solution. An attempt was also made to prove the existence of a $C^{2,\alpha}$ Hölder continuous solution. Details of this attempt are found in chapter 4.

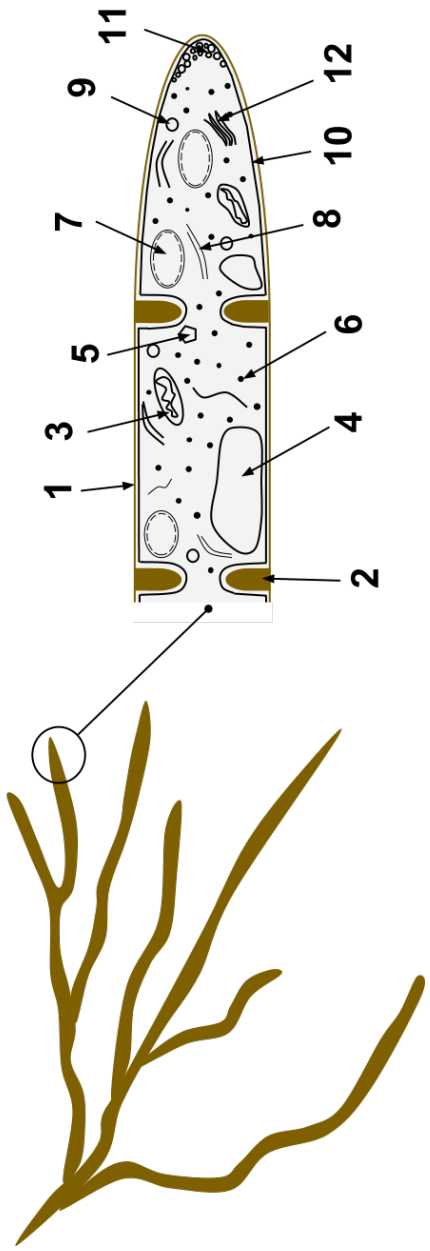

Figure 1: Fungal Hyphae Cells, 1-Hyphal wall, 2-Septum, 3-Mitochondrion, 4-Vacuole, 5-Ergosterol crystal, 6-Ribosome, 7-Nucleus, 8-Endoplasmic reticulum, 9-Lipid body, 10-Plasma membrane, 11-Spitzenkörper, 12-Golgi apparatus. (Source: AHiggins12 - CC BY-SA 3.0, `https://commons.wikimedia.org/wiki/File:HYPHAE.png`)

Chapter 1

Existence and Linear Stability of Solutions of the Ballistic VSC model

Abstract

An equation for the dynamics of the vesicle supply center model of tip growth in fungal hyphae is derived. For this we analytically prove the existence and uniqueness of a travelling wave solution which exhibits the experimentally observed behaviour. The linearized dynamics around this solution is analysed and we conclude that all eigenmodes decay in time. Numerical calculation of the first eigenvalue gives a timescale in which small perturbations will die out.

1.1 Introduction

Tip growth is a process in which fungi grow hairs, called hyphae, which lengthen at a constant speed, often achieving lengths much larger than their diameters. It is a mechanism by which organisms increase the ratio of surface area to volume probably in order to increase nutrient uptake. Experiments using markers on the cell wall [1] indicate that the wall expands orthogonally to its surface, with growth highly localized in the tip.

The concept of a vesicle supply center (VSC), first proposed by Bartnicki-Garcia *et al* [2], [11], lies at the basis for a whole hierarchy of mathematical models which attempt to explain tip growth. It assumes that there is a point source in the tip which distributes cell wall material for the tip. Vesicles travel from the VSC to the cell wall, producing growth of the cell wall orthogonal to the wall surface. A common result of these models is that the location of the VSC physically coincides with a body called a *Spitzenkörper* within the tip. This body was already suspected to play a role in tip growth.

The ballistic VSC model assumes that vesicles uniformly emanate from the VSC in all directions and travel in straight lines to the cell wall. Bartnicki-Garcia *et al* first derived an analytical expression for the shape of the travelling wave solution for a two dimensional model [2], and later numerically calculated the shape of cylindrically symmetric travelling wave solutions for the more realistic three dimensional model [11]. Koch [19] suggests replacing ballistic motion of the vesicles by a diffusive process. Tindemans [22], [23] has expanded further on this idea and has numerically calculated the shape of the travelling wave solutions. Other possible modifications of the model include adding elasticity of the cell wall [13], cell wall aging [7] or nonzero absorption times for vesicles [23].

Thus far, all research on VSC type models has focused on numerically determining the shape of the travelling wave solution, little analytical work has been done and no stability results have been proven. In this article we examine the mathematically simplest of the three dimensional models, the ballistic VSC model. We derive a second order parabolic PDE for the evolution of the tip shape.

Hyphoid solutions are travelling wave solutions to this PDE which look like fungal hyphae. They are cylindrically symmetric solutions with a smooth tip which approximate a cylinder of radius r_{max} as $z \to -\infty$. We analytically prove the existence, uniqueness and linear stability of a hyphoid solution. We numerically calculate the eigenvalues of the linearized operator, which should give an indication of the timescale in which small perturbations of the cell wall disappear. In a forthcoming paper we intend to combine the approach in this paper with a Schauder fixed point argument to establish the existence of hyphoid solutions for the diffusive VSC model.

The ballistic VSC model is based on the following assumptions:

- The hyphae are rotationally symmetric around the z axis.
- The VSC is located on the z axis and moving at a fixed velocity c. (A stationary VSC would result in a spherical cell)
- Vesicles are emitted uniformly in all direction and travel in straight lines from the VSC to the cell wall where they immediately are absorbed resulting in orthogonal growth. (Whether the VSC produces vesicles or redistributes vesicles produced elsewhere is irrelevant for modelling purposes, in either case we will refer to the total amount surface area added to the cell wall per unit of time as the production rate P of the VSC.)
- The amount of vesicles is large enough that this process can be approximated by a continuous flux of material arriving at the cell wall.

Eggen [7] showed that with these assumptions, the dynamics of the model can be expressed in terms of the mean curvature of the surface, we continue with this idea.

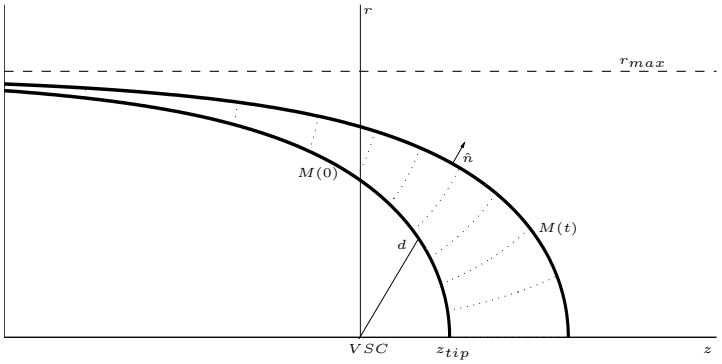

Figure 1.1: The manifold $M(t)$ and model definitions.

1.2 The evolution equation

We will model the cell wall as a 2D manifold $M(t)$, axisymmetric around the z axis, star-shaped with respect to the location of the VSC, and embedded in 3D Euclidean space. If we consider the evolution of any piece of the cell wall $A(t) \subset M(t)$, with surface area also denoted as $A(t)$, flowing according to a velocity field $\vec{u}$ defined in a neighbourhood of $A(t)$, we have Gauss' formula for the first variation of area:

$$\frac{\mathrm{d}A}{\mathrm{d}t} = -\int_{A(t)} H(\vec{u}\cdot\hat{n})\mathrm{d}A + \oint_{\partial A(t)} (\hat{n}_s \cdot \vec{u})\mathrm{d}s \tag{1.2.1}$$

where $\hat{n}$ is the outward pointing normal, $\hat{n}_s$ is the normal to the boundary curve lying in the tangent space of $M(t)$, and H is the mean curvature. Note that, due to our choice of normal, the mean curvature would be negative for a concave surface. We assume the velocity field to be normal to the surface, $\vec{u} = u_n\hat{n}$, the boundary term vanishes and only the integral over u_nH remains.

In the ballistic model, the VSC is moving at constant speed c in the z direction and is assumed to start at the origin at time zero. So its position is $ct\hat{e}_z$. It radiates vesicles in all directions, this can be described by a flux field $\vec{\Phi}$ of the form:

$$\vec{\Phi}(\vec{x}) = \frac{P}{4\pi}\frac{(\vec{x} - ct\hat{e}_z)}{|\vec{x} - ct\hat{e}_z|^3} \tag{1.2.2}$$

where P is the rate of change of the total area of the manifold, or the production rate of the VSC. The amount of material absorbed in $A(t)$ is:

$$\frac{\mathrm{d}A}{\mathrm{d}t} = \int_{A(t)} (\vec{\Phi}\cdot\hat{n})\mathrm{d}A \tag{1.2.3}$$

Combining (1.2.1) and (1.2.3) to maintain mass balance gives

$$-\int_{A(t)} u_n H \mathrm{d}A = \int_{A(t)} (\vec{\Phi} \cdot \hat{n}) \mathrm{d}A \tag{1.2.4}$$

Since $A(t)$ was chosen arbitrarily, the terms in the integrals must be equal:

$$u_n = -\frac{\vec{\Phi} \cdot \hat{n}}{H}. \tag{1.2.5}$$

This equation defines a geometric flow which is similar, differing only in the factor $\vec{\Phi} \cdot \hat{n}$, to the inverse mean curvature flow which has been studied extensively by Gerhardt [10], Huisken [14], [15], Urbas [25] and many others. Unfortunately, since we are interested in solutions which are not closed surfaces and because the flux term $\vec{\Phi} \cdot \hat{n}$ depends not only on the shape of the manifold, but also on the position, it is not clear whether their results and methods can be used for this problem.

The manifold $M(t)$ is embedded in $\mathbb{R}^3$ and we define $F : \Omega \times [0, T) \to \mathbb{R}^3$ for Ω a two dimensional coordinate space to be the embedding map. The manifold is now given by

$$M(t) = \{F(x, t) | x \in \Omega\}, \tag{1.2.6}$$

here x is a Lagrangian marker of some particle of the cell wall, and $F(x, t)$ gives its location in $\mathbb{R}^3$. The Laplace-Beltrami operator $\Delta_{M(t)}$ on a quantity A is defined as

$$\Delta_{M(t)} A = \frac{1}{\sqrt{g}} \partial_i (\sqrt{g} g^{ij} \partial_j A), \tag{1.2.7}$$

and a standard result from differential geometry relates the mean curvature vector to the Laplace-Beltrami operator on the embedding map, $H\hat{n} = \Delta_{M(t)} F$. Equation (1.2.5) can now be written as

$$\frac{\partial F}{\partial t} \cdot \Delta_{M(t)} F = -\frac{P}{4\pi} \frac{\hat{n} \cdot (F - ct\hat{e}_z)}{|F - ct\hat{e}_z|^3}, \tag{1.2.8}$$

and the condition that the velocity is normal to the surface of the manifold becomes

$$\frac{\partial F}{\partial t} \cdot \partial_i F = 0, \qquad \text{for} \qquad i = 1, 2. \tag{1.2.9}$$

One now sees that if F satisfies (1.2.8) with $c = 1$ and $P = 4\pi$, one can scale space and time and substitute

$$\tilde{F} = \frac{P}{4\pi c} F(x, \frac{4\pi c^2}{P} t) \tag{1.2.10}$$

into (1.2.8) to see that $\tilde{F}$ solves the equation for arbitrary c and P. So for the rest of this article we shall concern ourselves only with the case $c = 1$ and $P = 4\pi$.

1.3 Travelling waves

We want to study rotationally symmetric solutions of (1.2.8) with $P = 4\pi$ and $c = 1$. So $\Omega = I \times S^1$ where I is an interval, $p \in I \subset \mathbb{R}$, and we split F into a radial component $r(p,t)$ and a component in the z direction $z(p,t)$,

$$F(p,\theta,t) = r(p,t)\hat{e}_r(\theta) + z(p,t)\hat{e}_z. \tag{1.3.1}$$

We wish to study travelling wave solutions which move at a speed of one in the z direction. So

$$M(t) = M(0) + t\hat{e}_z. \tag{1.3.2}$$

In other words, for every p there is an unique q such that

$$F(p,\theta,t) = F(q,\theta,0) + t\hat{e}_z. \tag{1.3.3}$$

Each point on $M(t)$ can be seen as a point (with a different coordinate p) of $M(0)$ displaced in the z direction, we define the map $\xi : I \times [0,T) \to I$ which maps p into q as described above. Clearly $\xi(p,0) = p$ and

$$F(p,\theta,t) = F_1(\xi(p,t),\theta) + t\hat{e}_z = r_1(\xi(p,t))\hat{e}_r(\theta) + (z_1(\xi(p,t)) + t)\hat{e}_z, \tag{1.3.4}$$

where $F_1(p,\theta) = F(p,\theta,0)$, $r_1(p) = r(p,0)$ and $z_1(p) = z(p,0)$. The curve $(r_1(p), z_1(p)), p \in I$ describes the travelling wave solution in a coordinate frame moving at speed $c = 1$ in the z direction. Physically, if one were to place an ink marker on the fungal hyphae at coordinates (p,θ) at time zero, $F(p,\theta,t)$ would describe how this ink marker would move through space (the dotted curves in Figure 1.1), in a stationary reference frame the ink marker would appear to move in a direction perpendicular to the cell surface. If, however, one were to move along with the cell tip, the fungal hyphae would appear stationary and $\xi(p,t)$ would describe the p-coordinate of the ink marker as it appears to move backwards along the surface.

1.3.1 Geometry

We now calculate, using (1.2.8) and (1.3.4) some geometric quantities for the manifold $M(t)$. The tangent vectors at coordinates (p,θ) are given by,

$$\begin{aligned} \frac{\partial F}{\partial p} &= \frac{\partial \xi}{\partial p}\left(r_1'(\xi(p,t))\hat{e}_r(\theta) + z_1'(\xi(p,t))\hat{e}_z\right), \\ \frac{\partial F}{\partial \theta} &= r_1(\xi(p,t))\hat{e}_\theta, \end{aligned} \tag{1.3.5}$$

and so the metric tensor is

$$g = \begin{pmatrix} \left(\frac{\partial \xi}{\partial p}\right)^2 v^2 & 0 \\ 0 & r_1^2 \end{pmatrix}, \tag{1.3.6}$$

where $v^2 = {r_1'}^2 + {z_1'}^2$. The unit normal is given by

$$\hat{n} = \pm\frac{1}{v}(z_1'\hat{e}_r(\theta) - r_1'\hat{e}_z), \tag{1.3.7}$$

where the sign is chosen such that the normal points outward. If the parameter p is such that larger values denote points closer to the tip then the positive sign is chosen. This allows us to write the right hand side of (1.2.8) as

$$\frac{\hat{n}\cdot(F - t\hat{e}_z)}{|F - t\hat{e}_z|^3} = \pm\frac{1}{v}\frac{z_1'r_1 - r_1'z_1}{(r_1^2 + z_1^2)^{\frac{3}{2}}}. \tag{1.3.8}$$

The velocity vector is

$$\frac{\partial F}{\partial t} = \frac{\partial \xi}{\partial t}\left(r_1'(\xi(p,t))\hat{e}_r(\theta) + z_1'(\xi(p,t))\hat{e}_z\right) + \hat{e}_z. \tag{1.3.9}$$

Since the velocity vector is perpendicular to the tangent vectors,

$$\frac{\partial F}{\partial t}\cdot\frac{\partial F}{\partial p} = \frac{\partial \xi}{\partial p}\left(\frac{\partial \xi}{\partial t}v^2 + z_1'\right) = 0 \tag{1.3.10}$$

and we can solve for the time derivative of ξ

$$\frac{\partial \xi}{\partial t} = -\frac{z_1'}{v^2}. \tag{1.3.11}$$

The mean curvature vector, given by the Laplace-Beltrami operator on the embedding map, is

$$\begin{aligned}\Delta_{M(t)}F &= \frac{1}{r_1 v\frac{\partial \xi}{\partial p}}\left[\frac{\partial}{\partial p}\left(\frac{r_1}{v\frac{\partial \xi}{\partial p}}\frac{\partial F}{\partial p}\right) + \frac{\partial}{\partial \theta}\left(\frac{v\frac{\partial \xi}{\partial p}}{r_1}\frac{\partial F}{\partial \theta}\right)\right], \\ &= \frac{1}{r_1 v\frac{\partial \xi}{\partial p}}\frac{\partial}{\partial p}\left(\frac{r_1}{v}(r_1'\hat{e}_r(\theta) + z_1'\hat{e}_z)\right) - \frac{1}{r_1}\hat{e}_r(\theta).\end{aligned} \tag{1.3.12}$$

We now change to a new variable $\xi = \xi(p,t)$ and use the chain rule, the term $\frac{\partial \xi}{\partial p}$ disappears

$$\Delta_{M(t)}F = \frac{1}{r_1 v}\frac{\partial}{\partial \xi}\left(\frac{r_1}{v}(r_1'\hat{e}_r(\theta) + z_1'\hat{e}_z)\right) - \frac{1}{r_1}\hat{e}_r(\theta), \tag{1.3.13}$$

and we can write the left hand side of (1.2.8) as

$$-\frac{\partial F}{\partial t}\cdot\Delta_{M(t)}F = \frac{r_1'}{v}\left(\frac{z_1'r_1'' - r_1'z_1''}{v^3} - \frac{z_1'}{r_1 v}\right) \tag{1.3.14}$$

and (1.2.8) can be written entirely in terms of the initial manifold, as described by $r_1(\xi)$ and $z_1(\xi)$.

$$r_1'\left(\frac{z_1'r_1'' - r_1'z_1''}{v^3} - \frac{z_1'}{r_1 v}\right) = \pm\frac{z_1'r_1 - r_1'z_1}{(r_1^2 + z_1^2)^{\frac{3}{2}}} \tag{1.3.15}$$

1.4 Hyphoid solutions

Recall from the introduction that a hyphoid solution is a travelling wave solution which approximates a cylinder of radius r_{max} far away from the tip. In order to study the existence and uniqueness of such hyphoid solutions we choose our parameter p such that it is the z coordinate at time zero, $I = (-\infty, z_{tip})$. So for all p, $z_1(\xi(p,0)) = z_1(p) = p$ and clearly $z_1' = 1$ and $z_1'' = 0$. Now since $\frac{\partial}{\partial t} z_1(\xi(p,t)) = \frac{\partial \xi}{\partial t} z_1' = \frac{\partial \xi}{\partial t}$ we see that $\xi(p,t) = z_1(\xi(p,t))$. Setting $z = \xi(p,t)$ we can describe our manifold as the graph of a function $r_1(z)$. Using this parametrization (1.3.15) becomes

$$r_1' \left(\frac{r_1''}{v^3} - \frac{1}{r_1 v} \right) = \frac{r_1 - r_1' z}{(r_1^2 + z^2)^{\frac{3}{2}}}, \tag{1.4.1}$$

where $v^2 = 1 + r_1'^2$. Multiplying by r_1 we see that this is equivalent to

$$-\frac{\mathrm{d}}{\mathrm{d}z} \left(\frac{r_1}{\sqrt{1 + r_1'^2}} \right) = \frac{\mathrm{d}}{\mathrm{d}z} \left(\frac{z}{\sqrt{r_1^2 + z^2}} \right). \tag{1.4.2}$$

Integrating, we get a first order ODE,

$$\frac{r_1}{\sqrt{1 + r_1'^2}} = 1 - \frac{z}{\sqrt{r_1^2 + z^2}}, \tag{1.4.3}$$

where we have chosen the integration constant such that there is a z_{tip} such that $r_1(z_{tip}) = 0$. If we assume that r_1 has an asymptote $r_1 \to r_{max}$, $r_1' \to 0$ as $z \to -\infty$, we get $r_{max} = 2$ as expected from mass balance.

Solving for the derivative of r_1 gives

$$r_1' = -\sqrt{r_1^2 \left(1 - \frac{z}{\sqrt{r_1^2 + z^2}} \right)^{-2} - 1} = f(z, r_1). \tag{1.4.4}$$

This ODE is defined in the region

$$r \geq 1 - \frac{z}{\sqrt{r^2 + z^2}}, \tag{1.4.5}$$

outside this region, no travelling wave solutions can exist. Define B to be the boundary,

$$B = \left\{ (z, r) | r = 1 - \frac{z}{\sqrt{r^2 + z^2}} \right\}. \tag{1.4.6}$$

Solutions which hit B at some point cease to exist to the left of this point. Note that B lies below the line $r = 2$. We will refer to the region enclosed by B where the ODE is not defined as the forbidden zone.

Note that we have chosen the negative solution, $r_1' = f(z, r_1) \leq 0$, since we are looking for solutions with $z_{tip} > 0$ and extending in the negative z direction

with a positive asymptote $r_1 \to 2$. Choosing the positive square root would result in unrealistic solutions $r_1 < 0$ mirrored over the z axis.

Since any solution is decreasing (and thus solutions above the line $r = 2$ will always stay above this asymptote as $z \to -\infty$), we know that for a hyphoid solution:

$$1 - \frac{z}{\sqrt{r_1^2 + z^2}} \leq r_1 < 2. \tag{1.4.7}$$

1.4.1 Existence and uniqueness

Theorem 1.4.1 (Existence and Uniqueness) *There exists a unique hyphoid solution.*

Proof From (1.4.7), choosing $z = 0$, we see that a hyphoid solution must pass through a point $(0, x)$ for some $x \in [1, 2)$. We can immediately exclude the case $x = 1$ since this solution will not exist for $z < 0$. We examine all the remaining possible solutions, parametrized by x. For $x \in (1, 2)$ let $\gamma_x : I_x \to \mathbb{R}^+$ be the solution to (1.4.4) which passes through $(0, x)$, with I_x the corresponding existence interval. So,

$$\frac{\mathrm{d}}{\mathrm{d}z}\gamma_x(z) = f(z, \gamma_x(z)), \qquad \gamma_x(0) = x. \tag{1.4.8}$$

We will first examine those values of x for which γ_x is not a hyphoid solution. Let

$$\Sigma^- = \left\{ x \subset (1,2) | \exists z \in (-\infty, 0) : \gamma_x(z) = 1 - \frac{z}{\sqrt{\gamma_x(z)^2 + z^2}} \right\} \tag{1.4.9}$$

be the set of values of x for which γ_x hits the boundary B of the forbidden zone. Let

$$\Sigma^+ = \{ x \subset (1,2) | \exists z \in (-\infty, 0) : \gamma_x(z) = 2 \} \tag{1.4.10}$$

be the set of values of x which hits the line $r = 2$. For some $z^* < 0$ let $\tilde{\gamma}$ be a solution to (1.4.4) with $(z^*, \tilde{\gamma}(z^*)) \in B$ and let $\tilde{I}$ be the corresponding existence interval, note that $\min(\tilde{I}) = z^*$. Then $\tilde{\gamma}(z) \leq \tilde{\gamma}(z^*) < 2$ for all $z \in \tilde{I}$ due to the strict monotonicity of the ODE (1.4.4) outside B. Consequently, $1 < \tilde{\gamma}(0) < 2$ and so $\tilde{\gamma} = \gamma_{x^*}$ for some x^* and $\Sigma^- \neq \emptyset$. In an analogue way one sees that $\Sigma^+ \neq \emptyset$. Straightforward perturbation arguments yield that Σ^+ is an open interval. Finally, the mapping $\Psi : \Sigma^- \to (-\infty, 0)$ given by:

$$\Psi(r) = \Pi_z \left(\mathrm{graph}(\gamma_r) \cap B \right), \tag{1.4.11}$$

with Π_z the projection operator to z, is monotone and maps onto the open interval $(-\infty, 0)$ and thus Σ^- is an open interval. Since $\Sigma^- \subset (1,2), \Sigma^+ \subset (1,2)$ and $\Sigma^- \cap \Sigma^+ = \emptyset$ the set $\Sigma^0 = (1,2) \setminus (\Sigma^- \cup \Sigma^+)$ is closed, not empty and for $x \in \Sigma^0$, γ_x is a travelling wave solution.

We show now that Σ^0 has only one element, otherwise Σ^0 would have interior points. We examine the asymptotic behaviour of solutions $\gamma_{\tilde{x}}$ with $\tilde{x}$ in the

neighbourhood of an interior point x. Differentiating (1.4.8) with respect to x results in the following linear ODE for $\rho(z) = \frac{\partial}{\partial x}\gamma_x(z)$:

$$\frac{\partial}{\partial z}\rho(z) = \frac{\partial f}{\partial r}(z, \gamma_x(z))\rho(z), \qquad \rho(0) = 1, \tag{1.4.12}$$

where

$$\frac{\partial f}{\partial r}(z, r) = \frac{1}{f}\left(r\left(1 - \frac{z}{d}\right)^{-2} - \left(1 - \frac{z}{d}\right)^{-3}\left(\frac{zr^3}{d^3}\right)\right) \tag{1.4.13}$$

Since f is negative, negative z implies $\frac{\partial f}{\partial r}(z, r) < 0$ and $\lim_{z\to-\infty}\frac{\partial f}{\partial r}(z, \gamma_x(z)) = -\infty$, so $\rho(z)$ increases exponentially as $z \to -\infty$ and a solution close to γ_x diverges from γ_x as $z \to -\infty$ and so cannot have the same asymptotic behaviour. Therefore Σ^0 cannot have interior points and this interval must consist of a single point.

■

1.4.2 Properties of the hyphoid solution

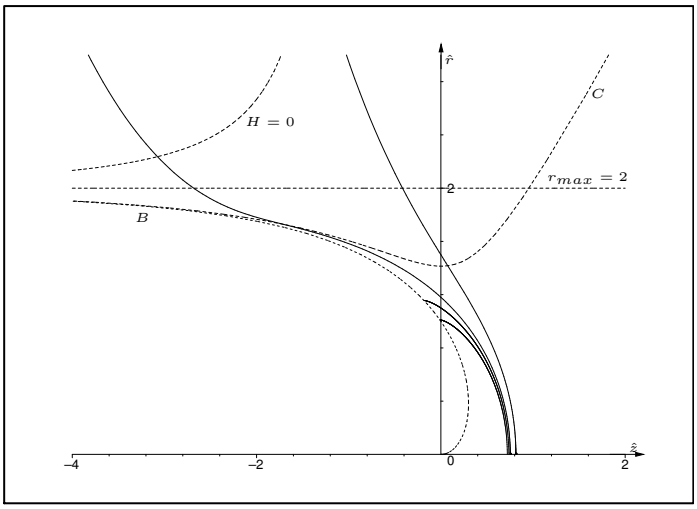

Figure 1.2: Solid lines: solutions γ_x to (1.4.8) for $x = 1.01$, $x = 1.1$ in Σ^- and $x = 1.1804$, $x = 1.5$ in Σ^+, Dashed lines: the line $r = 2$, and the curves defined in (1.4.6), (1.4.16) and (1.4.18).

Lemma 1.4.2 (Properties of the hyphoid solution) *The hyphoid solution has the following properties:*

1. *The tip has no corner.*
2. *The tip is the closest point to the VSC, and is the only extremum of the distance d to the VSC.*
3. *The solution is star-shaped and the mean curvature is strictly negative.*
4. *The solution is concave.*

Proof 1. Tip shape.

Note that if r_1' is finite then the left hand side of (1.4.3) is $O(r_1)$ as $r_1 \to 0$ while the right hand side is $O(r_1^2)$ for positive z; this yields a contradiction, hence $r_1' \to -\infty$ as $r_1 \to 0$. This means that the tip has no corner.

2. Tip location.

Since the tip has no corner, the distance d to the VSC has an extremum at the tip. If we consider other extrema of the distance, where $d' = \frac{r_1 r_1' + z}{d} = 0$ or $r_1' = -\frac{z}{r_1}$ then, since r_1' is negative, these extrema can only occur if $z \geq 0$. Substituting (1.4.4) we get an expression for the set of

points (z_D, r_D) where $f(z_D, r_D) = -\frac{z_D}{r_D}$. We show that this curve does not intersect the hyphoid solution. Solving for r_D gives the trivial solution $r_D = 0$ and

$$r_D^2 = 1 - 2z_D, \qquad 0 \leq z_D \leq \frac{1}{2}. \tag{1.4.14}$$

This parabola hits the line $r = 0$ at $z_D = \frac{1}{2}$ and hits the curve B at $(z_D, r_D) = (0, 1)$. Differentiating to get the slope m of the tangent to this curve, we get

$$m = -\frac{1}{r_D} < -\frac{z_D}{r_D} = f(z_D, r_D), \tag{1.4.15}$$

so any solution to (1.4.4) which has an extremum in the distance d other than at the tip, passes through this parabola from left to right and must originate from B. The hyphoid solution does not originate from B and therefore cannot intersect this parabola. So it only has one extremum in d which must be a minimum, the tip is the closest point to the VSC.

3. Star-shapedness.

   For the VSC model to make sense, the hyphoid solution has to be star-shaped with respect to the origin (the location of the VSC) and to have nonzero (and thus negative, due to our choice of normal $\hat{n}$) mean curvature. Since the flux $\vec{\Phi}$ always points away from the VSC, (1.2.5) says that the two requirements are equivalent. While it is possible to find solutions to (1.4.3) in which H and $\vec{\Phi} \cdot \hat{n}$ are zero or switch signs, these solutions are physically unrealistic. A solution is not star-shaped with respect to the origin if at any point $r - zr' < 0$. Since r is positive and r' is negative, this can only occur at negative z. We now consider the points where $r - zr' = 0$, combining this with (1.4.3) and solving for r at negative z one gets:

$$r = 2\frac{z^2}{z^2 - 1}. \tag{1.4.16}$$

   Since for $z < -1$ this curve lies above the line $r = 2$, any bounded solution to (1.4.3), in particular the hyphoid solution, will not cross this curve. Since for the hyphoid solution, $r - zr'$ is positive at the tip, it is positive everywhere and the hyphoid solution is star-shaped with respect to the origin and has negative mean curvature.

4. Concavity.

   Differentiating (1.4.4) gives:

$$r'' = \frac{rd^2}{(d-z)^2} - \frac{r^3 z}{(d-z)^3} + \frac{1}{f(z,r)}\frac{r^4}{(d-z)^3}, \tag{1.4.17}$$

   where $f(z, r)$ is given by (1.4.4). This equation gives the second derivative of r for any travelling wave solution passing through the point (z, r). We now consider the curve C where $r'' = 0$

$$C = \left\{ (z,r) | f(z,r) = \frac{r^3}{r^2 z - d^2(d-z)} \right\}. \tag{1.4.18}$$

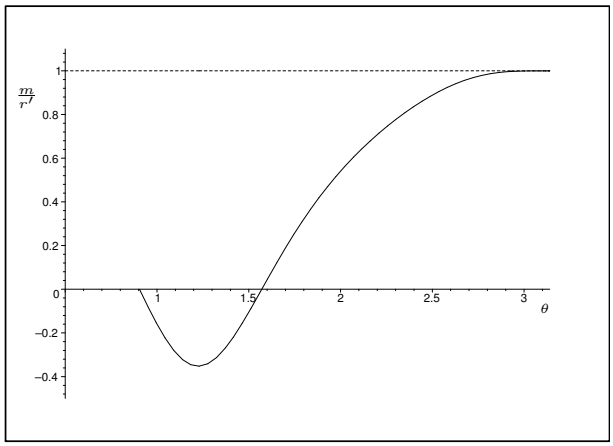

Figure 1.3: Ratio of the slope m of the curve C to the slope r' of the solution.

We parametrize this curve in polar coordinates $r = \rho(\phi)\sin\phi$, $z = \rho(\phi)\cos\phi$, $d = \rho(\phi)$. Substituting this in the definition (1.4.4) of f and the equation (1.4.18) for the curve C we get

$$-\sqrt{\frac{\rho(\phi)^2\sin^2\phi}{(1-\cos\phi)^2} - 1} = \frac{\sin^3\phi}{(1-\cos\phi)(\cos^2\phi + \cos\phi - 1)}. \tag{1.4.19}$$

Since $f(z,r)$ is negative and $\sin\phi$ is positive, the term $\cos^2\phi + \cos\phi - 1$ on the right hand side must be negative and we see that C stays above the line at angle $\phi_{min} = \arccos(\frac{\sqrt{5}-1}{2})$. Solving for $\rho(\phi)^2$ gives

$$\rho(\phi)^2 = \frac{\sin^4\phi}{(\cos^2\phi + \cos\phi - 1)^2} + \frac{(1-\cos\phi)^2}{\sin^2\phi} \tag{1.4.20}$$

and

$$C = \left\{(\rho(\phi)\cos\phi, \rho(\phi)\sin\phi) | \phi_{min} < \phi < \pi\right\}. \tag{1.4.21}$$

If we now examine the slope m of the curve C

$$m = \frac{\frac{\mathrm{d}}{\mathrm{d}\phi}\left(\rho(\phi)\sin\phi\right)}{\frac{\mathrm{d}}{\mathrm{d}\phi}\left(\rho(\phi)\cos\phi\right)} \tag{1.4.22}$$

and compare this to the slope $r' = f(\rho(\phi)\cos\phi, \rho(\phi)\sin\phi)$ of the travelling wave solution intersecting C we find, using Maple, a symbolic mathematical analysis program, that $\frac{m}{r'}$ has a supremum of 1 as $\phi \to \pi$, so $r' < m$. See also Figure 1.3. So travelling wave solutions cross the curve C from above to below as z increases, and can cross the curve C at most once. The hyphoid solution has $r'' < 0$ in the tip. If the hyphoid solution were

to intersect C, this would imply r'' is positive as $z \to -\infty$ which is in contradiction with the fact that $r' < 0$ and $r' \to 0$ as $z \to -\infty$. So the hyphoid solution cannot intersect C and must be concave. ■

1.5 Stability of the hyphoid solution

In order to study the stability of the hyphoid solution we consider the manifold to be the graph of the function $z(r,t)$ in a frame of coordinates moving along with the VSC, clearly the hyphoid solution found in the previous section is stationary in these coordinates. If a particle p is at radius $r(p,t)$ at time t the embedding map can now be written as

$$F(p,\theta,t) = (z(r(p,t),t) + ct)\,\hat{e}_z + r(p,t)\hat{e}_r(\theta). \tag{1.5.1}$$

As it will be helpful later to consider variations with respect to c, we choose to leave the parameter c in our equations, although we will do all our calculations at $c = 1$. The normal $\hat{n}$ and tangent $\hat{m}$ unit vectors to the manifold are now given by

$$\hat{n} = \frac{1}{v}(\hat{e}_z - z'\hat{e}_r(\theta)) \qquad \hat{m} = \frac{1}{v}(z'\hat{e}_z + \hat{e}_r(\theta)) \qquad v^2 = 1 + z'^2. \tag{1.5.2}$$

Examining the partial derivatives of F we get

$$\begin{aligned} \frac{\partial F}{\partial p} &= r'v\hat{m}, & g_{11} &= r'^2v^2, \\ \frac{\partial F}{\partial \theta} &= r\hat{e}_\theta, & g_{22} &= r^2, \\ \frac{\partial F}{\partial t} &= \dot{r}v\hat{m} + (\dot{z}+c)\hat{e}_z, & \sqrt{g} &= r'vr. \end{aligned} \tag{1.5.3}$$

Since $\frac{\partial F}{\partial p} \cdot \frac{\partial F}{\partial t} = 0$ we can solve for $\dot{r}$, and obtain

$$\dot{r} = -\frac{(\dot{z}+c)z'}{v^2}, \qquad \frac{\partial F}{\partial t} = \frac{(\dot{z}+c)}{v}\hat{n}. \tag{1.5.4}$$

Now the evolution equation (1.2.8) can be written as a PDE for $z(r,t)$ as

$$\Psi(\dot{z}, z'', z', z, c) = (\dot{z}+c)H - \frac{z'r - z}{(r^2+z^2)^{\frac{3}{2}}} = 0, \tag{1.5.5}$$

where the mean curvature H is given by

$$H = \frac{z''}{v^3} + \frac{z'}{rv}. \tag{1.5.6}$$

In Section 1.4 we showed the existence of an unique hyphoid solution $r_1(z)$ for $c = 1$, since $r_1' < 0$ we can invert this to get a stationary solution $z_1(r)$ to (1.5.5) at $c = 1$. Using the scaling (1.2.10) we see that for arbitrary c,

$$z_c(r) = \frac{1}{c}z_1(cr), \tag{1.5.7}$$

is an equilibrium solution to the PDE, we will make use of this in the proof of Theorem 1.5.5.

1.5.1 The linearized evolution equation

Linearizing around the solution at $c = 1$, $z(r,t) = z_1(r) + w(r,t)$ results in the following linear evolution for w

$$\dot{w} + L[w] = O(w^2), \tag{1.5.8}$$

with

$$L[w] = a(r)w'' + b(r)w' + c(r)w, \tag{1.5.9}$$

where

$$\begin{aligned} a(r) &= \frac{\partial \Psi}{\partial z''} \Big/ \frac{\partial \Psi}{\partial \dot{z}} &&= \frac{1}{v^3 H}, \\ b(r) &= \frac{\partial \Psi}{\partial z'} \Big/ \frac{\partial \Psi}{\partial \dot{z}} &&= \frac{1}{H}\left(-\frac{3z_1''z_1'}{v^5} + \frac{1}{v^3 r} - \frac{r}{d^3}\right), \\ c(r) &= \frac{\partial \Psi}{\partial z} \Big/ \frac{\partial \Psi}{\partial \dot{z}} &&= \frac{1}{H}\left(\frac{1}{d^3} + \frac{3z_1(z_1'r - z_1)}{d^5}\right). \end{aligned} \tag{1.5.10}$$

Here $d^2 = r^2 + z_1(r)^2$, $v^2 = 1 + z_1'(r)^2$, and H is the mean curvature of the unperturbed surface.

1.5.2 Divergence form

If we write $w(r,t) = Y(r)\phi(r,t)$ for $Y(r)$ nonzero everywhere, and define the linear operator

$$\tilde{L}[\phi] = \frac{1}{Y} L[Y(r)\phi(r,t)] = a\phi'' + \left(\frac{2aY'}{Y} + b\right)\phi' + \left(a\frac{Y''}{Y} + b\frac{Y'}{Y} + c\right)\phi. \tag{1.5.11}$$

If Y is chosen such that $\frac{2aY'}{Y} + b = a' + \frac{a}{r}$, or

$$\log Y = \int \frac{a' + \frac{a}{r} - b}{2a} \mathrm{d}r, \tag{1.5.12}$$

then $\tilde{L}[\phi]$ is in divergence form.

$$\tilde{L}[\phi] = -\frac{1}{r}\frac{\partial}{\partial r}\left(r\alpha(r)\frac{\partial}{\partial r}\phi(r,t)\right) + \beta(r)\phi(r,t), \tag{1.5.13}$$

where

$$\alpha(r) = -a(r), \tag{1.5.14}$$

$$\begin{aligned} \beta(r) &= a(r)\frac{Y''}{Y} + b(r)\frac{Y'}{Y} + c(r) \\ &= a\left(\frac{\mathrm{d}}{\mathrm{d}r}\left(\frac{a' + \frac{a}{r} - b}{2a}\right) + \left(\frac{a' + \frac{a}{r} - b}{2a}\right)^2\right) + b\left(\frac{a' + \frac{a}{r} - b}{2a}\right) + c. \end{aligned} \tag{1.5.15}$$

Using integration by parts one clearly sees that $\int \tilde{L}[u]v r\mathrm{d}r = \int u\tilde{L}[v]r\mathrm{d}r$ so $\tilde{L}$ is symmetric on L^2.

1.5.3 Asymptotics

One can find formal series solutions for the hyphoid solution $z_1(r)$, its derivatives, and thus for the functions $a(r)$, $b(r)$, $c(r)$, $Y(r)$, $\alpha(r)$ and $\beta(r)$ in the tip as $r \to 0$ and in the asymptote as $r \to 2$. Using a combination of Implicit Function Theorem with methods found in de Bruijn [4] for finding expansions for solutions of ODEs, one can show that these formal series are asymptotic expansions. However, these calculations are extremely lengthy and outside the scope of this article. To first order this gives the following estimates,

$(r \to 0)$	$(r \to 2)$
$z_1 = z_{tip} + O\left(r^2\right),$	$z_1 = -\sqrt{2}(2-r)^{-\frac{1}{2}} + O\left((2-r)^{\frac{1}{2}}\right),$
$z_1' = -\dfrac{1}{2z_{tip}^2} r + O\left(r^3\right),$	$z_1' = -\dfrac{\sqrt{2}}{2}(2-r)^{-\frac{3}{2}} + O\left((2-r)^{-\frac{1}{2}}\right),$
$z_1'' = -\dfrac{1}{2z_{tip}^2} + O\left(r^2\right),$	$z_1'' = -\dfrac{3\sqrt{2}}{4}(2-r)^{-\frac{5}{2}} + O\left((2-r)^{-\frac{3}{2}}\right),$
$H = -\dfrac{1}{z_{tip}^2} + O\left(r^2\right),$	$H = -\dfrac{1}{2} + O\left(2-r\right),$
$a = -z_{tip}^2 + O\left(r^2\right),$	$a = -4\sqrt{2}(2-r)^{\frac{9}{2}} + O\left((2-r)^{\frac{11}{2}}\right),$
$b = -z_{tip}^2 \dfrac{1}{r} + O\left(r\right),$	$b = \sqrt{2}(2-r)^{\frac{5}{2}} + O\left((2-r)^{\frac{5}{2}}\right),$
$c = \dfrac{2}{z_{tip}} + O\left(r^2\right),$	$c = -\dfrac{3\sqrt{2}}{2}(2-r)^{\frac{1}{2}} + O\left((2-r)^{\frac{3}{2}}\right),$
$\log Y = \left(\dfrac{3}{4z_{tip}^2} - \dfrac{1}{4z_{tip}^3}\right) r^2 + O\left(r^4\right),$	$\log Y = \dfrac{1}{16}(2-r)^{-2} + O\left((2-r)^{-1}\right),$
$\alpha = z_{tip}^2 + O\left(r^2\right),$	$\alpha = 4\sqrt{2}(2-r)^{\frac{9}{2}} + O\left((2-r)^{\frac{11}{2}}\right),$
$\beta = \dfrac{3}{z_{tip}} - 3 + O\left(r^2\right),$	$\beta = \dfrac{\sqrt{2}}{16}(2-r)^{-\frac{3}{2}} + O\left((2-r)^{-\frac{1}{2}}\right).$

From these asymptotics we can prove the following properties of α and β.

Lemma 1.5.1 *Properties of α and β.*

- *α is positive and bounded for all r, near the tip α stays away from zero.*
- *β is bounded near the tip, and is bounded by below by its minimum β_0.*

Proof Positivity of α follows from negativity of H. In the tip $v = 1$, so $\alpha(0) = -\frac{1}{H(0)}$. Since in the tip $z_1'(0) = 0$, from (1.5.5) we get that $H(0) = -\frac{1}{z_{tip}^2}$ and so $\alpha(0) = z_{tip}^2$. In the asymptote $r \to 2$, $\alpha(r) = O((2-r)^{\frac{9}{2}})$ and so α stays bounded.

From the asymptotics at $r \to 0$ it follows that β is bounded near the tip. From the asymptotics at $r \to 2$ it follows that β is positive and explodes as $r \to 2$, by continuity it follows that it is bounded from below, we define β_0 to be its minimum. Numerical calculations in Section 1.6 suggest that $\beta_0 \approx 0.56$ and thus positive, however for now we shall assume nothing about its sign. ■

Corollary 1.5.2 *$\tilde{L}$ is bounded from below.*

Proof Integrating by parts we obtain,

$$(\tilde{L}u, u)_{L^2} = \int_0^2 (\alpha u'^2 + \beta u^2) r \mathrm{d}r \geq \beta_0 ||u||_{L^2}^2. \tag{1.5.16}$$

1.5.4 Eigenvalues of $\tilde{L}$

Naively, since in Section 1.4 we found a class of travelling wave solutions of which the hyphoid solution was a special case, one would expect a zero eigenvalue. However this is not the case. Consider those solutions $r_p(z)$ which cross the line $r = 2$ at the point $(r, z) = (2, p)$. Since $r_p'(z) < 0$ we can invert these solutions to get functions $z_p(r)$ for $r \in [0, 2]$. If one were to linearize around one such solution at finite p we would certainly get a zero eigenvalue with eigenfunction $\frac{\partial z_p}{\partial p}$. The hyphoid solution can be considered to be the point wise limit of $z_p(r)$ as $p \to -\infty$. Since for $r < 2$ the functions $z_p(r)$ are bounded from below by the hyphoid solution, and since these solutions are monotone in p (since solutions to a first order ODE cannot cross paths), $\frac{\partial z_p}{\partial p}(r) \to 0$. However, by construction, $\frac{\partial z_p}{\partial p}(2) \to 1$. So the pointwise limit as $p \to -\infty$ of the zero eigenfunction is not a continuous function of r. In fact, in this section we will show that all eigenvalues are positive.

We now construct an energetic Hilbert space V as a subspace of $L^2(0, 2)$ with measure $r\mathrm{d}r$ (or equivalently, L^2 on the disc of radius 2 with the standard area measure, restricted to rotationally symmetric functions), and define the Friedrichs' extension of $\tilde{L}$, also denoted as $\tilde{L}$ on V. For more details see Weidmann [29] §5.5.

For test functions $u, v \in C_0^\infty(0, 2)$ the inner product on V is given by

$$\begin{aligned} \langle u, v \rangle_V &= (1 - \beta_0)(u, v)_{L^2} + (\tilde{L}[u], v)_{L^2} \\ &= \int_0^2 (\alpha u' v' + (1 + \beta - \beta_0) uv) r \mathrm{d}r. \end{aligned} \tag{1.5.17}$$

The space V is the completion of test function under the norm $||u||_V^2 = \langle u, u \rangle_V$. The extended operator $\tilde{L} : D(\tilde{L}) \to L^2$ has a domain $D(\tilde{L})$ which is dense in V and is self-adjoint on L^2.

Lemma 1.5.3 *V is compactly embedded in L^2.*

$$V \subset\subset L^2(0,2) \tag{1.5.18}$$

Proof By construction, V is continuously embedded in L^2. Now choose a bounded sequence $\{\phi_n\}$ in V. Since $\beta = O((2-r)^{-\frac{3}{2}})$ there are constants $A > 0$ and r_0 such that for all $r \in (r_0, 2)$, $1 + \beta(r) - \beta_0 \geq A(2-r)^{-\frac{3}{2}}$. So for positive $\delta \leq 2 - r_0$, if $2 - \delta < r < 2$ then $\frac{1}{A}\delta^{\frac{3}{2}}(1 + \beta(r) - \beta_0) \geq 1$ and

$$\int_{2-\delta}^{2} \phi_n^2 r \mathrm{d}r \leq \frac{1}{A}\delta^{\frac{3}{2}} \int_{2-\delta}^{2} (1 + \beta - \beta_0)\phi_n^2 r \mathrm{d}r \leq \frac{1}{A}\delta^{\frac{3}{2}} ||\phi_n||_V^2. \tag{1.5.19}$$

and

$$\lim_{\delta \to 0} ||\phi_n||_{L^2(2-\delta,2)} = 0 \qquad \text{uniformly in } n. \tag{1.5.20}$$

As $\{\phi_n\}$ is bounded in L^2 it has a subsequence, again denoted by $\{\phi_n\}$, which weakly converges to some $\phi \in L^2$. For $k = 1, 2, \ldots$, define $\delta_k \in (0,1)$ such that

$$\begin{aligned} ||\phi||_{L^2(2-\delta_k,2)} &\leq \frac{1}{3k}, \qquad \text{and} \\ ||\phi_n||_{L^2(2-\delta_k,2)} &\leq \frac{1}{3k}. \end{aligned} \tag{1.5.21}$$

Note that by Lemma 1.5.1, α and β are well behaved outside the asymptote $r \to 2$, so the sequence of restrictions of ϕ_n to $(0, 2-\delta_k)$ is bounded in $H^1(0, 2-\delta_k)$. Due to the compactness of the embedding $H^1(0, 2-\delta) \hookrightarrow L^2(0, 2-\delta)$ (one sees this compactness by considering these spaces with measure $r\mathrm{d}r$ as function spaces on the disc with the usual area measure) we can find convergent subsequences for any fixed δ. Let $n_k^{(0)}$ be the sequence $1, 2, 3, \ldots$. For each $i \geq 1$ we find a subsequence $n_k^{(i)}$ of $n_k^{(i-1)}$ such that

$$||\phi_{n_k^{(i)}} - \phi||_{L^2(0,2-\delta_i)} \leq \frac{1}{3k}. \tag{1.5.22}$$

The diagonal sequence now satisfies

$$||\phi_{n_k^{(k)}} - \phi||_{L^2(0,2-\delta_k)} \leq \frac{1}{3k}. \tag{1.5.23}$$

Hence

$$\begin{aligned} ||\phi_{n_k^{(k)}} - \phi||_{L^2(0,2)} &\leq ||\phi_{n_k^{(k)}} - \phi||_{L^2(0,2-\delta_k)} \\ &\quad + ||\phi_{n_k^{(k)}}||_{L^2(2-\delta_k,2)} \\ &\quad + ||\phi||_{L^2(2-\delta_k,2)} \qquad\qquad \leq \frac{1}{k}, \end{aligned} \tag{1.5.24}$$

and we see that the subsequence $\{\phi_{n_k^{(k)}}\}$ converges to ϕ strongly in L^2. ∎

Corollary 1.5.4 *$\tilde{L}$ has a pure point spectrum.*

Proof From Lemma 1.5.3 this follows directly by Rellich's criterion ([24] Theorem 4.5.3).

Theorem 1.5.5 (Linear stability of the hyphoid solution) *All eigenvalues of $\tilde{L}$ are positive.*

Proof We consider variations of the hyphoid solution with respect to the velocity c of the VSC. From (1.5.5) and (1.5.7) we know that $z_c(r) = \frac{1}{c} z_1(cr)$ is a solution to $\Psi(0, z_c'', z_c', z_c, c) = 0$. Differentiating by c at $c = 1$ one sees that $L[\frac{\partial z_c}{\partial c}|_{c=1}] + 1 = 0$. Now let $\psi = -\frac{1}{Y}\frac{\partial z_c}{\partial c}|_{c=1} = -\frac{1}{Y}(z_1' r - z_1)$. Since, by Lemma 1.4.2, the hyphoid solution is star shaped, $z_1' r - z_1 < 0$ and ψ is a positive function. Furthermore $\tilde{L}[\psi] = \frac{1}{Y}$ is positive. Since $\tilde{L}$ is a self-adjoint operator and bounded from below,it has a smallest eigenvalue λ_1 which can be calculated using the Rayleigh quotient. Let ϕ_1 be a function with $||\phi_1||_{L^2} = 1$ which minimizes $(\phi, \tilde{L}[\phi])_{L^2}$, then λ_1 is this minimum and ϕ_1 lies in its corresponding eigenspace. The absolute value of ϕ_1 also minimizes the Rayleigh quotient, so without loss of generality ϕ_1 may be assumed positive. Now since ϕ_1 is an eigenfunction, $(\psi, \tilde{L}[\phi_1])_{L^2} = (\psi, \lambda_1\phi_1)_{L^2} = \lambda_1(\psi, \phi_1)_{L^2}$, but since $\tilde{L}$ is self-adjoint, $(\psi, \tilde{L}[\phi_1])_{L^2} = (\tilde{L}[\psi], \phi_1)_{L^2} = (\frac{1}{Y}, \phi_1)_{L^2}$. Since $\frac{1}{Y}$, ψ, and ϕ_1 are positive, and the L^2 inner product of two positive functions is positive, the smallest eigenvalue λ_1 must be positive. ■

1.5.5 Asymptotics of the eigenfunctions

One can find formal series solutions for the eigenfunctions of $\tilde{L}$. Using similar techniques as in Section 1.5.3 one can show that these formal series are asymptotic expansions. The asymptotic expansion of the eigenfunction ϕ_λ at eigenvalue λ as $r \to 2$ is

$$\begin{aligned}\log \phi_\lambda = &-\frac{1}{16}(2-r)^{-2} - \frac{1}{2}(2-r)^{-1} \\ &+ \sqrt{2}\lambda(2-r)^{-\frac{1}{2}} + \frac{15}{32}\log(2-r) + O\left(\sqrt{2-r}\right).\end{aligned} \tag{1.5.25}$$

Since $w_\lambda(r) = Y(r)\phi_\lambda$ we can combine this with the asymptotic expansion for Y

$$\begin{aligned}\log Y = &\frac{1}{16}(2-r)^{-2} + \frac{1}{2}(2-r)^{-1} \\ &- \frac{63}{32}\log(2-r) + \frac{57}{32}(2-r) + O((2-r)^2).\end{aligned} \tag{1.5.26}$$

We see that the first two terms of the expansion cancel out, resulting in the following asymptotic expansion for the eigenfunctions w.

$$w = (2-r)^{-\frac{3}{2}} e^{\sqrt{2}\lambda(2-r)^{-\frac{1}{2}} + O(\sqrt{2-r})}. \tag{1.5.27}$$

For positive (stable) λ these eigenfunctions increase exponentially as $r \to 2$.

1.6 Numerical calculations

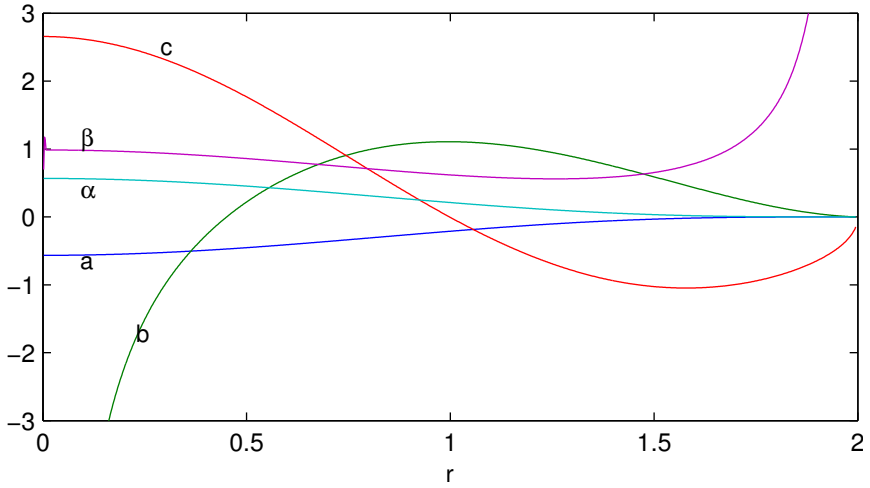

Figure 1.4: Functions $a(r)$, $b(r)$, $c(r)$, $\alpha(r)$ and $\beta(r)$.

Starting from the second order PDE (1.5.5) with $c = 1$ and assuming $\dot{z} = 0$ we get a second order ODE in $z(r)$ for the shape of the hyphoid solution. Setting $z_1' = u$ we get the following first order system of differential equations.

$$\frac{\partial}{\partial r}\begin{pmatrix} z_1 \\ u \end{pmatrix} = \begin{pmatrix} u \\ \left(\frac{1+u^2}{r^2+z_1^2}\right)^{\frac{3}{2}}(ur - z_1) - \frac{u}{r}(1+u^2) \end{pmatrix} \tag{1.6.1}$$

Starting from $r = 1.9951$, $z_1 = -20$ and $u = -2050.3$, as given by the asymptotic expansion as given in Section 1.5.3 we compute a numerical solution using an initial value solver available in a package such as MatLab. The resulting points (z_1, z_1', r) enables us to calculate higher derivatives using central difference methods and thus we can calculate $a(r)$, $b(r)$, $c(r)$, $\alpha(r)$ and $\beta(r)$. These functions are shown in Figure 1.4. From these, using finite difference methods and assuming boundary conditions of $\frac{\mathrm{d}\phi}{\mathrm{d}r}(0) = 0$, $\phi(2) = 0$ we can discretize $\tilde{L}$ to obtain a tridiagonal matrix, of which the eigenvalues and eigenvectors can subsequently be calculated.

The five smallest eigenvalues are $\lambda_1 = 0.7145, \lambda_2 = 1.4292, \lambda_3 = 2.1134, \lambda_4 = 2.7726$, and $\lambda_5 = 3.4109$, corresponding eigenfunctions $\phi_1 \cdots \phi_5$ are given in Figure 1.5. Note that it is necessary to calculate the eigenfunctions of the symmetric operator $\tilde{L}$. The eigenfunctions of the operator L are related to these by $w_i = Y\phi_i$ but since the factor Y grows faster than the eigenfunctions decay, the functions w_i will reach the floating point upper boundary of a computer around $r = 1.9$.

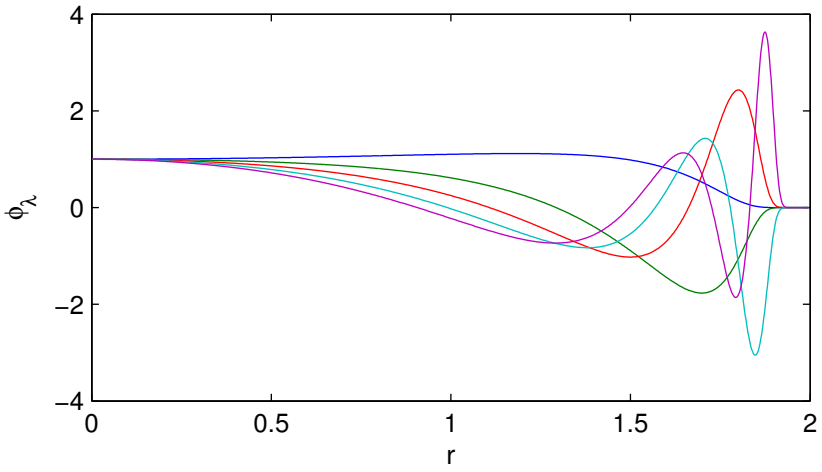

Figure 1.5: The first five eigenfunctions of the self-adjoint operator $\tilde{L}$.

This would imply a generic perturbation will die out at a rate dictated by the first eigenvalue, so with a timescale of $1/\lambda_1 \approx 1.4$. Given a generic hypha with production factor P travelling at a velocity c one can use the rescaling described in (1.2.10) to get the timescale τ in which perturbations die out. (For convenience, using mass balance $P = 2\pi r_{max} c$, we also express τ in terms of the radius r_{max} of the base of the hypha.)

$$\tau \approx 1.4 \frac{P}{4\pi c^2} = 1.4 \frac{r_{max}}{2c} \tag{1.6.2}$$

1.7 Conclusions

We have shown that the VSC model has hyphoid solutions, travelling wave solutions similar in shape to fungal hyphae. Moreover, we have shown that these solutions are linearly stable. However, whether this implies nonlinear stability is a nontrivial open problem, especially since the eigenfunctions of L do not decay as $r \to 2$. In this limit the operator degenerates to a transport operator (in coordinates moving along with the tip) and a perturbation away from the tip will move further down the asymptote without decaying. It should however be possible, when restricting ourselves to a compact area near the tip, to show that perturbations do decay at a rate dictated by the first eigenvalue. We intend to discuss this in a forthcoming paper.

Chapter 2

Asymptotics for the Ballistic VSC Model

2.1 Introduction

In the previous chapter we proved the existence and uniqueness of a so-called hyphoid solution $r : (-\infty, z_{tip}] \to [0, 2)$ to the travelling wave ODE

$$\frac{r(z)}{\sqrt{1 + r'(z)^2}} = 1 - \frac{z}{\sqrt{r(z)^2 + z^2}}. \tag{2.1.1}$$

This solution satisfies $r(z_{tip}) = 0$, $r(z) \to 2$ as $z \to -\infty$ and $r'(z) < 0$.

We denote the inverse of the hyphoid solution as $z : [0, 2) \to (-\infty, z_{tip}]$, in section 1.5 we derived a second order ODE for $z(r)$,

$$\frac{z''(r)}{(1 + z'(r)^2)^{3/2}} + \frac{z'(r)}{r\sqrt{1 + z'(r)^2}} = \frac{rz'(r) - z(r)}{(r^2 + z(r)^2)^{3/2}}. \tag{2.1.2}$$

In section 1.5.3 we stated that there are formal series solutions for $z(r)$ as $r \to 0$ and $r \to 2$. We claimed that these series are in fact asymptotic expansions, cutting the series off after a certain amount of terms provides an estimate for the asymptotic behaviour of $z(r)$. In section 1.5.5 we made similar statements concerning the eigenfunctions of the symmetric operator $\tilde{L}$. The goal of this chapter is to derive these formal series and to prove these estimates.

In section 2.2 we will derive a formal series solution for $r(z)$ as $z \to -\infty$, we will then show that this series is an asymptotic expansion. This expansion can then be inverted to give an asymptotic expansion for $z(r)$ as $r \to 2$. In section 2.3 we will derive a formal series solution for $z(r)$ and show this is an asymptotic expansion. Finally, in section 2.4 we will derive asymptotic expansion for the eigenfunctions.

2.2 Asymptotics as $z \to -\infty$

If we rewrite (2.1.1), squaring and transposing terms twice to get rid of square roots and denominators, we get de following equation.

$$A_4 r'(z)^4 + A_2 r'(z)^2 + A_0 = 0, \tag{2.2.1}$$

where

$$\begin{aligned} A_0 &= r(z)^6 + (2z^2 - 2)r(z)^4 + (z^4 - 6z^2 + 1)r(z)^2 - 4z^4, \\ A_2 &= -2r(z)^4 + (-6z^2 + 2)r(z)^2 - 4z^4, \qquad \text{and} \\ A_4 &= r(z)^2. \end{aligned} \tag{2.2.2}$$

2.2.1 Formal asymptotics as $z \to -\infty$

We now define a formal asymptotic series for $r(z)$, let

$$r(z) = \sum_{m=0}^{\infty} r_{0,1,m} z^{-m}, \tag{2.2.3}$$

this allows us to express the formal derivative $r'(z)$ and powers of $r(z)$ and $r'(z)$ in terms of the coefficients $r_{0,1,m}$,

$$\begin{aligned} r(z)^2 &= \sum_{m=0}^{\infty} r_{0,2,m} z^{-m}, \quad \text{where} \quad r_{0,2,m} = \sum_{i=0}^{m} r_{0,1,i} r_{0,1,m-i}, \\ r(z)^4 &= \sum_{m=0}^{\infty} r_{0,4,m} z^{-m}, \quad \text{where} \quad r_{0,4,m} = \sum_{i=0}^{m} r_{0,2,i} r_{0,2,m-i}, \\ r(z)^6 &= \sum_{m=0}^{\infty} r_{0,6,m} z^{-m}, \quad \text{where} \quad r_{0,6,m} = \sum_{i=0}^{m} r_{0,4,i} r_{0,2,m-i}, \\ r'(z) &= \sum_{m=2}^{\infty} r_{1,1,m} z^{-m}, \quad \text{where} \quad r_{1,1,m} = (1-m) r_{0,1,m-1}, \\ r'(z)^2 &= \sum_{m=4}^{\infty} r_{1,2,m} z^{-m}, \quad \text{where} \quad r_{1,2,m} = \sum_{i=2}^{m-2} r_{1,1,i} r_{1,1,m-i}, \\ r'(z)^4 &= \sum_{m=8}^{\infty} r_{1,4,m} z^{-m}, \quad \text{where} \quad r_{1,4,m} = \sum_{i=4}^{m-4} r_{1,2,i} r_{1,2,m-i}. \end{aligned} \tag{2.2.4}$$

Our notation is chosen in such a way that $r_{p,n,m}$ is the coefficient before z^{-m} in the formal series for the n-th power of the p-th derivative of $r(z)$. Important to note is that if $n \geq 2$ the coefficient $r_{0,n,m}$ depends only on $r_{0,1,i}$ for $0 \leq i \leq m$, where the dependence on $r_{0,1,m}$ is linear if $m \geq 1$. Similarly, the coefficient $r_{1,n,m}$ depends only on $r_{0,1,i}$ for $0 \leq i \leq m-1$. We can now calculate formal

series for the A_0 term in (2.2.1),

$$\begin{aligned} A_0 &= r(z)^6 + (2z^2-2)r(z)^4 + (z^4-6z^2+1)r(z)^2 - 4z^4 \\ &= \sum_{m=0}^{\infty} r_{0,6,m} z^{-m} + 2\sum_{m=-2}^{\infty} r_{0,4,m+2} z^{-m} - 2\sum_{m=0}^{\infty} r_{0,4,m} \\ &\quad + \sum_{m=-4}^{\infty} r_{0,2,m+4} z^{-m} - 6\sum_{m=-2}^{\infty} r_{0,2,m+2} z^{-m} + \sum_{m=0}^{\infty} r_{0,2,m} z^{-m} - 4z^4 \\ &= \sum_{m=-2}^{\infty} c_{0,m} z^{-m}, \end{aligned} \tag{2.2.5}$$

where,

$$\begin{aligned} c_{0,-4} &= r_{0,2,0} - 4, \\ c_{0,-3} &= r_{0,2,1}, \\ c_{0,-2} &= 2r_{0,4,0} + r_{0,2,2} - 6r_{0,2,0}, \\ c_{0,-1} &= 2r_{0,4,1} + r_{0,2,3} - 6r_{0,2,1}, \\ c_{0,m} &= r_{0,6,m} + 2r_{0,4,m+2} - 2r_{0,4,m} \\ &\qquad + r_{0,2,m+4} - 6r_{0,2,m+2} + r_{0,2,m} \qquad \text{for } m \geq 0. \end{aligned} \tag{2.2.6}$$

The formal series for the A_2 term is given by

$$\begin{aligned} A_2 &= -2r(z)^4 + (-6z^2+2)r(z)^2 - 4z^4 \\ &= -2\sum_{m=0}^{\infty} r_{0,4,m} z^{-m} - 6\sum_{m=-2}^{\infty} r_{0,2,m+2} z^{-m} + 2\sum_{m=0}^{\infty} r_{0,2,m} z^{-m} - 4z^4 \\ &= \sum_{m=-4}^{\infty} c_{2,m} z^{-m}, \end{aligned} \tag{2.2.7}$$

where,

$$\begin{aligned} c_{2,-4} &= -4, \\ c_{2,-3} &= 0, \\ c_{2,-2} &= -6r_{0,2,0}, \\ c_{2,-1} &= -6r_{0,2,1}, \\ c_{2,m} &= -2r_{0,4,m} - 6r_{0,2,m+2} + 2r_{0,2,m} \qquad \text{for } m \geq 0, \end{aligned} \tag{2.2.8}$$

and the formal series for the A_4 term is given by $A_4 = \sum_{m=0}^{\infty} r_{0,2,m} z^{-m}$. Substituting this into (2.2.1) we get

$$\sum_{m=8}^{\infty} \sum_{k=0}^{m-8} r_{0,2,k} r_{1,4,m-k} z^{-m} + \sum_{m=0}^{\infty} \sum_{k=-4}^{m-4} c_{2,k} r_{1,2,m-k} z^{-m} + \sum_{m=-4}^{\infty} c_{0,m} z^{-m} = 0. \tag{2.2.9}$$

We need to choose $r_{0,1,m}$ such that the coefficients for all powers z^{-m} in this equation are zero. Examining the coefficient for z^4 we get $c_{0,-4} = r_{0,2,0} - 4 = r_{0,1,0}^2 - 4 = 0$. Since $r(z) > 0$ we choose the positive root so $r_{0,1,0} = 2$. For $m = -3 \cdots -1$ we get $c_{0,m} = 0$, these equations can be solved to give $r_{0,1,1} = 0$, $r_{0,1,2} = -2$ and $r_{0,1,3} = 0$. For $m = 0 \cdots 7$ we get

$$c_{0,m} + \sum_{k=-4}^{m-4} c_{2,k} r_{1,2,m-k} = 0. \tag{2.2.10}$$

We rewrite the definition of $r_{0,2,m}$ in (2.2.4), extracting the first and last terms in the sum,

$$r_{0,2,m} = 2r_{0,1,0}r_{0,1,m} + \sum_{i=1}^{m-1} r_{0,1,i} r_{0,1,m-i}. \tag{2.2.11}$$

Combining the above two equations with (2.2.6) and substituting $l = m + 4$ we get

$$\begin{aligned} r_{0,1,l} = -\frac{1}{2r_{0,1,0}} \Bigg(& r_{0,6,l-4} + 2r_{0,4,l-2} - 2r_{0,4,l-4} - 6r_{0,2,l-2} + r_{0,2,l-4} \\ & + \sum_{k=-4}^{l-8} c_{2,k} r_{1,2,l-k-4} \Bigg), \end{aligned} \tag{2.2.12}$$

for $l = 4 \cdots 11$. Now, all the coefficients on the right hand side depend only on $r_{0,1,i}$ with $i < l$ so we can iteratively calculate $r_{0,1,4}$ through $r_{0,1,11}$. Similarly, examining the coefficient of z^{-m} in (2.2.9) for $m \geq 8$ we get,

$$c_{0,m} + \sum_{k=-4}^{m-4} c_{2,k} r_{1,2,m-k} + \sum_{k=0}^{m-8} r_{0,2,k} r_{1,4,m-k} = 0, \tag{2.2.13}$$

and so, again combining this with (2.2.6) and (2.2.11), and substituting $l = m+4$ we get

$$\begin{aligned} r_{0,1,l} = -\frac{1}{2r_{0,1,0}} \Bigg(& r_{0,6,l-4} + 2r_{0,4,l-2} - 2r_{0,4,l-4} - 6r_{0,2,l-2} + r_{0,2,l-4} \\ & + \sum_{k=-4}^{l-8} c_{2,k} r_{1,2,l-k-4} + \sum_{k=0}^{l-12} r_{0,2,k} r_{1,4,l-k-4} \Bigg), \end{aligned} \tag{2.2.14}$$

for $l \geq 12$. Again the right hand side only depends on $r_{0,1,i}$ with $i < l$ so we can iteratively calculate all $r_{0,1,l}$.

Calculating the first 20 terms gives us the following formal series solution to (2.1.1),

$$\begin{aligned} r(z) = 2 - \frac{2}{z^2} + \frac{10}{z^4} - \frac{50}{z^6} + \frac{130}{z^8} + \frac{1294}{z^{10}} - \frac{21110}{z^{12}} + \frac{66718}{z^{14}} \\ + \frac{2239234}{z^{16}} - \frac{39132770}{z^{18}} + \frac{99949706}{z^{20}} + \cdots . \end{aligned} \tag{2.2.15}$$

Looking at these first terms, one might suspect we only get even powers of $\frac{1}{z}$, this is in fact the case.

Lemma 2.2.1 *For odd m, $r_{0,1,m} = 0$.*

Proof We prove this by induction. The calculations preceding this lemma show that the first few odd coefficients are zero. Given an odd m and assuming $r_{0,1,i} = 0$ for all odd i between 1 and $m-2$ we need to show that $r_{0,1,l} = 0$.

First of all, if m is odd, then for arbitrary i, either i or $m-i$ will be odd but never both. Combining this, the induction hypothesis, and (2.2.4) yields that

$$\begin{aligned} r_{1,1,i} &= 0 \qquad && \text{for } i = 2, 4, \cdots, m-1, \\ r_{1,n,i} &= 0 && \text{for } i = 1, 3, 5, \cdots, m \text{ and } n = 2, 4, \\ r_{0,n,i} &= 0 && \text{for } i = 1, 3, 5, \cdots, m-2 \text{ and } n = 2, 4, 6. \end{aligned}$$

From (2.2.8) we then see that $c_{2,i} = 0$ for odd i between 1 and $m-4$. Now given odd l and arbitrary k, either k or $l-k-4$ is odd, so (2.2.14) yields that $r_{0,1,l} = 0$. ■

2.2.2 Asymptotic expansions for $r(z)$ as $z \to -\infty$

We will now show that this formal series is an asymptotic expansion, terminating the series at the z^{-2n} term results in an error estimate of $O(z^{-2(n+1)})$. In order to do this, we will first prove some a general result about the asymptotics of certain differential equations.

Theorem 2.2.2 Asymptotics of a nonlinear ODE of polynomial form. *We consider a nonlinear, first order, ordinary differential equation for $f(x)$ of the form*

$$G(x, f, f') = \sum_{i=0}^{M} \sum_{j=0}^{N_i} A_{i,j}(f) f'^i x^j = 0 \tag{2.2.16}$$

where M is the highest power of the derivative f' of f, N_i is the highest power of x by which the i-th power of f' is multiplied and $A_{i,j}(f)$ are continuous differentiable functions of f. If the following conditions hold

1. *A_{0,N_0} has a root at f_{zero} and its derivative $A'_{0,N_0}(f_{zero}) \neq 0$,*
2. *$A_{1,N_1}(f_{zero})$ is nonzero,*
3. *$N_0 > N_1 > N_2, ..., N_M$,*

then there exists a x_0 and at least one solution $f(x)$ to the ODE defined for $x > x_0$ such that

$$\begin{aligned} \lim_{x \to \infty} f(x) &= f_{zero}, \qquad \text{and} \\ \lim_{x \to \infty} f'(x) &= 0. \end{aligned}$$

We will prove this theorem in section 2.2.2, but first we will examine a simplified version of (2.2.16).

Simplified problem

If, in the ODE of theorem 2.2.2 we assume that f' is small, we can drop all but the zeroth and first power of f'. In the first summation we therefore only consider the terms $i = 0$ and $i = 1$. If we then only consider the solution at large values of x, we can drop all but the highest powers x^{N_0} and x^{N_1}. We then approximate A_{0,N_0} by its first order Taylor polynomial around f_{zero},

$$A_{0,N_0}(f) = \alpha(f - f_{zero}), \tag{2.2.17}$$

where

$$\alpha = A'_{0,N_0}(f_{zero}). \tag{2.2.18}$$

We then approximate A_{1,N_1} by its value β at f_{zero},

$$A_{1,N_1}(f) = A_{1,N_1}(f_{zero}) = \beta. \tag{2.2.19}$$

After dividing by x^{N_1}, the ODE then reduces to

$$\alpha(f(x) - f_{zero})x^{N_0-N_1} + \beta f'(x) = 0. \tag{2.2.20}$$

This ODE is separable, starting with an initial condition $f(x_0) = f_0$ it has as solution

$$f(x) = f_{zero} + (f_0 - f_{zero})e^{-\frac{\alpha}{(N_0-N_1+1)\beta}(x^{N_0-N_1+1}-x_0^{N_0-N_1+1})} \tag{2.2.21}$$

Now if $\frac{\alpha}{\beta} > 0$ all solutions $f(x) \to f_{zero}$ regardless of the initial condition. If on the other hand $\frac{\alpha}{\beta} < 0$, there is exactly one solution, with initial condition $f_0 = f_{zero}$ such that $f(x) \to f_{zero}$, solutions at all other initial conditions become unbounded. We will see similar behaviour in the analysis of the full problem in the next section.

The full problem

We will now give the proof of theorem 2.2.2.

Proof Similar to the simplified problem, we define

$$\begin{aligned} \alpha &= A_{0,N_0}(f_{zero}), \\ \beta &= A'_{1,N_1}(f_{zero}). \end{aligned} \tag{2.2.22}$$

Our first goal is to use the Implicit Function Theorem to restate the ODE in the form $f' = g(x, f)$ in some region of the (x, f) plane. In order to do this, we fix a sufficiently small μ and examine the μ-clines, the sets of points in the (x, f) plane where $f' = \mu$ for some constant value of μ. We first prove that for sufficiently large x there exist functions $f_\mu(x)$ such that $G(x, f_\mu(x), \mu) = 0$.

Substituting $f' = \mu$ into equation (2.2.16), dividing by x^{N_0} and substituting $y = \frac{1}{x}$ we get

$$F_\mu(y,f) = A_{0,N_0}(f) + y\sum_{j=0}^{N_0-1} A_{0,j}(f)y^{N_0-1-j} + y^{N_0-N_1}\sum_{i=1}^{M}\sum_{j=0}^{N_i} A_{i,j}(f)\mu^i y^{N_1-j} = 0.$$

Because of condition 3 all powers of y are positive. Because of condition 1 $F_\mu(0, f_{zero}) = A_{0,N_0}(f_{zero}) = 0$ and $\frac{\partial F_\mu}{\partial f}(0, f_{zero}) = \alpha \neq 0$, so by the Implicit Function Theorem for small y there is a function $\tilde{f}_\mu(y)$ such that $F_\mu(y, \tilde{f}_\mu(y)) = 0$ and $\tilde{f}_\mu(0) = f_{zero}$. Reformulating this in terms of x means that there is an x_0 and a function $f_\mu(x)$ defined for $x > x_0$ such that $G(x, f_\mu(x), \mu) = 0$ and $\lim_{x\to\infty} f_\mu(x) = f_{zero}$. Furthermore, the slope of the μ-cline is given by

$$\begin{aligned}\frac{\mathrm{d}f_\mu}{\mathrm{d}x} &= -\frac{\frac{\partial G}{\partial x}(x, f_\mu(x), \mu)}{\frac{\partial G}{\partial f}(x, f_\mu(x), \mu)} \\ &= -\frac{\sum_{i=0}^{M}\sum_{j=0}^{N_i} A_{i,j}(f_\mu(x))\mu^i j x^{j-1}}{\sum_{i=0}^{M}\sum_{j=0}^{N_i} A'_{i,j}(f_\mu(x))\mu^i x^j}.\end{aligned}$$

In the limit $x \to \infty$ the highest power of x dominates in the sums and

$$\lim_{x\to\infty}\frac{\mathrm{d}f_\mu}{\mathrm{d}x} = -\lim_{x\to\infty}\frac{A_{0,N_0}(f_\mu(x))x^{N_0-1}}{A'_{0,N_0}(f_\mu(x))x^{N_0}} = -\lim_{x\to\infty}\frac{\beta}{\alpha}x^{-1} = 0.$$

If we now specifically examine the null-cline $f_0(x)$ we see that for $x > x_0$, $G(x, f_0(x), 0) = 0$. Furthermore if we examine $\frac{\partial G}{\partial f'}$ at the null-cline, we see that only the parts of the sum with $i = 0$ remain.

$$\frac{\partial G}{\partial f'}(x, f_0(x), 0) = \sum_{j=0}^{N_1} A_{1,j}(f_0(x))x^j$$

Since $f_0(x) \to f_{zero}$ all the factors $A_{1,j}(f_0(x))$ remain bounded. Since $A_{1,j}(f_{zero}) \neq 0$ the x^{N_1} term will dominate for large enough x, $|A_{1,N_1}(f_0(x))x^j| > |\sum_{j=0}^{N_1-1} A_{1,j}(f_0(x))x^j|$ and therefore $\frac{\partial G}{\partial f'}(x, f_0(x), 0) \neq 0$. So by the Implicit Function Theorem, in the neighbourhood of the null-cline $f_0(x)$ and for sufficiently large x, there is a continuous differentiable function $g(x, f)$ such that $G(x, f, g(x, f)) = 0$ and $g(x, f_0(x)) = 0$.

In the neighbourhood of the null-cline the ODE can now be written as

$$f'(x) = g(x, f(x)).$$

Furthermore,

$$\frac{\partial g}{\partial f} = -\frac{\frac{\partial G}{\partial f}}{\frac{\partial G}{\partial f'}} = -\frac{\sum_{i=0}^{M}\sum_{j=0}^{N_i} A'_{i,j}(f)f'^i x^j}{\sum_{i=1}^{M}\sum_{j=0}^{N_i} A_{i,j}(f)f'^{i-1}x^j},$$

and so

$$\lim_{x\to\infty}\frac{\partial g}{\partial f}(x,f_0(x)) = -\frac{\alpha}{\beta}. \tag{2.2.23}$$

Thus for sufficiently large x, $\frac{\partial g}{\partial f}$ will have the same sign as $-\frac{\alpha}{\beta}$ giving an ordering to the μ-clines. We now consider solutions to this ODE, around the null-cline, for the different signs of $\frac{\alpha}{\beta}$.

1. If $\frac{\alpha}{\beta} > 0$:

   Given a $\mu > 0$, the μ-cline lies below the $-\mu$-cline. We consider solutions to the ODE in an area Ω of the (x, f) plane bounded by x_0 to the left, $f_{-\mu(x)}$ above and $f_\mu(x)$ below. Since the slopes of the upper and lower bound go to zero as $x \to \infty$, there is a x_0 such that for all $x > x_0$, $\frac{\mathrm{d}f_\mu}{\mathrm{d}x} < \mu$ and $\frac{\mathrm{d}f_{-\mu}}{\mathrm{d}x} > -\mu$. Therefore solutions starting on x_0 cannot leave the area Ω and must stay between the μ-cline and the $-\mu$-cline, since both these curves approach f_{zero} these solutions approach f_{zero}. Since μ can be chosen arbitrarily small, there must be solutions $f(x)$ for which $\frac{\mathrm{d}f}{\mathrm{d}x} \to 0$.

2. If $\frac{\alpha}{\beta} < 0$:

   Given a $\mu > 0$, the μ-cline lies above the $-\mu$-cline. We consider solutions to the ODE in an area Ω of the (x, f) plane bounded by x_0 to the left, $f_\mu(x)$ above and $f_{-\mu}(x)$ below. Since the slopes of the upper and lower bound go to zero as $x \to \infty$, there is a x_0 such that for all $x > x_0$, $\frac{\mathrm{d}f_\mu}{\mathrm{d}x} < \mu$ and $\frac{\mathrm{d}f_{-\mu}}{\mathrm{d}x} > -\mu$. For $c \in C = (f_{-\mu}(x_0), f_\mu(x_0))$ consider solutions $\gamma_c(x)$ to the ODE such that $\gamma_c(x_0) = c$. There is an set $\Sigma^+ \subset C$ such that for $c \in \Sigma^+$ the solution γ_c exits Ω through the upper boundary. Likewise there is a set $\Sigma^- \subset C$ such that for $c \in \Sigma^-$ the solution γ_c exits Ω through the lower boundary. Since the solutions are ordered and the upper and lower boundaries are open sets, Σ^+ and Σ^- are open intervals. Since a solution cannot reenter Ω, $\Sigma^+ \cap \Sigma^- = \emptyset$, therefore there must be a nonempty closed interval $\Sigma^0 = C \setminus (\Sigma^+ \cup \Sigma^-)$ such that for $c \in \Sigma^0$, the solution γ_c stays between the upper and lower bounds. Since both these curves approach f_{zero} these solutions approach f_{zero}. Since μ can be chosen arbitrarily small, there must be solutions $f(x)$ for which $\frac{\mathrm{d}f}{\mathrm{d}x} \to 0$.

■

If we rewrite the ODE for the hyphoid solution (1.4.4), squaring twice in order to eliminate the square roots, this ODE can be written as

$$r^2 r'^4 + \left(-2r^4 + (-6z^2+2)r^2 - 4z^4\right) r'^2 \qquad + \tag{2.2.24}$$

$$r^6 + (2z^2-2)r^4 + (-6z^2+z^4+1)r^2 - 4z^4 \qquad = \qquad 0. \tag{2.2.25}$$

We can use this form of the ODE, together with Theorem 2.2.2 to prove that the formal asymptotic series described in (2.2.15), cut off after a certain amount of terms, describes a good estimate of the solution in the asymptote.

We can use this theorem to derive a two term estimate for $r(z)$. If we substitute

$$r(z) = 2 - \frac{2}{z^2} + \frac{g(z)}{z^4} \qquad \text{and} \qquad r'(z) = \frac{4}{z^3} + \frac{g'(z)}{z^4} - 4\frac{g(z)}{z^5},$$

into (2.2.24) and multiplying out the powers of z in the denominator, we get an equation of the following form

$$\sum_{i=0}^{4} \cdot \sum_{j=0}^{N_i} A_{ij}(g) g'^i z^j = 0 \tag{2.2.26}$$

where $A_{ij}(g)$ are polynomials of finite order in g and $N_0 \cdots N_4 = 28, 25, 24, 13, 12$. Specifically,

$$\begin{aligned} &A_{0,28}(g) = 4(g-10) && \text{and} && A_{0,j}(g) = 0 && \text{for } j \text{ odd} \\ &A_{1,25}(g) = -32 && \text{and} && A_{1,j}(g) = 0 && \text{for } j \text{ even.} \end{aligned}$$

So, setting $x = -z$, the requirements of Theorem 2.2.2 are met and we know there exists at least one solution with such that

$$\lim_{z\to-\infty} g(z) = 10, \qquad \lim_{z\to\infty} \frac{\mathrm{d}}{\mathrm{d}z} g(z) = 0.$$

Uniqueness of this solution follows from the uniqueness of the hyphoid solution. If we now substitute $f(z,r) = \frac{4}{z^3} + \frac{g'(z)}{z^4} - 4\frac{g(z)}{z^5}$ into the equation (1.4.17) for the second derivative and take the limit $z \to -\infty$ we get

$$\begin{aligned} \lim_{z\to-\infty} r'' &= \lim_{z\to-\infty} \frac{rd^2}{(d-z)^2} - \frac{r^3 z}{(d-z)^3} + \frac{1}{f(z,r)} \frac{r^4}{(d-z)^3} \\ &= \lim_{z\to-\infty} \frac{1}{2} - \frac{1}{f(z,r)} \frac{2}{z^3} = \lim_{z\to-\infty} \frac{1}{2} - \frac{2}{(\frac{4}{z^3} - 4\frac{10}{z^5})z^3} = 0. \end{aligned}$$

Now, since $r'' \to 0$ and $r' \to 0$, we get

$$\lim_{z\to-\infty} H = \lim_{z\to-\infty} \left(\frac{r''}{(1+r'^2)^{\frac{3}{2}}} - \frac{1}{r(1+r'^2)^{\frac{1}{2}}} \right) = \lim_{z\to-\infty} -\frac{1}{r} = -\frac{1}{2}.$$

So the second derivative r'' tends to zero and the mean curvature H of the hyphoid solution approaches the mean curvature of a cylinder of radius 2 as $z \to -\infty$.

In the next theorem we will show that we can cut off the formal series (2.2.15) at any term of power $z^{-2(N-1)}$ and that the error made is $O(z^{-2N})$, and so this series is an asymptotic series.

Theorem 2.2.3 Asymptotic N-term estimate of $r(z)$ *For $N \geq 2$, if we write*

$$r(z) = \sum_{n=0}^{N-1} a_n z^{-2n} + g(z) z^{-2N} \tag{2.2.27}$$

with $a_0 \cdots a_n$ the coefficients of the formal asymptotic series as given by (2.2.15), then there is a unique function g(z) such that r(z) is the hyphoid solution. Furthermore,

$$\lim_{z\to-\infty} g(z) = a_N \qquad \textit{and} \qquad \lim_{z\to-\infty} g'(z) = 0.$$

Proof The derivative of $r(z)$ is

$$r'(z) = -2z^{-3}\sum_{n=0}^{N-2}(n+1)a_{n+1}z^{-2n} + g'(z)z^{-2N} - 2Ng(z)z^{-2N-1}.$$

Expanding using Newton's binomium, we first examine terms in (2.2.24) contributing the highest power of z combined with a certain power of g or g'.

- The term contributing the highest power of z containing g is

  $$z^4 r^2 \sim 2a_0 g z^{-2N+4} \sim 4g z^{-2N+4}.$$

  Higher powers of g can only be found at lower powers of z.

- The term contributing the highest power of z containing g'^1 is

  $$-2r'^2(2z^4) \sim 16a_1 g' z^{-3-2N+4} \sim -32g' z^{-2N+1}.$$

- The term contributing the highest power of z containing g'^2 is

  $$-2r'^2(2z^4) \sim -4g' z^{-4N+4}.$$

- The term contributing the highest power of z containing g'^3 is

  $$r^2 r'^4 \sim -8a_0^2 a_1 g'^3 z^{-3-6N} \sim 64 g'^3 z^{-6N-3}.$$

- The term contributing the highest power of z containing g'^4 is

  $$r^2 r'^4 \sim a_0^2 g'^4 z^{-8N} \sim 4g'^4 z^{-8N}.$$

- The term contributing to the lowest power of z is

  $$r^2 r'^4 \sim g^2 z^{-4N}(2N)^4 g^4 z^{4(-2N-1} \sim 16N^4 g^6 z^{-12N-4}$$

If we multiply our ODE by z^{12N+4} we get a polynomial equation as described in Theorem 2.2.2 (by setting $x = -z$). For $N \geq 2$ the powers of z described above are decreasing, so the coefficients of powers of z greater than $-2N+4+(12N+4)$ will not contain any g or g' and can thus only be combinations of $a_0 \cdots a_{N-1}$. Since $a_0 \cdots a_{N-1}$ were chosen such that the highest order terms of a formal series expansion of the ODE would evaluate to zero, these terms must be zero. Similarly, the coefficient of the term $z^{-2N+4+(12N+4)}$ will, besides the $4g$ part

described above, contain a combination of $a_0 \cdots a_{N-1}$ which we will for now call k. We will later see that $k = -4a_N$. So,

$$\begin{aligned}
N_0 &= -2N + 4 + (12N + 4) & A_{0,N_0}(g) &= 4g + k, \\
N_1 &= -2N + 1 + (12N + 4) & A_{1,N_1}(g) &= -32, \\
N_2 &= -4N + 4 + (12N + 4) & A_{2,N_2}(g) &= -4, \\
N_3 &= -6N - 3 + (12N + 4) & A_{3,N_3}(g) &= 64, \\
N_4 &= -8N + (12N + 4) & A_{4,N_4}(g) &= 4,
\end{aligned}$$

and all the requirements for Theorem 2.2.2 are satisfied. Therefore there exists a solution $g(z)$ such that

$$\lim_{z\to-\infty} g(z) = -\frac{1}{4}k \qquad \text{and} \qquad \lim_{z\to-\infty} g'(z) = 0.$$

If we now repeat the above with higher N we see that clearly $k = -4a_N$. ■

2.2.3 Asymptotics of $z(r)$ as $r \to 2$

For the study of the stability of the hyphoid solution, we are interested in perturbations of this solution near the tip. These are best expressed if we choose r as our coordinate and study variations in the z direction. Therefore we invert $r(z)$ to obtain a description of the z coordinate of the hyphoid solution in terms of r. We do this in two steps, we first show that there is a formal inverse $z(r)$ in terms of powers of $(2-r)^{1/2}$, then we show that this formal series is again an asymptotic expansion.

Lemma 2.2.4 Formal inverse for $r(z)$. *The formal expansion for $r(z)$,*

$$r(z) = 2 - \sum_{m=1}^{\infty} r_{0,1,m} z^{-2m} \qquad \text{as } z \to -\infty, \tag{2.2.28}$$

can be formally inverted to obtain a formal series $z(r)$,

$$z(r) = \sum_{m=0}^{\infty} z_{0,1,m} (2-r)^{m-1/2} \qquad \text{as } r \to 2. \tag{2.2.29}$$

These series satisfy

$$z_n(r_{n+1}(z)) = z + O(z^{-2n-1}) \tag{2.2.30}$$

where z_n and r_n are the functions obtained by truncating the formal series for z and r after the n^{th} term.

Proof If we square the estimate (2.2.30) and multiply by $(2 - r_{n+1}(z))$, we see that we can equivalently prove that

$$z_n(r_{n+1}(z))^2(2 - r_{n+1}(z)) - z^2(2 - r_{n+1}(z)) = O(z^{-2n-2}).$$

Substituting the expansions for z_n and r_{n+1} and substituting $x = z^{-2}$ we obtain

$$f_n(x)^2 - g_n(x) = O(x^{n+1}), \tag{2.2.31}$$

where f_n and g_n are the polynomials defined by

$$f_n(x) = \sum_{i=0}^{n} z_{0,1,j} \left(\sum_{j=1}^{n+1} r_{0,1,j} x^j \right)^i, \qquad \text{and}$$
$$g_n(x) = \sum_{j=0}^{n} r_{0,1,j} x^j.$$

We wish to find values for the coefficients $z_{0,1,j}$ such that the above holds for all n, we will do so using induction.

We first examine the $n = 0$ case,

$$f_0(x)^2 - g_0(x) = z_{0,1,0}^2 - r_{0,1,0}.$$

If we choose the negative root, $z_{0,1,0} = -\sqrt{r_{0,1,0}}$ then (2.2.31) holds and $z(r) \to -\infty$ as expected.

If we examine the $n = 1$ case,

$$\begin{aligned} f_1(x)^2 - g_1(x) &= \left[z_{0,1,0} + z_{0,1,1}(r_{0,1,1}x + r_{0,1,2}x^2) \right]^2 - r_{0,1,1} - r_{0,1,2}x \\ &= 2z_{0,1,0}z_{0,1,1}r_{0,1,1}x - r_{0,1,2}x + O(x^2) \end{aligned}$$

and so if we choose

$$z_{0,1,1} = \frac{r_{0,1,2}}{2z_{0,1,0}r_{0,1,0}} = -\frac{r_{0,1,2}}{2r_{0,1,0}^{(3/2)}},$$

then (2.2.31) holds.

We now assume that $f_k(x)^2 - g_k(x) = O(x^{k+1})$ for some $k \geq 1$. Since both f_k and g_k are polynomials, this implies there is some c_k, (depending only on $z_{0,1,0}$ to $z_{0,1,k}$ and $r_{0,1,1}$ $r_{0,1,k+1}$) such that $f_k(x)^2 - g_k(x) = c_k x^{k+1} + O(x^{k+2})$. Now

$$\begin{aligned} &f_{k+1}(x)^2 - g_{k+1}(x) \\ &\quad = \left[f_k(x) + z_{0,1,k+1} \left(\sum_{j=1}^{k+2} r_{0,1,j} x^j \right)^{k+1} \right]^2 - g_n(x) - r_{0,1,k+2} x^{k+1}, \\ &\quad = c_k x^{k+1} + 2z_{0,1,k+1} f_k(x) \left(\sum_{j=1}^{k+2} r_{0,1,j} x^j \right)^{k+1} - r_{0,1,k+2} x^{k+1} + O(x^{k+2}). \end{aligned}$$

Now

$$f_k(x)\left(\sum_{j=1}^{k+2} r_{0,1,j}x^j\right)^{k+1} = f_k(x)\left(r_{0,1,1}x + \sum_{j=2}^{k+2} r_{0,1,j}x^j\right)^{k+1}$$
$$= z_{0,1,0}r_{0,1,1}^{k+1}x^{k+1} + O(x^{k+2}),$$

and so if we choose

$$z_{0,1,k+1} = \frac{r_{0,1,k+1} - c_k}{2z_{0,1,0}r_{0,1,1}^{k+1}}$$

then

$$f_{k+1}(x)^2 - g_{k+1}(x) = O(x^{k+2}).$$

By induction, (2.2.31) holds for all $n \geq 0$. ■

Lemma 2.2.5 Invertibility of the asymptotic expansion for $r(z)$. *If the formal expansion for $r(z)$ is an asymptotic expansion, i.e. there are constants C_n such that for sufficiently large $|z|$,*

$$|r(z) - r_n(z)| \leq Cz^{-2n-2}, \tag{2.2.32}$$

then the formal inverse of $r(z)$ is also an asymptotic expansion for $z(r)$, specifically there are constants $\tilde{C}_n$ such that for r sufficiently close to 2,

$$|z(r) - z_n(r)| \leq \tilde{C}_n(2-r)^{n+1/2}. \tag{2.2.33}$$

Proof Our proof makes use of the following identity for the difference of whole powers of a and b,

$$a^n - b^n = (a-b)\sum_{i=0}^{n-1} a^{n-1-i}b^i. \tag{2.2.34}$$

For half powers of a and b we modify this as

$$\begin{aligned}(a^{n-1/2} - b^{n-1/2}) &= \frac{a^{2n-1} - b^{2n-1}}{a^{n-1/2} + b^{n-1/2}} \\ &= (a-b)\frac{\sum_{i=0}^{2n-2} a^{2n-2-i}b^i}{a^{n-1/2} + b^{n-1/2}},\end{aligned} \tag{2.2.35}$$

for $n \geq 1$. We will apply this to differences of powers of $(2 - r(z))$ and $(2 - r_{n+1}(z))$. We fix $n \geq 0$ and r. Since $r(z)$ is invertible, there is some z such that $r = r(z)$, if r is chosen sufficiently close to 2 (or equivalently, for $|z|$ sufficiently large) then

$$\begin{aligned}\frac{1}{2}r_{0,1,1}z^{-2} \leq 2 - r(z) &\leq 2r_{0,1,1}z^{-2}, \\ \frac{1}{2}r_{0,1,1}z^{-2} \leq 2 - r_{n+1}(z) &\leq 2r_{0,1,1}z^{-2}.\end{aligned} \tag{2.2.36}$$

Looking at the difference of $-1/2$ powers of $(2-r(z))$ and $(2-r_{n+1}(z))$ we see that

$$\begin{aligned}
&\left|\frac{1}{\sqrt{2-r_{n+1}(z)}}-\frac{1}{\sqrt{2-r(z)}}\right| \\
&\qquad\leq \frac{\sqrt{2-r(z)}-\sqrt{2-r_{n+1}(z)}}{\sqrt{2-r_{n+1}(z)}\sqrt{2-r(z)}} \\
&\qquad\leq \frac{|r_{n+1}(z)-r(z)|}{\sqrt{2-r_{n+1}(z)}\sqrt{2-r(z)}(\sqrt{2-r_{n+1}(z)}+\sqrt{2-r(z)})} \\
&\qquad\leq C\,|z|^{-2(n+2)+3}\leq C\,|z|^{-2n-1}\,.
\end{aligned}$$

Similarly, looking at this difference at higher powers $m-\frac{1}{2}$ for $m\geq 1$ we use (2.2.35) to see that

$$\begin{aligned}
&\left|(2-r_(z))^{m-1/2}-(2-r_{n+1}(z))^{m-1/2}\right| \\
&\qquad\leq |r(z)-r_{n+1}(z)|\,\frac{\sum_{i=0}^{2m-2}(2-r(z))^{2m-2-i}(2-r_{n+1}(z))^{i}}{(2-r(z))^{m-1/2}+(2-r_{n+1}(z))^{m-1/2}} \\
&\qquad\leq |r_{n+1}(z)-r(z)|\,\frac{\sum_{i=0}^{2m-2}(2-r_{n+1}(z))^{2m-2-i}(2-r(z))^{i}}{(2-r_{n+1}(z))^{m-1/2}+(2-r(z))^{m-1/2}} \qquad (2.2.37)\\
&\qquad\leq C\,|z|^{-2(n+2)-2(2m-2)+2(m-1/2)}\leq C\,|z|^{-2n-2m-1}
\end{aligned}$$

We now examine the difference between $z(r)$ and its n-term estimate $z_n(r)$. Substituting $r=r(z)$, and using theorem 2.2.4 we obtain

$$\begin{aligned}
|z(r)-z_n(r)| &\leq |z(r(z))-z_n(r_{n+1}(z))|+|z_n(r_{n+1}(z))-z_n(r(z))| \\
&\leq |z_n(r_{n+1}(z))-z_n(r(z))|+O(z^{-2n-2}) \\
&\leq \sum_{m=0}^{n}|z_{0,1,m}|\cdot\left|(2-r_(z))^{m-1/2}-(2-r_{n+1}(z))^{m-1/2}\right|+O(z^{-2n-2}) \\
&= O(|z|^{-2n-1}),
\end{aligned} \qquad (2.2.38)$$

by the estimates derived above.

By Lemma 2.2.5 we can invert the power series found by Theorem 2.2.3 and calculate asymptotic series for $z(r)$ and its derivatives.

$$\begin{aligned}
z_0(r) &= -\sqrt{2}(2-r)^{-\frac{1}{2}} &&+\frac{5\sqrt{2}}{4}(2-r)^{\frac{1}{2}} &&+\frac{25\sqrt{2}}{32}(2-r)^{\frac{3}{2}} &&+O\left((2-r)^{\frac{5}{2}}\right),\\
z_0'(r) &= -\frac{\sqrt{2}}{2}(2-r)^{-\frac{3}{2}} &&-\frac{5\sqrt{2}}{8}(2-r)^{-\frac{1}{2}} &&+\frac{75\sqrt{2}}{64}(2-r)^{\frac{1}{2}} &&+O\left((2-r)^{\frac{3}{2}}\right),\\
z_0''(r) &= -\frac{3\sqrt{2}}{4}(2-r)^{-\frac{5}{2}} &&-\frac{5\sqrt{2}}{16}(2-r)^{-\frac{3}{2}} &&+\frac{75\sqrt{2}}{128}(2-r)^{-\frac{1}{2}} &&+O\left((2-r)^{\frac{1}{2}}\right).
\end{aligned}$$

Using these we can calculate the asymptotic series for the mean curvature H of the hyphoid solution.

$$H = -\frac{1}{2} - \frac{1}{4}(2-r) - \frac{25}{8}(2-r)^2 + O\left((2-r)^3\right).$$

Using this enables us to calculate the asymptotic series for the coefficients a, b and c of the linearized operator L.

$$\begin{aligned}
a(r) &= -4\sqrt{2}(2-r)^{\frac{9}{2}} &&+ 17\sqrt{2}(2-r)^{\frac{11}{2}} &&+ \frac{57\sqrt{2}}{8}(2-r)^{\frac{13}{2}} &&+O\left((2-r)^{\frac{15}{2}}\right),\\
b(r) &= \sqrt{2}(2-r)^{\frac{3}{2}} &&- \frac{\sqrt{2}}{4}(2-r)^{\frac{5}{2}} &&+ \frac{479\sqrt{2}}{32}(2-r)^{\frac{7}{2}} &&+O\left((2-r)^{\frac{9}{2}}\right),\\
c(r) &= -\frac{3\sqrt{2}}{2}(2-r)^{\frac{1}{2}} &&+ \frac{5\sqrt{2}}{8}(2-r)^{\frac{3}{2}} &&- \frac{89\sqrt{2}}{64}(2-r)^{\frac{5}{2}} &&+O\left((2-r)^{\frac{7}{2}}\right).
\end{aligned}$$

With these we can examine the asymptotic series for the integrating factor Y required to transform L to divergence form, and to calculate the coefficients α and β of this self adjoint operator $\tilde{L}$.

$$Y = (2-r)^{-\frac{63}{32}} e^{\left(\frac{1}{16}(2-r)^{-2} + \frac{1}{2}(2-r)^{-1} + O(2-r)\right)}, \tag{2.2.39}$$

$$\begin{aligned}
\alpha(r) &= 4\sqrt{2}(2-r)^{\frac{9}{2}} &&- 17\sqrt{2}(2-r)^{\frac{11}{2}} &&- \frac{57\sqrt{2}}{8}(2-r)^{\frac{13}{2}} &&+O\left((2-r)^{\frac{15}{2}}\right),\\
\beta(r) &= \frac{\sqrt{2}}{16}(2-r)^{-\frac{3}{2}} &&+ \frac{15\sqrt{2}}{64}(2-r)^{-\frac{1}{2}} &&- \frac{9\sqrt{2}}{512}(2-r)^{\frac{1}{2}} &&+O\left((2-r)^{\frac{3}{2}}\right).
\end{aligned}$$

2.3 Asymptotics in the tip

In order to derive a formal series solution to (2.1.2) we first rewrite this ODE in order to remove square roots.

$$(rz''(r) + z'(r)v^2)^2 d^6 = (rz'(r) - z(r))^2 v^6 r^2, \tag{2.3.1}$$

where,

$$v^2 = 1 + z'(r)^2, \qquad \text{and} \qquad d^2 = r^2 + z(r)^2. \tag{2.3.2}$$

This form of the ODE allows us to derive asymptotic expansions using similar methods as in section 2.3.

2.3.1 Formal asymptotics as $r \to 0$

We introduce a formal series for $z(r)$ and its derivatives. Since $z(-r)$ is also a solution to (2.1.2) and the solution to the ODE is unique, $z(-r) = z(r)$ and so

we expect only even powers of r in the expansions of $z(r)$.

$$\begin{aligned} z(r) &= \sum_{m=0}^{\infty} z_{1,m} r^{2m}, \\ z'(r) &= \sum_{m=1}^{\infty} 2m z_{1,m} r^{2m-1}, \\ z''(r) &= \sum_{m=0}^{\infty} 2(m+1)(2m+1) z_{1,m+1} r^{2m}. \end{aligned} \tag{2.3.3}$$

We can now calculate formal series for powers of d and v,

$$\begin{aligned} v^2 &= \sum_{m=0}^{\infty} v_{2,m} r^{2m}, \quad \text{where} \quad v_{2,0} = 1, \\ &\qquad\qquad \text{and} \quad v_{2,m} = \sum_{i=1}^{m} 4i(m-i+1) z_{1,i} z_{1,m-i+1}, \\ v^4 &= \sum_{m=0}^{\infty} v_{4,m} r^{2m}, \quad \text{where} \quad v_{4,m} = \sum_{i=0}^{m} v_{2,i} v_{2,m-i}, \\ v^6 &= \sum_{m=0}^{\infty} v_{6,m} r^{2m} \quad \text{where} \quad v_{6,m} = \sum_{i=0}^{m} v_{2,i} v_{4,m-i}, \\ d^2 &= \sum_{m=0}^{\infty} d_{2,m} r^{2m}, \quad \text{where} \quad d_{2,0} = z_{1,0}^2, \\ &\qquad\qquad d_{2,1} = 2 z_{1,0} z_{1,1} + 1, \\ &\qquad\qquad \text{and} \quad d_{2,m} = \sum_{i=0}^{m} z_{1,i} z_{1,m-i}, \qquad \text{for } m \geq 2, \\ d^4 &= \sum_{m=0}^{\infty} d_{4,m} r^{2m}, \quad \text{where} \quad d_{4,m} = \sum_{i=0}^{m} d_{2,i} d_{2,m-i}, \\ d^6 &= \sum_{m=0}^{\infty} d_{6,m} r^{2m}, \quad \text{where} \quad d_{6,m} = \sum_{i=0}^{m} d_{2,i} d_{4,m-i}. \end{aligned} \tag{2.3.4}$$

Our notation is chosen in such a way that $v_{n,m}$ is the coefficient before r^{2m} of the n-th power of v. Similarly, $d_{n,m}$ is the coefficient before r^{2m} of the n-th power of d. It is important to note that $v_{n,m}$ and $d_{n,m}$ depend only on $z_{1,0}$ to $z_{1,m}$ and no higher coefficients. We now calculate formal series for various

terms in (2.3.1),

$$\begin{aligned}
rz'(r) - z(r) &= \sum_{m=0}^{\infty} a_{1,m} r^{2m}, \qquad \text{where} \qquad a_{1,m} = (2m-1) z_{1,m} \\
(rz'(r) - z(r))^2 &= \sum_{m=0}^{\infty} a_{2,m} r^{2m}, \qquad \text{where} \qquad a_{2,m} = \sum_{i=0}^{m} a_{1,i} a_{1,m-i} \\
rz''(r) + z'(r)v^2 &= \sum_{m=1}^{\infty} b_{1,m} r^{2m-1} \quad \text{where} \qquad b_{1,m} = 2m(2m-1) z_{1,m} \\
&\qquad\qquad + 2 \sum_{i=1}^{m} i z_{1,i} v_{2,m-i}, \\
(rz''(r) + z'(r)v^2)^2 &= \sum_{m=1}^{\infty} b_{2,m} r^{2m}, \qquad \text{where} \qquad b_{2,m} = \sum_{i=1}^{m} b_{1,i} b_{1,m-i+1}.
\end{aligned} \tag{2.3.5}$$

Here again, $a_{n,m}$ and $b_{n,m}$ depend only $z_{1,0}$ to $z_{1,m}$. Substituting (2.3.5) into (2.3.1) we get

$$\begin{aligned}
\sum_{m=1}^{\infty} \sum_{i=1}^{m} b_{2,i} d_{6,m-i} r^{2m} &= \sum_{m=0}^{\infty} \sum_{i=0}^{m} a_{2,i} v_{6,m-i} r^{2m+2}, \\
&= \sum_{m=1}^{\infty} \sum_{i=0}^{m-1} a_{2,i} v_{6,m-i-1} r^{2m}.
\end{aligned} \tag{2.3.6}$$

We need to choose $z_{1,m}$ such that each coefficient before r^{2m} is equal on the left and right hand sides of this equal, so for each $m \geq 1$,

$$\sum_{i=1}^{m} b_{2,i} d_{6,m-i} = \sum_{i=0}^{m-1} a_{2,i} v_{6,m-i-1}. \tag{2.3.7}$$

Now, the left hand side depends on the coefficients $z_{1,0}$ to $z_{1,m}$ while the right hand side depends only on $z_{1,0}$ to $z_{1,m-1}$. We use this to set up a recurrence relation for $z_{1,m}$ where we choose $z_{1,0} = z_{tip}$. Examining the case $m = 1$ we get,

$$b_{2,1} d_{6,0} = a_{2,0} v_{6,0}, \tag{2.3.8}$$

or

$$16 z_{1,1}^2 z_{tip}^6 = z_{tip}^2. \tag{2.3.9}$$

Since for the hyphoid solution $z < z_{tip}$, we choose the negative root to get

$$z_{1,1} = -\frac{1}{4 z_{tip}^2}. \tag{2.3.10}$$

For $m \geq 2$ we get

$$b_{2,m} d_{6,0} = \sum_{i=0}^{m-1} a_{2,i} v_{6,m-i-1} - \sum_{i=1}^{m-1} b_{2,i} d_{6,m-i}. \tag{2.3.11}$$

Splitting off the first and last terms in the sum for $b_{2,m}$ we obtain

$$2b_{1,1}b_{1,m}d_{6,0} = \sum_{i=0}^{m-1} a_{2,i}v_{6,m-i-1} - \sum_{i=1}^{m-1} b_{2,i}d_{6,m-i} - d_{6,0}\sum_{i=2}^{m-1} b_{1,i}b_{m-i+1}, \quad (2.3.12)$$

now substituting the expression for $b_{1,m}$ in (2.3.5) we get a recursive relation for $z_{1,m}$,

$$\begin{aligned} 2b_{1,1}d_{6,0}\left(2m(2m-1)z_{1,m} + 2\sum_{i=1}^{m-1} iz_{1,i}v_{2,m-i} + 2mz_{1,m}v_{2,0}\right) \\ = \sum_{i=0}^{m-1} a_{2,i}v_{6,m-i-1} - \sum_{i=1}^{m-1} b_{2,i}d_{6,m-i} - d_{6,0}\sum_{i=2}^{m-1} b_{1,i}b_{m-i+1}, \end{aligned} \quad (2.3.13)$$

so,

$$\begin{aligned} z_{1,m} = \frac{1}{4m^2b_{1,1}d_{6,0}}\sum_{i=0}^{m-1} a_{2,i}v_{6,m-i-1} - \frac{1}{4m^2b_{1,1}d_{6,0}}\sum_{i=1}^{m-1} b_{2,i}d_{6,m-i} \\ - \frac{1}{4m^2b_{1,1}}\sum_{i=2}^{m-1} b_{1,i}b_{m-i+1} - \frac{1}{m^2}\sum_{i=1}^{m-1} iz_{1,i}v_{2,m-i}. \end{aligned} \quad (2.3.14)$$

The right hand side of this equation depends only on $z_{1,0}$ to $z_{1,m-1}$ so we can iterate this equation to calculate all coefficients $z_{1,m}$, doing so gives the following formal series solution to (2.1.2),

$$z(r) = z_{tip} - \frac{1}{4}z_{tip}^{-2}r^2 + \left(\frac{3}{32}z_{tip}^{-4} - \frac{1}{16}z_{tip}^{-5} - \frac{1}{64}z_{tip}^{-6}\right)r^4 + \cdots. \quad (2.3.15)$$

2.3.2 Asymptotic expansions as $r \to 0$

2.4 Linear stability of the hyphoid solution

In Section 1.5.1 we linearized around the hyphoid solution $z_1(r)$ by setting $z(r,t) = z_1(r) + w(r,t)$. For small perturbations $w(r,t)$ these perturbations evolve according to

$$\dot{w} + L[w] = 0, \quad (2.4.1)$$

with

$$L[w] = aw'' + bw' + cw, \quad (2.4.2)$$

where a, b and c are functions of r given in (1.5.10).

If we write $w(r,t) = Y(r)\phi(r,t)$ for nonzero $Y(r)$, we can examine the modified operator $\tilde{L}[\phi] = \frac{1}{Y}L[Y\phi]$. With suitable choices of Y, we can make $\tilde{L}$ symmetric in L^2 with either the measure $\mathrm{d}r$ or $r\mathrm{d}r$. We will refer to $\tilde{L}$ as being in 1D or 2D-divergence form respectively. Specifically, if we set

$$\log Y_{1D} = \int \frac{a' - b}{2a}\mathrm{d}r, \quad (2.4.3)$$

then

$$\tilde{L}_{1D}[\phi] = -\frac{\mathrm{d}}{\mathrm{d}r}\left(\alpha_{1D}\frac{\mathrm{d}\phi}{\mathrm{d}r}\right) + \beta_{1D}\phi, \tag{2.4.4}$$

with

$$\begin{aligned}
&\alpha_{1D}(r) = -a(r),\\
&\beta_{1D}(r) = a(r)\left[\frac{\mathrm{d}}{\mathrm{d}r}\left(\frac{a'-b}{2a}\right) + \left(\frac{a'-b}{2a}\right)^2\right] + b(r)\left(\frac{a'-b}{2a}\right) + c(r),
\end{aligned} \tag{2.4.5}$$

and partial integration yields that $\int_0^2 \tilde{L}_{1D}[\phi]\psi \mathrm{d}r = \int_0^2 \psi\tilde{L}_{1D}[\phi]\mathrm{d}r$. Similarly, if we set

$$\log Y_{2D} = \int \frac{a' + \frac{a}{r} - b}{2a}\mathrm{d}r, \tag{2.4.6}$$

then

$$\tilde{L}_{2D}[\phi] = -\frac{1}{r}\frac{\mathrm{d}}{\mathrm{d}r}\left(r\alpha_{2D}\frac{\mathrm{d}\phi}{\mathrm{d}r}\right) + \beta_{2D}\phi, \tag{2.4.7}$$

with

$$\begin{aligned}
&\alpha_{2D}(r) = -a(r),\\
&\beta_{2D}(r) = a(r)\left[\frac{\mathrm{d}}{\mathrm{d}r}\left(\frac{a' + \frac{a}{r} - b}{2a}\right) + \left(\frac{a' + \frac{a}{r} - b}{2a}\right)^2\right] + b(r)\left(\frac{a' + \frac{a}{r} - b}{2a}\right) + c(r),
\end{aligned} \tag{2.4.8}$$

and partial integration yields that $\int_0^2 \tilde{L}_{2D}[\phi]\psi r \mathrm{d}r = \int_0^2 \psi\tilde{L}_{2D}[\phi] r\mathrm{d}r$.

2.4.1 Eigenfunctions of $\tilde{L}[\phi]$ in 1D-divergence form

Eigenfunctions ϕ_λ of $\tilde{L}[\phi]$ are solutions of the equation

$$\tilde{L}[\phi_\lambda] = \lambda\phi_\lambda \tag{2.4.9}$$

where $\frac{\partial}{\partial r}\phi_\lambda = 0$ at $r = 0$ and a second boundary condition at the asymptote $r \to 2$ still has to be determined by exceptional behaviour of the solution to (2.4.9) near this asymptote. We change coordinates such that

$$\frac{\partial}{\partial\xi} = \alpha\frac{\partial}{\partial r} \tag{2.4.10}$$

so

$$\begin{aligned}
\xi(r) = \int_0^r \frac{1}{\alpha(s)}\mathrm{d}s \qquad &= \frac{\sqrt{2}}{28}(2-r)^{-\frac{7}{2}} \qquad &&+\frac{17\sqrt{2}}{80}(2-r)^{-\frac{5}{2}}\\
&+\frac{635\sqrt{2}}{384}(2-r)^{-\frac{3}{2}} \qquad &&+O\left((2-r)^{-\frac{1}{2}}\right).
\end{aligned}$$

Inverting this we get an asymptotic series at large ξ for $r(\xi)$, so we can define $\alpha(\xi) = \alpha(r(\xi))$ and $\beta(\xi) = \beta(r(\xi))$ and calculate their asymptotic series.

$$\begin{aligned}
2 - r(\xi) &= 28^{-\frac{2}{7}} 2^{\frac{1}{7}} \xi^{-\frac{2}{7}} + \frac{17}{5} 28^{-\frac{4}{7}} 2^{-\frac{5}{7}} \xi^{-\frac{4}{7}} + \frac{67}{75} 28^{\frac{1}{7}} 2^{-\frac{4}{7}} \xi^{-\frac{6}{7}} + O(\xi^{-\frac{8}{7}}), \\
\alpha(\xi) &= \frac{2^{\frac{4}{7}} 7^{\frac{5}{7}}}{49} \xi^{-\frac{9}{7}} + \frac{2^{\frac{1}{7}} 7^{\frac{3}{7}} 17}{245} \xi^{-\frac{11}{7}} - \frac{2^{\frac{5}{7}} 7^{\frac{1}{7}} 57}{3136} \xi^{-\frac{13}{7}} + O(\xi^{-\frac{13}{7}}), \\
\beta(\xi) &= \frac{2^{\frac{1}{7}} 7^{\frac{3}{7}}}{8} \xi^{\frac{3}{7}} + \frac{2^{\frac{5}{7}} 7^{\frac{1}{7}} 3}{40} \xi^{\frac{1}{7}} - \frac{2^{\frac{2}{7}} 7^{\frac{6}{7}} 1681}{11200} \xi^{-\frac{1}{7}} + O(\xi^{-\frac{3}{7}}).
\end{aligned}$$

By multiplying by α, (2.4.9) transforms to

$$\frac{\partial^2}{\partial \xi^2} \phi_\lambda - \gamma(\xi) \phi_\lambda = 0, \tag{2.4.11}$$

with $\gamma(\xi) = \alpha(\xi)(\beta(\xi) - \lambda)$ having the following asymptotic series

$$\gamma(\xi) = \frac{2^{\frac{5}{7}} 7^{\frac{1}{7}}}{56} \xi^{-\frac{6}{7}} + \frac{2^{\frac{2}{7}} 7^{\frac{6}{7}} 23}{1960} \xi^{-\frac{8}{7}} - \frac{2^{\frac{4}{7}} 7^{\frac{5}{7}} \lambda}{49} \xi^{-\frac{9}{7}} + O(\xi^{-\frac{10}{7}}).$$

Note that while α and β have asymptotic expansions in powers of $\xi^{\frac{2}{7}}$, the expansion of γ is in powers of $\xi^{\frac{1}{7}}$. We will now examine the asymptotic behaviour of general solutions to (2.4.11). Setting $\phi_\lambda = e^{\upsilon}$ and dividing out the e^{υ}, (2.4.11) transforms to

$$\frac{\partial^2}{\partial \xi^2} \upsilon = \gamma(\xi) - (\frac{\partial}{\partial \xi} \upsilon)^2, \tag{2.4.12}$$

after setting $\psi = \frac{\partial}{\partial \xi} \upsilon$ we get the following first order ODE

$$\frac{\partial}{\partial \xi} \psi = \alpha(\xi)(\beta(\xi) - \lambda) - \psi^2. \tag{2.4.13}$$

Numerical integrations, with $\gamma(\xi) = c_1 \xi^{-\frac{6}{7}} - c_2 \lambda \xi^{-\frac{9}{7}}$, c_1 and c_2 appropriate constants taken from the asymptotic expansion of γ and $\lambda = 1$, shown in Figure 2.1, suggest that this equation has many solutions for which in the asymptote $\psi(\xi) \simeq \sqrt{\alpha(\xi)\beta(\xi)}$ and a single solution for which in the asymptote $\psi(\xi) \simeq -\sqrt{\alpha(\xi)\beta(\xi)}$. We will define ψ_0 to be this asymptote.

$$\psi_0(\xi) = -\sqrt{\alpha(\xi)\beta(\xi)} \tag{2.4.14}$$

2.4.2 Eigenfunctions for $\lambda \in \mathbb{C}$

To prove that (2.4.13) has a unique solution ψ_* with the same asymptotic behaviour as ψ_0 we will transform this ODE to an integral equation. We have

$$\begin{aligned}
\frac{\partial}{\partial \xi} \psi &= \alpha(\beta - \lambda) - \psi^2 \\
&= \alpha(\beta - \lambda) - (\psi - \psi_0)^2 - 2\psi_0 \psi + \psi_0^2,
\end{aligned}$$

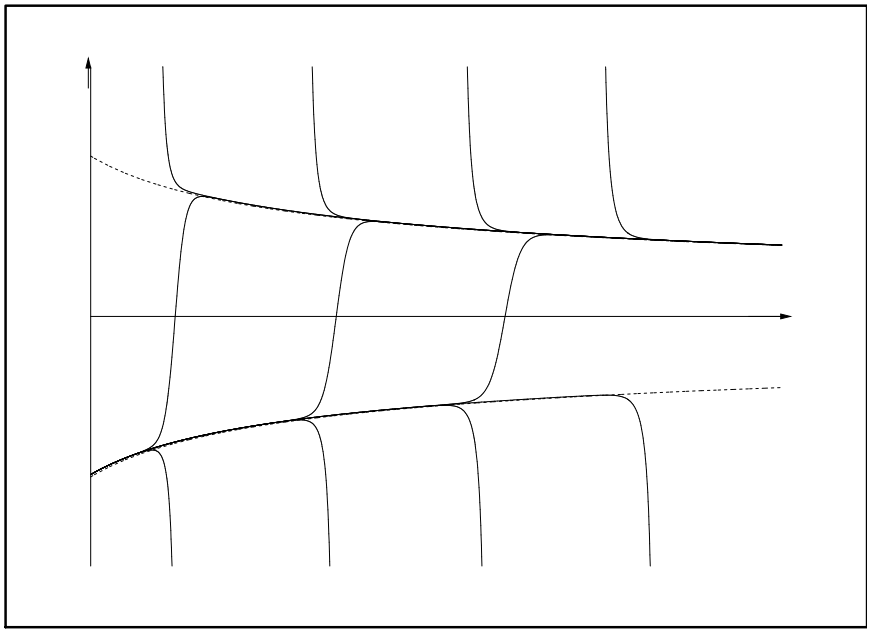

Figure 2.1: Solid lines: solutions to (2.4.13) with $\gamma(\xi) = c_1\xi^{-\frac{6}{7}} - c_2\lambda\xi^{-\frac{9}{7}}$ and $\lambda = 1$. Dashed line: the curve $\psi^2 = \gamma(\xi)$.

so

$$\frac{\partial}{\partial \xi}\psi + 2\psi_0\psi = 2\psi_0^2 - \alpha\lambda - (\psi - \psi_0)^2. \tag{2.4.15}$$

Define ζ to be a primitive of $-\psi_0$

$$\frac{\partial}{\partial \xi}\zeta = -\psi_0,$$
$$\zeta(\xi) = -\int_{\xi_0}^{\xi} \psi_0(s)\mathrm{d}s.$$

Multiplying by $e^{-2\zeta}$ and integrating from ξ to infinity gives

$$\psi(\xi) = -e^{2\zeta(\xi)} \int_{\xi}^{\infty} e^{-2\zeta(s)} \left[2\psi_0(s)^2 - \alpha(s)\lambda - (\psi(s) - \psi_0(s))^2\right] \mathrm{d}s \tag{2.4.16}$$
$$= \Phi(\psi, \lambda)(\xi). \tag{2.4.17}$$

Before continuing our analysis of the operator $\Phi(\cdot, \lambda)(\xi)$ we will provide some estimates of terms within the integral equation.

Lemma 2.4.1 Estimate of the integral over $e^{-2\zeta}\psi_0^2$.

For some sufficiently large ξ_0 the following inequality holds for all $\xi > \xi_0$

$$0 < -\frac{e^{2\zeta(\xi)}}{\psi_0(\xi)} \int_{\xi}^{\infty} e^{-2\zeta(s)}\psi_0(s)^2\mathrm{d}s < \frac{1}{2}. \tag{2.4.18}$$

Proof Since ψ_0 is negative and all other terms in the integral are positive it is clear that the integral itself must be positive. To establish the upper bound we integrate by parts

$$\begin{aligned} & -\frac{e^{2\zeta(\xi)}}{\psi_0(\xi)} \int_{\xi}^{\infty} e^{-2\zeta(s)}\psi_0(s)^2\mathrm{d}s \\ = & -\frac{1}{2}\frac{e^{2\zeta(\xi)}}{\psi_0(\xi)} \int_{\xi}^{\infty} \frac{\mathrm{d}}{\mathrm{d}s}\left(e^{-2\zeta(s)}\right)\psi_0(s)\mathrm{d}s \\ = & \frac{1}{2} + \frac{1}{2}\frac{e^{2\zeta(\xi)}}{\psi_0} \int_{\xi}^{\infty} e^{-2\zeta(s)}\frac{\mathrm{d}}{\mathrm{d}s}\psi_0\mathrm{d}s \end{aligned}$$

Since $\psi_0(\xi)$ is negative and increasing and all other terms in the integral on the right hand side are positive, the inequality is proven. ■

Lemma 2.4.2 Estimate of the integral over $e^{-2\zeta}\frac{\mathrm{d}}{\mathrm{d}s}\psi_0$

$$\lim_{\xi\to\infty} -\frac{e^{2\zeta(\xi)}}{\psi_0(\xi)} \int_{\xi}^{\infty} e^{-2\zeta(s)}\frac{\mathrm{d}}{\mathrm{d}s}\psi_0(s)\mathrm{d}s = 0 \tag{2.4.19}$$

Proof Since ψ_0 is negative and all other terms are positive it is clear that the term in the limit is positive. Since $\psi_0(\xi)^2 = \alpha(\xi)\beta(\xi) \sim \xi^{-\frac{6}{7}}$, $\frac{\mathrm{d}}{\mathrm{d}\xi}\psi_0(\xi) \sim \xi^{-\frac{10}{7}}$, so

given $\epsilon > 0$ finite, we can choose a ξ_0 such that for all $\xi > \xi_0$, $\frac{\mathrm{d}}{\mathrm{d}\xi}\psi_0 < \epsilon\alpha(\xi)\beta(\xi)$. So, applying Lemma 2.4.1,

$$\begin{aligned}
&- \frac{e^{2\zeta(\xi)}}{\psi_0(\xi)} \int_\xi^\infty e^{-2\zeta(s)} \frac{\mathrm{d}}{\mathrm{d}s}\psi_0(s)\mathrm{d}s \\
&< -\epsilon \frac{e^{2\zeta(\xi)}}{\psi_0(\xi)} \int_\xi^\infty e^{-2\zeta(s)} \psi_0(s)^2 \mathrm{d}s \\
&< \frac{1}{2}\epsilon.
\end{aligned}$$

■

Lemma 2.4.3 Estimate of the integral over $e^{-2\zeta}\alpha|\lambda|$.

$$\lim_{\xi\to\infty} -\frac{e^{2\zeta(\xi)}}{\psi_0(\xi)} \int_\xi^\infty e^{-2\zeta(s)} \alpha(s)|\lambda|\mathrm{d}s = 0 \tag{2.4.20}$$

Proof Since ψ_0 is negative and all other terms are positive it is clear that the term in the limit is positive. Since $\beta \to \infty$ we can choose ξ_0 sufficiently large such that for $\xi > \xi_0$, $|\lambda| < \epsilon\beta(\xi)$, so $\alpha(\xi)|\lambda| < \epsilon\psi_0(\xi)^2$. Applying Lemma 2.4.1 we get

$$\begin{aligned}
&- \frac{e^{2\zeta(\xi)}}{\psi_0(\xi)} \int_\xi^\infty e^{-2\zeta(s)} \alpha(s)|\lambda|\mathrm{d}s \\
&< -\epsilon \frac{e^{2\zeta(\xi)}}{\psi_0(\xi)} \int_\xi^\infty e^{-2\zeta(s)} \psi_0(s)^2 \mathrm{d}s \\
&< \frac{1}{2}\epsilon
\end{aligned}$$

■

We now consider the Banach space $(X, ||\cdot||)$ defined by the norm

$$||\psi|| = \sup_{\xi>\xi_0} \left| \frac{\psi(\xi)}{\psi_0(\xi)} \right|, \tag{2.4.21}$$

for some sufficiently large ξ_0 such that Lemmas 2.4.1, 2.4.2 and 2.4.3 can be applied.

Lemma 2.4.4 *The image of X under $\Phi(\cdot,\lambda)$ lies in X.*

Proof We will show that for $\psi \in X$ the norm of $\Phi(\psi,\lambda)$ is finite.

$$\begin{aligned}
||\Phi(\psi,\lambda)|| &= \sup_{\xi>\xi_0} \left| \frac{e^{2\zeta(\xi)}}{\psi_0(\xi)} \int_\xi^\infty e^{-2\zeta(s)} \left(2\psi_0(s)^2 - \alpha(s)\lambda - (\psi(s)-\psi_0(s))^2\right) \mathrm{d}s \right| \\
&\leq \sup_{\xi>\xi_0} -\frac{e^{2\zeta(\xi)}}{\psi_0(\xi)} \int_\xi^\infty e^{-2\zeta(s)} \left(2\psi_0(s)^2 + \alpha(s)|\lambda| + (|\psi(s)| + |\psi_0(s)|)^2\right) \mathrm{d}s \\
&\leq \sup_{\xi>\xi_0} -\frac{e^{2\zeta(\xi)}}{\psi_0(\xi)} \int_\xi^\infty e^{-2\zeta(s)} \left(2\psi_0(s)^2 + \alpha(s)|\lambda| + \psi_0(s)^2(||\psi|| + 1)^2\right) \mathrm{d}s
\end{aligned}$$

By Lemmas 2.4.3 we can choose ξ_0 sufficiently large that the term $\alpha(s)|\lambda|$ can be neglected. Applying Lemma 2.4.1 we get

$$||\Phi(\psi,\lambda)|| \leq \frac{1}{2}(2+(||\psi||+1)^2)+\frac{1}{2}\epsilon < \infty, \tag{2.4.22}$$

since all terms are finite. ■

We now examine $\Phi(\cdot,\lambda)$ in an closed ball B_R of radius $R<1$ around ψ_0.

$$B_R = \{\psi : ||\psi-\psi_0|| \leq R\} \tag{2.4.23}$$

Lemma 2.4.5 *There is an R such that the image under $\Phi(\cdot,\lambda)$ of B_R is a subset of B_R.*

Proof We estimate the distance of $\Phi(\psi,\lambda)$ to ψ_0 for $\psi \in B_R$. First note that

$$\begin{aligned}
1 &= -\frac{e^{2\zeta(\xi)}}{\psi_0(\xi)}\int_\xi^\infty \frac{\mathrm{d}}{\mathrm{d}s}\left(e^{-2\zeta(s)}\psi_0(s)\right)\mathrm{d}s \\
&= -\frac{e^{2\zeta(\xi)}}{\psi_0(\xi)}\int_\xi^\infty e^{-2\zeta(s)}\left(\frac{\mathrm{d}}{\mathrm{d}s}\psi_0(s)+2\psi_0(s)^2\right)\mathrm{d}s.
\end{aligned}$$

So

$$\begin{aligned}
&||\psi_0-\Phi(\psi,\lambda)|| \\
&= \sup_{\xi>\xi_0}\left|1+\frac{e^{2\zeta(\xi)}}{\psi_0(\xi)}\int_\xi^\infty e^{-2\zeta(s)}\left(2\psi_0(s)^2-\alpha(s)\lambda-(\psi(s)\psi_0(s))^2\right)\mathrm{d}s\right| \\
&= \sup_{\xi>\xi_0}\left|\frac{e^{2\zeta(\xi)}}{\psi_0(\xi)}\int_\xi^\infty e^{-2\zeta(s)}\left(-\frac{\mathrm{d}}{\mathrm{d}s}\psi_0(s)-\alpha(s)\lambda-(\psi(s)-\psi_0(s))^2\right)\mathrm{d}s\right| \\
&\leq \sup_{\xi>\xi_0}-\frac{e^{2\zeta(\xi)}}{\psi_0(\xi)}\int_\xi^\infty e^{-2\zeta(s)}\left(\frac{\mathrm{d}}{\mathrm{d}s}\psi_0(s)+\alpha(s)|\lambda|+|\psi(s)-\psi_0(s)|^2\right)\mathrm{d}s \\
&\leq \sup_{\xi>\xi_0}-\frac{e^{2\zeta(\xi)}}{\psi_0(\xi)}\int_\xi^\infty e^{-2\zeta(s)}\left(\frac{\mathrm{d}}{\mathrm{d}s}\psi_0(s)+\alpha(s)|\lambda|+R^2\psi_0(s)^2\right)\mathrm{d}s.
\end{aligned}$$

By Lemmas 2.4.2 and 2.4.3 we can choose ξ_0 sufficiently large such that the terms $\frac{\mathrm{d}}{\mathrm{d}s}\psi_0(s)$ and $\alpha(s)|\lambda|$ can be neglected. Using Lemma 2.4.1 we get

$$\begin{aligned}
||\psi_0-\Phi(\psi,\lambda)|| &< \frac{1}{2}R^2 - \sup_{\xi>\xi_0}\frac{e^{2\zeta(\xi)}}{\psi_0(\xi)}\int_\xi^\infty e^{-2\zeta(s)}\left(\frac{\mathrm{d}}{\mathrm{d}s}\psi_0+\alpha(s)|\lambda|\right)\mathrm{d}s \\
&< \frac{1}{2}R^2.
\end{aligned}$$

Since $R<1$, $\frac{1}{2}R^2 < R$ proving the lemma. ■

Lemma 2.4.6 Differentiability of $\Phi(\psi,\lambda)$.

1. *$\Phi(\psi, \lambda)$ is differentiable in λ, this derivative lies in X and is given by*

$$\frac{\partial \Phi}{\partial \lambda} = \Phi((1+\sqrt{2})\psi, 1). \tag{2.4.24}$$

2. *For $\psi \in B_R$, $\Phi(\psi, \lambda)$ is differentiable in ψ and the derivative is given by*

$$\frac{\partial \Phi}{\partial \psi}(\psi)[h](\xi) = -2e^{2\zeta(\xi)} \int_{\xi}^{\infty} e^{-2\zeta(s)}(\psi(s) - \psi_0(s))h(s)\mathrm{d}s. \tag{2.4.25}$$

3. *$\Phi(\psi, \lambda)$ is a contraction on B_R, for $\psi_1, \psi_2 \in B_R$, $||\Phi(\psi_2, \lambda) - \Phi(\psi_1, \lambda)|| < R||\psi_2 - \psi_1||$.*

Proof 1. Rewriting (2.4.16) one sees that

$$\Phi(\psi, \lambda) = \Phi(\psi, 0) + \lambda\Phi((1+\sqrt{2})\psi, 1), \tag{2.4.26}$$

so $\Phi(\psi, \lambda)$ is affine linear in λ and by Lemma 2.4.4 its derivative lies in X.

2. For each $\psi \in B_R$ consider the linear operator $A(\psi)[h]$ acting on $h \in X$ defined by

$$A(\psi)[h](\xi) = -2e^{2\zeta(\xi)} \int_{\xi}^{\infty} e^{-2\zeta(s)}(\psi(s) - \psi_0(s))h(s)\mathrm{d}s. \tag{2.4.27}$$

One sees that A is a bounded linear operator from X to X with operator norm less than or equal to R since,

$$\begin{aligned} ||A(\psi)[h]|| &= \left| \sup_{\xi > \xi_0} 2\frac{e^{2\zeta(\xi)}}{\psi_0(\xi)} \int_{\xi}^{\infty} e^{-2\zeta(s)}(\psi(s) - \psi_0(s))h(s)\mathrm{d}s \right| \\ &\leq 2R||h|| \sup_{\xi > \xi_0} -\frac{e^{2\zeta(\xi)}}{\psi_0(\xi)} \int_{\xi}^{\infty} e^{-2\zeta(s)}\psi_0(s)^2\mathrm{d}s \\ &< R||h||. \end{aligned}$$

Furthermore, $A(\psi)$ is the Fréchet derivative of $\Phi(\psi, \lambda)$ since

$$\begin{aligned} &\lim_{h\to 0} \frac{||\Phi(\psi + h, \lambda) - \Phi(\psi, \lambda) - A(\psi)[h]||}{||h||} \\ &= \lim_{h\to 0} \frac{\sup_{\xi > \xi_0} \left| \frac{e^{2\zeta(\xi)}}{\psi_0(\xi)} \int_{\xi}^{\infty} e^{-2\zeta(s)} h(s)^2 \mathrm{d}s \right|}{||h||} \\ &= \lim_{h\to 0} \frac{||h||^2 \sup_{\xi > \xi_0} \left| \frac{e^{2\zeta(\xi)}}{\psi_0(\xi)} \int_{\xi}^{\infty} e^{-2\zeta(s)} \psi_0(s)^2 \mathrm{d}s \right|}{||h||} \\ &= \lim_{h\to 0} \frac{||h||^2 \cdot \frac{1}{2}||\Phi(\psi_0, 0)||}{||h||} = 0, \end{aligned}$$

since $||\Phi(\psi_0, 0)||$ is finite.

3. All terms other than the terms containing ψ_2 and ψ_1 cancel in the integrals

$$\begin{aligned}
&\Phi(\psi_2,\lambda)-\Phi(\psi_1,\lambda)\\
=&e^{2\zeta(\xi)}\int_\xi^\infty e^{-2\zeta(s)}\left((\psi_2(s)-\psi_0(s))^2-(\psi_1(s)-\psi_0(s))^2\right)\mathrm{d}s\\
=&e^{2\zeta(\xi)}\int_\xi^\infty e^{-2\zeta(s)}(\psi_2(s)+\psi_1(s)-2\psi_0(s))\cdot(\psi_2(s)-\psi_1(s))\mathrm{d}s\\
=&A\left(\frac{\psi_2+\psi_1}{2}\right)[\psi_2-\psi_1].
\end{aligned}$$

Since B_R is concave, $\frac{1}{2}(\psi_2+\psi_1)\in B_R$ and

$$||\Phi(\psi_2,\lambda)-\Phi(\psi_1,\lambda)||=\left|\left|A\left(\frac{\psi_2+\psi_1}{2}\right)[\psi_2-\psi_1]\right|\right|<R||\psi_2-\psi_1||.$$

■

Theorem 2.4.7 Existence, uniqueness and analyticity of the exceptional solution.

There exists a unique solution $\psi_*\in B_R$ to (2.4.13), this solution is analytic in λ.

Proof By Lemma 2.4.4 and point 3 of Lemma 2.4.6, $\Phi(\cdot,\lambda)$ maps from B_R to B_R and is a contraction on B_R. Therefore, by the Banach fixed point theorem, this map has a unique fixed point ψ_* which solves (2.4.13). Moreover, this solution is the limit of the following sequence:

$$\begin{aligned}
\psi_0&=-\sqrt{\alpha\beta},\\
\psi_{n+1}&=\Phi(\psi_n,\lambda).
\end{aligned}$$

By Lemma 2.4.6 we also know that $\Phi(\lambda,\psi)$ is differentiable in λ and ψ and that the operator norm of the derivative to ψ of $\Phi(\lambda,\psi)$ is less than one. Since, ψ_* is the solution of the equation $\psi-\Phi(\lambda,\psi)=0$, by the implicit function theorem ψ_* is differentiable, and thus analytic, in λ. ■

Corollary 2.4.8 Asymptotic behaviour of the exceptional solution.

The asymptotic behaviour of the exceptional solution ψ_* is the same as the asymptotic behaviour of ψ_0.

Proof Since $\psi_*\in B_R$ and $R<1$ we know that, for all $\xi>\xi_0$

$$\left|\frac{\psi_*(\xi)}{\psi_0(\xi)}\right|<R. \tag{2.4.28}$$

So,

$$-R-1<\frac{\psi_*(\xi)}{\psi_0(\xi)}<R-1<0, \tag{2.4.29}$$

and $\frac{\psi_*(\xi)}{\sqrt{\alpha(\xi)\beta(\xi)}}$ is finite and stays away from zero in the asymptote. ■

2.4.3 Asymptotics of the eigenfunctions

Now that we've shown that the ODE (2.4.13) for the eigenfunctions has an unique exceptional solution, we can examine a formal asymptotic series for this solution. Since we expect the first term of the expansion for ψ_* to be equal to the first term of ψ_0 we substitute the following ansatz

$$\psi_* = \xi^{-\frac{3}{7}} \left(\sum_{n=0}^{n_{max}} \psi_{*n} \xi^{-\frac{n}{7}} \right), \tag{2.4.30}$$

Setting $\psi_{*0} = -\frac{2^{\frac{6}{7}} 7^{\frac{4}{7}}}{28}$, the first coefficient of ψ_0, allows us to isolate each power of ξ and calculate each coefficient ψ_{*n} resulting in the following expansion

$$\psi_* = -\frac{2^{\frac{6}{7}} 7^{\frac{4}{7}}}{28} \xi^{-\frac{3}{7}} - \frac{2^{\frac{3}{7}} 7^{\frac{2}{7}} 23}{280} \xi^{-\frac{5}{7}} + \frac{2^{\frac{5}{7}} 7^{\frac{1}{7}} \lambda}{7} \xi^{-\frac{6}{7}} + O(\xi^{-\frac{7}{7}}), \tag{2.4.31}$$

and so,

$$\begin{aligned} \phi = e^{v} = e^{\int \psi_*} \quad &= e^{-\frac{2^{\frac{6}{7}} 7^{\frac{4}{7}}}{16} \xi^{\frac{4}{7}} - \frac{2^{\frac{3}{7}} 7^{\frac{2}{7}} 23}{80} \xi^{\frac{2}{7}} + 2^{\frac{5}{7}} 7^{\frac{1}{7}} \lambda \xi^{\frac{1}{7}} - \frac{15}{112} \ln \xi + O\left(\xi^{-\frac{1}{7}}\right)} \\ &= (2-r)^{-\frac{15}{32}} e^{-\frac{1}{16}(2-r)^{-2} - \frac{1}{2}(2-r)^{-1} + \sqrt{2}\lambda(2-r)^{-\frac{1}{2}} + O\left(\sqrt{2-r}\right)}. \end{aligned}$$

The generic solutions of (2.4.9) which do not converge to ψ_0 have opposite signs in the first few terms of their expansions and so increase exponentially for all λ as $r \to 2$. For the exceptional solution $w(r) = Y(r)\phi$, if we combine the asymptotic expansion for Y given in (2.2.39) with the expansion given above we see that the first two terms of the expansion cancel out, resulting in the following asymptotic expansion for the eigenfunctions.

$$w = (2-r)^{-\frac{3}{2}} e^{\sqrt{2}\lambda(2-r)^{-\frac{1}{2}} + O(\sqrt{2-r})}. \tag{2.4.32}$$

For positive λ these eigenfunctions increase exponentially as $r \to 2$.

2.5 Eigenfunctions of $\tilde{L}[\phi]$ in 2D-divergence form

We now show that $\tilde{L}$ has eigenfunctions and eigenvalues in V. Eigenfunctions ϕ_λ of $\tilde{L}[\phi]$ are solutions of the equation

$$\tilde{L}[\phi_\lambda] = \lambda \phi_\lambda \tag{2.5.1}$$

where $\frac{\partial}{\partial r}\phi_\lambda = 0$ at $r = 0$ and the behaviour in the asymptote is such that $\phi_\lambda \in V$. We define a new coordinate x,

$$x = \frac{1}{\sqrt{2-r}} \qquad r(x) = 2 - x^{-2} \qquad \frac{\partial}{\partial r} = \frac{\partial x}{\partial r}\frac{\partial}{\partial x} = \frac{1}{2}x^3 \frac{\partial}{\partial x}, \tag{2.5.2}$$

the asymptotic behaviour now lies at $x \to \infty$ and (2.5.1) can now be written as

$$-\frac{1}{r}\frac{\partial}{\partial r}\left(r\alpha(r)\frac{\partial}{\partial r}\phi\right) + (\beta(r) - \lambda) =$$
$$-\frac{x^3}{4r(x)}\frac{\partial}{\partial x}\left(r(x)\alpha(x)x^3\frac{\partial\phi}{\partial x}\right) + (\beta(r) - \lambda) =$$
$$A(x)\frac{\partial^2\phi}{\partial x^2} + B(x)\frac{\partial\phi}{\partial x} + C(x) = 0,$$

where

$$\begin{aligned}
A(x) &= -\frac{1}{4}\alpha(x)x^6 &&= -\frac{\sqrt{2}}{x^3} + \frac{17}{4}\frac{\sqrt{2}}{x^5} + \frac{57}{32}\frac{\sqrt{2}}{x^7} + O\left(x^{-9}\right), \\
B(x) &= -\frac{x^3}{4r(x)}\frac{\partial}{\partial x}\left(r(x)\alpha(x)x^3\right) &&= 6\frac{\sqrt{2}}{x^4} - 35\frac{\sqrt{2}}{x^6} - \frac{225}{16}\frac{\sqrt{2}}{x^8} + O\left(x^{-10}\right), \\
C(x) &= \beta(x) - \lambda &&= \frac{\sqrt{2}}{16}x^3 + \frac{15}{64}\sqrt{2}x - \lambda + O\left(x^{-1}\right).
\end{aligned}$$

We now substitute $\psi = \frac{\phi'}{\phi}$ to transform our second order ODE into a nonlinear first order ODE

$$\psi' + \psi^2 + P(x)\psi + Q(x) = 0 \tag{2.5.3}$$

where

$$\begin{aligned}
P(x) &= \frac{B(x)}{A(x)} &&= -6x^{-1} + \frac{19}{2}x^{-3} + \frac{175}{4}x^{-5} + O\left(x^{-7}\right), \\
Q(x) &= \frac{C(x)}{A(x)} &&= -\frac{1}{16}x^6 - \frac{1}{2}x^4 + \frac{\sqrt{2}}{2}\lambda x^3 + O\left(x^2\right).
\end{aligned}$$

Formally we can solve this ODE to get two possible series for $\psi(x)$

$$\psi_1(x) = -\frac{1}{4}x^3 - x + \sqrt{2}\lambda - \frac{15}{16}x^{-1} + \frac{\sqrt{2}}{4}\lambda x^{-2} + O\left(x^{-3}\right), \tag{2.5.4}$$
$$\psi_2(x) = \frac{1}{4}x^3 + x - \sqrt{2}\lambda + \frac{63}{16}x^{-1} - \frac{\sqrt{2}}{4}\lambda x^{-2} + O\left(x^{-3}\right). \tag{2.5.5}$$

Transforming these back to the corresponding $\phi = \exp(\int \psi)$ the general solution to (2.5.1) becomes $\phi_\lambda = C_1\phi_1 + C_2\phi_2$. Now, since ϕ_2 increases exponentially as $r \to 2$ and so $\phi_2 \notin V$, while ϕ_1 decreases exponentially and $\phi_1 \in V$, we formally expect an eigenfunction, unique modulo a multiplicative constant, corresponding to $C_2 = 0$, in V.

In order to prove that (2.5.1) has a unique solution with an asymptotic expansion given by our formal series, we use the following theorem by de Bruijn [4].

Theorem 2.5.1 de Bruijn [4], ¶9.3 An unstable case.

Consider the equation

$$t^{-k}\rho'(t) = \alpha(t) + \beta(t)\rho(t) + \gamma(t)\rho^2(t) \tag{2.5.6}$$

where α, β and γ have asymptotic developments

$$\begin{aligned}
\alpha(t) &= a_0 + a_1 t^{-1} + a_2 t^{-2} + \cdots && (t \to \infty),\\
\beta(t) &= b_0 + b_1 t^{-1} + b_2 t^{-2} + \cdots && (t \to \infty),\\
\gamma(t) &= c_0 + c_1 t^{-1} + c_2 t^{-2} + \cdots && (t \to \infty).
\end{aligned}$$

Assume that $b_0 > 0$ and $c_0 = 0$, then there is a formal series $r_0 + r_1 t^{-1} + r_2 t^{-2} + \cdots$ which formally satisfies the equation. There is only one solution having this series as its development, and this one is the only bounded solution (i.e. the only solution which is $O(1)$ when $t \to \infty$.)

Now, in our case $P(x) = O(x^{-1})$ and $Q(x) = O(x^6)$ corresponding to $b_0 = 0$ and $c_0 \neq 0$ so we cannot use this theorem immediately, however if we substitute

$$\psi(x) = \psi_0(x) + \tilde{\psi}(x) \tag{2.5.7}$$

where $\psi_0(x) = -\frac{1}{4}x^3 - x + \sqrt{2}\lambda$ is the first few terms of our formal series for ψ we get

$$\tilde{\psi}' + \tilde{\psi}^2 + \tilde{P}(x)\tilde{\psi} + \tilde{Q}(x) = 0 \tag{2.5.8}$$

where

$$\begin{aligned}
\tilde{P}(x) &= -\frac{1}{2}x^3 - 2x + 2\lambda\sqrt{2} + O\left(x^{-1}\right),\\
\tilde{Q}(x) &= -\frac{15}{32}x^2 + \frac{\sqrt{2}\lambda}{8}x + O\left(1\right).
\end{aligned}$$

if we now divide by x^3 our ODE is in the required form and we know that for every λ there is a unique solution to (2.5.1) in V. Similarly, using the theorem found in de Bruijn [4] ¶9.2, one can show that there is a class of solutions with asymptotic expansions (2.5.5) which do not lie in V. Eigenfunctions now are those solutions ϕ_λ for which $\phi'_\lambda(0) = 0$.

2.5.1 Asymptotics of the eigenfunctions

Since $w(r) = Y(r)\phi$, if we combine the asymptotic expansions of ϕ (2.5.4) and Y given in (2.2.39) with the expansion given above we see that the first two terms of the expansion cancel out, resulting in the following asymptotic expansion for the eigenfunctions w.

$$w = (2-r)^{-\frac{3}{2}} e^{\sqrt{2}\lambda(2-r)^{-\frac{1}{2}} + O(\sqrt{2-r})}. \tag{2.5.9}$$

For positive (stable) λ these eigenfunctions increase exponentially as $r \to 2$.

Chapter 3

Existence of solutions to the Diffusive VSC model

Abstract

We prove existence of classical solutions to the so-called diffusive Vesicle Supply Centre (VSC) model describing the growth of fungal hyphae. It is supposed in this model that the local expansion of the cell wall is caused by a flux of vesicles into the wall and that the cell wall particles move orthogonally to the cell surface. The vesicles are assumed to emerge from a single point inside the cell (the VSC) and to move by diffusion.

For this model, we derive a non-linear, non-local evolution equation and show the existence of solutions relevant to our application context, namely, axially symmetric surfaces of fixed shape, travelling along with the VSC at constant speed. Technically, the proof is based on the Schauder fixed point theorem applied to Hölder spaces of functions. The necessary estimates rely on comparison and regularity arguments from elliptic PDE theory.

3.1 Introduction

Describing the growth behaviour of living cells is a challenging pursuit, both from the point of view of biological modelling and from the point of view of the mathematical treatment of the resulting models. Since growth of a cell proceeds primarily by incorporating new material into the cell wall and membrane, models for cell growth have to describe how the shape of a cell changes as a result of this process. In geometric models, the cell wall and the membrane are treated as a single surface without thickness. This allows one to mathematically describe the cell wall as an embedded two-dimensional manifold. In this case, the well-known "first variation of area formula" relates the local growth of cell surface area to the velocity of its particles, more precisely, to their normal velocity and

the divergence of their tangential velocity.

Extreme growth behaviour can be observed in fungal hyphae cells, i.e. very long, hair-shaped cells that form the mycelium of fungi. Accordingly, modelling their growth has attracted particular interest, with an emphasis on solutions given by a fixed, travelling profile. In most models for these cells, it is assumed that cell wall particles move in a direction orthogonal to the cell surface. (An exception to this is the isometric model described by Tindemans [22].) This assumption of orthogonal growth is mostly justified by observations, with turgor pressure given as a possible physical mechanism. It will also be adopted in the present paper. Moreover, conservation of mass dictates that the surface area growth equals the local flux F of material into the cell boundary. In Section 3.2 we show that these assumptions determine the normal velocity as $v_n = -F/H$ where H is the mean curvature of the manifold.

Some models express this flux solely as a function of the local geometry of the cell wall. For example, Goriely *et al.* [13] define the flux as a function of the curvature. The Vesicle Supply Centre (VSC) models, first proposed by Bartnicki-Garcia *et al.* [2], assume that material is transported towards the wall in so-called vesicles, i.e. small "sacks" bounded by a membrane. These vesicles are created at the Golgi apparatus, and transported via the cytoskeleton to the VSC, from which they are released and transported to the cell wall. On arrival at the cell wall the contents of the vesicles are used to make cell wall material while the vesicle membrane merges with the cell membrane. For modelling purposes it is not important whether the VSC acts as a distribution centre for vesicles created elsewhere, or whether it produces them itself; in both cases it can be treated as a source of vesicles. In models for tip growth, the location of the VSC often coincides with an organelle called the Spitzenkörper.

The VSC models are divided in two classes, depending on how vesicles move from the VSC to the cell wall. In the so-called ballistic model, vesicles travel in straight lines towards the cell wall. The model by Bartnicki-Garcia *et al.* [2] is of this kind, with vesicles sent in every direction isotropically. The advantage of ballistic models lies in their mathematical simplicity: The flux of vesicles arriving at a point on the cell wall can be calculated directly from its distance to the VSC and the slope of the wall. A travelling wave ansatz then yields an ordinary differential equation for the shape of the hypha. In a previous article [17] we used this to show that this model has unique, stable, travelling solutions. These solutions are tubular elongating cells growing mostly at the tip, as observed in fungal hyphae. Possible variations of the ballistic model involve including a directional preference to the release of vesicles so that more of them are focussed on the tip, or having multiple sources.

One criticism of the ballistic model, given e.g. by Koch [19], is that inside a living cell, it is highly unlikely that a vesicle will travel in a straight line to its destination. Instead it will perform a random walk and will be absorbed when it hits the cell boundary. Accordingly, the concentration of vesicles obeys a Poisson equation with a point source at the VSC and homogeneous Dirichlet boundary conditions.

Numerical calculations on this model were done by Tindemans *et al.* [23].

Possible variations of the diffusive model include further physical properties of the cell wall, e.g. elasticity or reduced absorption due to ageing [7]. A very good overview of many of the models available is given by De Keijzer *et al* [5].

The aim of all these models is to find a travelling solution corresponding to a fungal hypha. These are solutions which are stationary in a frame of reference travelling along with the VSC (or at some fixed velocity if no VSC is present in the models). As usual, we introduce the assumption of cylindrical symmetry, i.e. the surface can then be expressed as a curve rotated around the z axis. We seek solutions which asymptotically approximate a cylinder as $z \to -\infty$.

We want to stress that the diffusive VSC models are essentially nonlocal. In fact, the equations for the tip shape involve an unknown flux function which itself depends on the tip shape. Therefore this shape is determined by a condition which cannot be formulated as an ordinary differential equation.

So far, most research has focussed on numerically approximating the tip shape for these models. In this article we provide a theoretical foundation for the simplest of them by rigorously proving the existence of these travelling solutions using a Schauder fixed point argument. However, the methods described in this article should work as well for certain related models involving orthogonal growth and a flux dependent on the cell shape; on this, see also the Conclusions section.

3.1.1 Notation and conventions

In this article we will often make use of the following notation: Ω is an open subset of $\mathbb{R}^3$, not necessarily compact, rotationally symmetric around the z axis with boundary $\partial\Omega$. Since we are working in this axially symmetric case, we will use a cylindrical coordinate system $(r, z, \theta)^T$ in $\mathbb{R}^3$. The transformation to Euclidian coordinates is given by $(x_1, x_2, x_3)^T = (r\cos\theta, r\sin\theta, z)^T$. Often we will not mention the coordinate θ in our calculations. The rotationally symmetric surface $\partial\Omega$ will be parametrized by two functions $s \mapsto r(s)$ and $s \mapsto z(s)$. The surface implied is the curve parametrized by these two functions at some fixed value of θ, rotated around the z axis. When we refer to a point on the surface at pathlength s or the point $(r(s), z(s))$, we mean a point $(r(s), z(s), \theta) \in \partial\Omega$ at some arbitrary, but fixed value of θ.

For the (scalar) mean curvature H we use the conventions as found in [9]. The mean curvature is the sum (and thus not the true mean) of the principal curvatures with respect to an outward pointing normal $\hat{n}$. For example, the sphere of radius R has mean curvature $-\frac{2}{R}$ at every point.

When u is a (harmonic) function defined on Ω, the flux F_u of u will always be the negative normal derivative of u on $\partial\Omega$. Often u will depend on a parameter ξ, we will denote this as u_ξ. If it is clear the flux mentioned is the flux of u we will write F_ξ to denote the flux at parameter value ξ.

The proof in this article relies heavily on the use of Hölder spaces. For these spaces and their norms we will use the notation as found in [12], with $\|\cdot\|_{k,\alpha;X}$ denoting the $C^{k,\alpha}$ norm on the domain of definition X. The space of continuous

functions from X to Y with bounded Hölder norm is denoted as $C^{k,\alpha}(X;Y)$. The domain X or codomain Y will be omitted if they are clear from the context.

3.2 The diffusive VSC model

3.2.1 The diffusive flux

In the diffusive VSC model, we assume the VSC is a source of vesicles which diffuse outwards toward the cell wall, where they are completely absorbed, causing growth. Each vesicle is a membrane sack containing the materials to build new cell wall. Upon absorption, the membrane of the vesicle merges with the cell membrane, while the contents build new cell wall. In the VSC model, the membrane and cell wall are treated as a single manifold, and each vesicle contributes a fixed amount of surface area to this manifold. The total amount of surface area produced by the VSC per unit of time is denoted by P. The VSC is moving in the positive z direction at speed c. We assume the motion of the cell wall is slow on the diffusion time scale of the vesicles, and so the density of vesicles is always in equilibrium. As such, it can be found by solving a Poisson equation. The assumption that vesicles are completely absorbed at the boundary yields a homogeneous Dirichlet boundary condition. Furthermore, we assume that the motion of the cell wall is slow on the diffusion time scale of the vesicles.

If at time $t = 0$ the tip of the cell wall is at the origin, and the VSC is at distance ξ from the tip, then the density u_ξ of vesicles can be found by solving

$$\begin{aligned} \Delta u_\xi &= -P\delta(r, z+\xi-ct) && \text{in } \Omega, \\ u_\xi &= 0 && \text{on } \partial\Omega. \end{aligned} \tag{3.2.1}$$

The flux of material arriving at a point is now given by $F_\xi = -\frac{\partial u_\xi}{\partial \hat{n}}$ where $\hat{n}$ is the outward pointing normal of $\partial\Omega$. This flux gives the rate per unit of area at which the surface area increases.

3.2.2 Mass balance

If one takes an arbitrary bounded region $\Gamma \subset \partial\Omega$ of the surface of the cell, with surface area $\|\Gamma\|$ and boundary curve $\partial\Gamma$, then the total flux of material absorbed in Γ is given by

$$\frac{\mathrm{d}\,\|\Gamma\|}{\mathrm{d}t} = \int_\Gamma F_\xi \,\mathrm{d}S. \tag{3.2.2}$$

If one assumes Γ is transported by a velocity field v, then Gauss' formula for the first variation of area states that

$$\frac{\mathrm{d}\,\|\Gamma\|}{\mathrm{d}t} = -\int_\Gamma H(\hat{n}\cdot v)\mathrm{d}S + \oint_{\partial\Gamma} (\hat{m}\cdot v)\mathrm{d}l \tag{3.2.3}$$

where $\hat{m}$ is the outward pointing normal to $\partial\Gamma$ tangent to $\partial\Omega$ and H is the (scalar) mean curvature. By assumption, the surface of the cell moves orthogonally to the cell surface, so $v = v_n\hat{n}$ and the integral over $\partial\Gamma$ vanishes. As Γ was chosen arbitrarily, we get from (3.2.2) and (3.2.3) that

$$v_n = -\frac{F_\xi}{H}. \tag{3.2.4}$$

3.2.3 Main result

Equation (3.2.4), with flux defined by (3.2.1) as explained in Section 3.2.1, describes the evolution of an embedded two-dimensional manifold. The aim of this article is to show there exist solutions to this evolution which evolve similarly to the growth of fungal hyphae.

Theorem 3.2.1 Main result. *For each speed c of the VSC and production rate P there exists a manifold and distance ξ such that, when evolving under evolution equation* (3.2.4)*, this manifold appears stationary in a coordinate frame moving at speed c in the z direction. The manifold is cylindrically symmetric and approximates a cylinder of radius $\frac{P}{2\pi c}$ as $z \to -\infty$.*

This theorem will be proved in the course of this article.

3.2.4 Scaling

We define the typical length scale X and time-scale T of the model as follows,

$$X = \frac{P}{4\pi c} \qquad T = \frac{P}{4\pi c^2}. \tag{3.2.5}$$

Rescaling our spacial coordinates by $x = X\tilde{x}$ and $t = T\tilde{t}$ we denote the rescaled domain as $\tilde{\Omega}$. It is now natural to rescale the dependant variables and constants as

$$\begin{aligned} u_\xi = \frac{X}{T}\tilde{u}_{\tilde{\xi}}, \quad F_\xi = \frac{1}{T}\tilde{F}_{\tilde{\xi}}, \quad H = \frac{1}{X}\tilde{H}, \quad v_n = \frac{X}{T}\tilde{v}_n, \\ \xi = X\tilde{\xi}, \qquad \tilde{c} = 1, \qquad \tilde{P} = 4\pi. \end{aligned} \tag{3.2.6}$$

We now see that the rescaled model satisfies

$$\tilde{v}_n = -\frac{\tilde{F}_{\tilde{\xi}}}{\tilde{H}}, \tag{3.2.7}$$

where $\tilde{F}_{\tilde{\xi}} = -\frac{\partial\tilde{u}_{\tilde{\xi}}}{\partial\tilde{n}}$ and $\tilde{u}_{\tilde{\xi}}$ satisfies

$$\begin{aligned} \Delta\tilde{u}_{\tilde{\xi}} &= -4\pi\delta(\tilde{r}, \tilde{z} + \tilde{\xi} - t) \qquad \text{in } \tilde{\Omega}, \\ \tilde{u}_{\tilde{\xi}} &= 0 \qquad\qquad\qquad\qquad\quad \text{on } \partial\tilde{\Omega}. \end{aligned} \tag{3.2.8}$$

For the remainder of this article we will drop the tildes and work with this rescaled model.

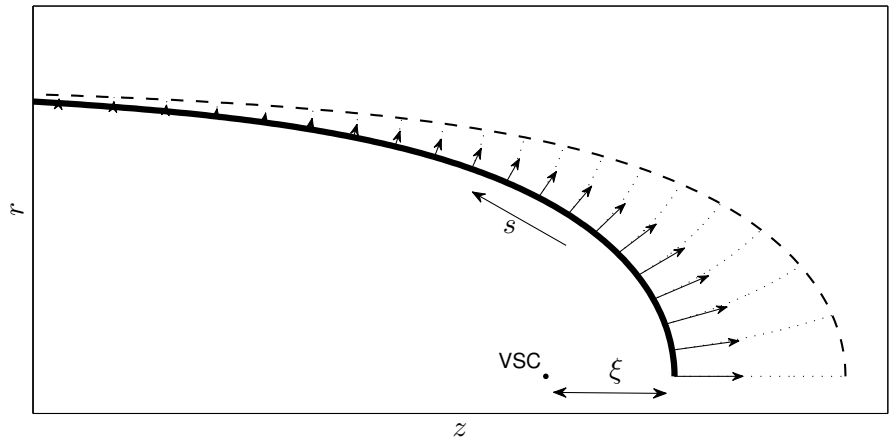

Figure 3.1: Travelling wave profile with model definitions. The solid curve, rotated around the z axis, is the cell boundary $\partial\Omega$. The arrows indicate the normal velocity and the dotted lines are the particle trajectories. The dashed curve indicates the location of the cell boundary at some later time.

3.2.5 The unbounded travelling wave problem

We wish to find a surface satisfying the evolution equation (3.2.4) which moves along with the VSC, see for example Figure 3.1. In other words, in a coordinate system moving along with the VSC, $\partial\Omega$ appears stationary. In this coordinate system, Gauss' formula for the variation of area on an arbitrary subsurface Γ states that:

$$\int_\Gamma F_\xi \mathrm{d}S = -\int_\Gamma H(\hat{n}\cdot(v-\hat{e}_z))\mathrm{d}S + \oint_{\partial\Gamma}(\hat{m}\cdot(v-\hat{e}_z))\mathrm{d}l \tag{3.2.9}$$

For a stationary solution, $v-\hat{e}_z$ must lie tangent to $\partial\Omega$ and the integral over Γ vanishes. By assumption, v is perpendicular to $\hat{m}$ and so

$$-\oint_{\partial\Gamma}\hat{m}\cdot\hat{e_z}\mathrm{d}l = \int_\Gamma F_\xi \mathrm{d}S. \tag{3.2.10}$$

We now choose Γ to be the region from the tip up to the plane located at $z=z(s)$, then $\hat{m}\cdot\hat{e}_z$ is constant over $\partial\Gamma$. We choose cylindrical coordinates r and z, and describe $\partial\Omega$ as the curve $(r(s),z(s))$ rotated around the z axis. We parametrize such that s is the pathlength over $\partial\Omega$ from the tip.

In these coordinates $\hat{m}=r'(s)\hat{e}_r+z'(s)\hat{e}_z$, and (3.2.10) simplifies to

$$z'(s)=-\frac{G_\xi(s)}{r(s)}, \qquad r'(s)=\sqrt{1-\left(\frac{G_\xi(s)}{r(s)}\right)^2}, \tag{3.2.11}$$

where

$$G_\xi(s) = \frac{1}{2\pi}\int_\Gamma F_\xi \mathrm{d}S = \int_0^s F_\xi(\sigma) r(\sigma)\mathrm{d}\sigma, \tag{3.2.12}$$

and $F_\xi(\sigma)$ is the flux passing through the point on the boundary at pathlength σ.

We wish to find functions $r(s)$, $z(s)$ and a number ξ^* such that when (3.2.1) is solved on the domain defined by the functions, the corresponding cumulative flux G_{ξ^*} and the functions r and z satisfy (3.2.11) with boundary conditions $r(0) = z(0) = 0$, $r'(0) = 1$. We wish $r(s)$ to remain bounded. Since by the divergence theorem $G_\xi(s) \to 2$, this can only be accomplished if $r(s) \to 2$ as $s \to \infty$. In the rest of the article we will refer to this as the unbounded travelling wave problem.

3.2.6 The bounded travelling wave problem

The fact that the domain of the functions r and z is infinite, and therefore that the domain Ω is unbounded makes analysis difficult. In order to handle these difficulties, we first restrict ourselves to bounded domains with a no flux condition at $z = z(s_{max})$ for some sufficiently large s_{max}. We apply the method of reflection and define the following problem: given functions $r(s)$ and $z(s)$ on $(0, s_{max})$ we define $\partial\Omega$ to be the curve $(r(s), z(s))$ rotated around the z axis and reflected at the plane $z = z(s_{max})$. If the VSC is located at a distance ξ from the tip, the density of vesicles $u_\xi(r, z)$ is found by solving

$$\begin{aligned} \Delta u_\xi &= -4\pi\delta(r, z+\xi) - 4\pi\delta(r, z+\eta) && \text{in } \Omega, \\ u_\xi &= 0 && \text{on } \partial\Omega. \end{aligned} \tag{3.2.13}$$

where $\eta = -2z(s_{max}) - \xi$ is the distance from the reflected VSC to the tip at $z = 0$. The functions F_ξ and G_ξ are still defined as above. Note that by symmetry and the divergence theorem, $G_\xi(s_{max}) = 2$.

Given s_{max} we wish to find functions $r(s)$, $z(s)$ and a number ξ^*, such that when (3.2.13) is solved on the domain defined by these functions, the corresponding cumulative flux G_{ξ^*} and the functions r and z satisfy (3.5.2) with boundary conditions $r(0) = z(0) = 0$, $r'(0) = 1$, and $r(s_{max}) = 2$. We will refer to this problem as the bounded travelling wave problem. In Section 3.7 we take the limit as $s_{max} \to \infty$ to show the existence of a solution for the unbounded travelling wave problem described in the previous section.

3.3 The Schauder map

Our approach to solve this problem relies on a Schauder fixed point argument on a subset of the product space $C^{1,\alpha} \times C^{0,\alpha}$ containing Hölder continuous functions $s \mapsto r(s)$ and $s \mapsto z'(s)$, for some $\alpha \leq \frac{1}{2}$. We equip this space with the $C^{1,\beta} \times C^{0,\beta}$ topology for some $\beta < \alpha$. Defining $z(s) = \int_0^s z'(\sigma)\mathrm{d}\sigma$, the functions $r(s)$ and $z(s)$ describe a boundary $\partial\Omega$ with certain properties. (Note that since $z \to -\infty$ if $s_{max} \to \infty$, we cannot claim that $z \in C^{1,\alpha}$ is bounded uniformly in s_{max}, instead we demand this only of its derivative z'.) Since the Schauder fixed point theorem requires that we work on a closed convex subset of this product space, we cannot require that $\partial\Omega$ is parametrized by pathlength ($r'^2 + z'^2 = 1$ is not a convex requirement.) Instead we require that $r'^2 + z'^2 \leq 1$ and $r' - z' \geq 1$, see Figure 3.2. Note, however, that the image of the Schauder map does satisfy the pathlength requirement $r'^2 + z'^2 = 1$.

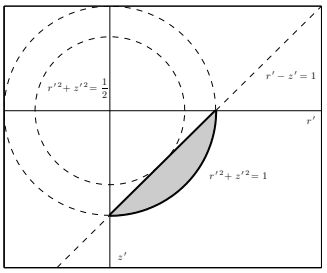

Figure 3.2: Convex bounds on r' and z'.

3.3.1 The domain of the Schauder map

Given a sufficiently large s_{max} we define the domain of the Schauder map $\Xi(M, A, C; s_{max})$ as the subset of $C^{1,\alpha}([0, s_{max}]; \mathbb{R}) \times C^{0,\alpha}([0, s_{max}]; \mathbb{R})$ containing functions r and z' satisfying the following convex properties:

$$\|r\|_{1,\alpha} \leq M, \qquad \|z'\|_{0,\alpha} \leq M, \tag{3.3.1}$$

$$r'(s)^2 + z'(s)^2 \leq 1, \qquad r'(s) - z'(s) \geq 1, \tag{3.3.2}$$

$$r(s_{max}) = 2, \qquad r'(s_{max}) = 0, \tag{3.3.3}$$

$$\frac{r'(s_2) - r'(s_1)}{s_2 - s_1} \leq A, \qquad \frac{z'(s_2) - z'(s_1)}{s_2 - s_1} \leq A, \quad \text{for} \quad s_1 < s_2, \tag{3.3.4}$$

$$s - \frac{1}{9}C^2 s^3 \leq r(s) \leq 2 \quad \text{for} \quad 0 \leq s \leq C^{-1}, . \tag{3.3.5}$$

In Section 3.4 we will show that one can solve the Dirichlet problem (3.2.13) for every ξ, $\xi_{min} \leq \xi \leq \xi_{max}$, with ξ_{min} and ξ_{max} to be determined later, and obtain a family G_ξ of cumulative fluxes, parametrized by ξ, with certain properties. This defines a map $\Psi_1 : \Xi(M, A, C; s_{max}) \to C^1([\xi_{min}, \xi_{max}]; C^{1,\alpha}([0, s_{max}]; \mathbb{R}))$. Given $G_\xi \in Im(\Psi_1)$ and a value of the parameter ξ, (3.2.11) can be seen as an ordinary differential equation, which can be solved to obtain functions $r_\xi(s)$ and $z_\xi(s)$. In Section 3.5 we will show that one can find a unique value ξ^* such that $r_{\xi^*}(s_{max}) = 2$. This defines a map $\Psi_2 : Im(\Psi_1) \to \Xi(\tilde{M}, \tilde{A}, \tilde{C})$. In Section

3.6 we will choose M, A and C such that the composition $\Psi = \Psi_2 \circ \Psi_1$ maps from $\Xi(M, A, C; s_{max})$ to itself. We then use Schauder's fixed point theorem to show that the map Ψ, which we will refer to as the Schauder map, has a fixed point. Since solutions to (3.2.11) satisfy $r'^2 + z'^2 = 1$, this fixed point describes a surface parametrized by pathlength and solves the bounded travelling wave problem defined in Section 3.2.6.

Lemma 3.3.1 *The set $\Xi(M, A, C; s_{max})$ is closed in the $C^{1,\beta} \times C^{0,\beta}$ topology.*

Proof Let (r_n, z'_n) be a sequence in $\Xi(M, A, C; s_{max})$ which converges to (r, z') in $C^{1,\beta} \times C^{0,\beta}$. We need to prove that (r, z') satisfies (3.3.1) to (3.3.5). We can clearly take the limit to see that (r, z) satisfies (3.3.2) to (3.3.5) so we need only concern ourselves with the Hölder norm established in (3.3.1). Now since r_n is bounded in the $C^{1,\alpha}$ norm it has a convergent subsequence in the $C^{1,\beta}$ norm, clearly the limit of this subsequence is r and thus $\|r\|_{1,\alpha} \leq M$. Similarly $\|z'\|_{0.\alpha} \leq M$.

■

3.3.2 Estimates on $r(s)$, $z(s)$ and distances

The definition of the set $\Xi(M, A, C; s_{max})$ yields several estimates on $r(s)$, $z(s)$ and distances between points on the boundary that will be used throughout this article.

First of all, (3.3.2) gives $0 \leq r' \leq 1$, $-1 \leq z' \leq 0$, $r'^2 + z'^2 \geq \frac{1}{2}$, $r(0) = 0$, $r'(0) = 1$ and $z'(0) = 0$. The estimate given by (3.3.5) gives an asymptotic approximation for $r(s)$ in the tip, at small s. The monotonicity of r then gives a lower bound away from the tip,

$$\frac{8}{9}C^{-1} \leq r(s) \leq 2 \qquad \text{for } C^{-1} \leq s \leq s_{max}. \tag{3.3.6}$$

Using this we can establish an asymptotic estimate for $z(s)$ at small s,

$$z(s) \geq -\sqrt{s^2 - r(s)^2} \geq -\frac{1}{2}Cs^2 \quad \text{for} \quad 0 \leq s \leq C^{-1}. \tag{3.3.7}$$

while the requirement that $r' - z' \geq 1$ implies that

$$-s \leq z(s) \leq 2 - s. \tag{3.3.8}$$

for all s.

The choice of parametrization of the curve $s \mapsto (r(s), z(s))$ yield various useful bounds on the distances between points on the curve.

Lemma 3.3.2 *The distance between points $(r(s_2), z(s_2))$ and $(r(s_1), z(s_1))$ is bounded from above and below by the difference in parameter values $s_2 - s_1$.*

$$\frac{1}{2}(s_2 - s_1)^2 \leq (r(s_2) - r(s_1))^2 + (z(s_2) - z(s_1))^2 \leq (s_2 - s_1)^2. \tag{3.3.9}$$

Proof Let $d(s)$ be the distance from $(r(s), z(s))$ to $r(s_1), z(s_1)$,

$$d(s) = \sqrt{(r(s) - r(s_1))^2 + (z(s) - z(s_1))^2}. \tag{3.3.10}$$

By the Cauchy-Schwarz inequality,

$$\begin{aligned}\left(\frac{\mathrm{d}}{\mathrm{d}s} d(s)\right)^2 &= \left(\frac{r(s) - r(s_1)}{d(s)} r'(s) + \frac{z(s) - z(s_1)}{d(s)} z'(s)\right)^2 \\ &\leq r'(s)^2 + z'(s)^2 \leq 1\end{aligned} \tag{3.3.11}$$

so $d(s_2) \leq (s_2 - s_1)$. For the lower bound we see that

$$\begin{aligned}d(s_2)^2 &= \frac{1}{2}\left((r(s_2) - r(s_1)) - (z(s_2) - z(s_1))\right)^2 + \frac{1}{2}((r(s_2) - r(s_1)) + (z(s_2) - z(s_1)))^2 \\ &\geq \frac{1}{2}(s_2 - s_1)^2,\end{aligned} \tag{3.3.12}$$

since $r'(s) - z'(s) \geq 1$.

Geometrically, the upper bound is achieved when the path between the points at pathlength s_1 and s_2 consists of a straight line. The lower bound is achieved when the path consists solely of vertical and horizontal segments. ■

Furthermore, the estimates for $r(s)$ and $z(s)$ established in the previous section allow us to calculate a lower bound for the distance between the VSC and the boundary of the cell, an important ingredient for bounding the flux.

Lemma 3.3.3 *If $\frac{1}{2}C^{-1} < \xi_{min} \leq \xi$ then the distance $d_\xi(s)$ from the point $(r(s), z(s))$ to the VSC is bounded from below by a nonzero constant d_{min} depending only on C and ξ_{min}.*

Proof Using the asymptotics for r and z at small s, (3.3.5) and (3.3.7),

$$d_\xi(s) = \sqrt{r(s)^2 + (\xi + z(s))^2} \geq \xi + z(s) \geq \xi_{min} - \frac{1}{2}C^{-1} \quad \text{for} \quad 0 \leq s \leq C^{-1},$$

while for large s,

$$d_\xi(s) \geq r(s) \geq \frac{8}{9}C^{-1} \quad \text{for} \quad C^{-1} \leq s \leq s_{max},$$

by (3.3.6). The minimum of these two estimates gives a lower bound for the distance. ■

3.3.3 Exterior spheres

For bounds on the flux in the next section we require that it is possible to be able to touch a sphere of fixed radius to every point of the boundary, in such a way that the interior of the sphere does not intersect Ω. If the second derivatives of r and z were bounded from above, this would be a relatively straightforward task involving the calculation of the first principle curvature. The upper bound on the difference quotient given by (3.3.4) is in fact sufficient for this task.

Lemma 3.3.4 *Let B_R be a ball of radius $R \leq \frac{1}{4A}$ touching $\partial\Omega$ at the point $(r(s_1)z(s_1))$. Then the distance from any point $(r(s_2), z(s_2)) \in \partial\Omega$ to the centre (r_c, z_c) of B_R is always greater than R.*

Proof Let $\frac{1}{2}\pi \leq \theta \leq \pi$ be such that

$$\cos\theta = \frac{z'(s_1)}{\sqrt{r'(s_1)^2 + z'(s_1)^2}}, \qquad \sin\theta = \frac{r'(s_1)}{\sqrt{r'(s_1)^2 + z'(s_1)^2}}. \tag{3.3.13}$$

The centre of the ball B_R is then given by

$$r_c = r(s_1) - R\cos\theta, \qquad z_c = z(s_1) + R\sin\theta. \tag{3.3.14}$$

The distance d_c between the point $(r(s_2), z(s_2))$ and the centre of this sphere is given by

$$\begin{aligned} d_c^2 &= (r(s_2) - r(s_1))^2 + (z(s_2) - z(s_1))^2 + R^2 \\ &\quad + 2R\left((r(s_2) - r(s_1))\cos\theta - (z(s_2) - z(s_1))\sin\theta\right). \end{aligned} \tag{3.3.15}$$

Integrating the difference quotients (3.3.4) we can estimate

$$\begin{aligned} r(s_2) - r(s_1) &\leq r'(s_1)(s_2 - s_1) + \frac{1}{2}A(s_2 - s_1)^2, \\ z(s_2) - z(s_1) &\leq z'(s_1)(s_2 - s_1) + \frac{1}{2}A(s_2 - s_1)^2. \end{aligned} \tag{3.3.16}$$

Substituting this, the linear terms in $(s_2 - s_1)$ drop out and

$$d_c^2 \geq (r(s_2) - r(s_1))^2 + (z(s_2) - z(s_1))^2 + R^2 + AR(s_2 - s_1)^2(\cos\theta - \sin\theta). \tag{3.3.17}$$

The distance between points at parameter values s_2 and s_1 can be estimated using Lemma (3.3.2) and so,

$$d_c^2 \geq \frac{1}{2}(s_2 - s_1)^2 + R^2 - 2AR(s_2 - s_1)^2, \tag{3.3.18}$$

and so if we choose $R \leq \frac{1}{4A}$ this distance will always be greater than R. ∎

3.4 The Dirichlet problem

Given a domain Ω given by the functions $r(s)$ and $z(s)$ as described in the previous section, we wish to find a solution u_ξ to (3.2.13). We then wish to find various estimates for the flux $F_\xi(s)$ passing through the point $(r(s), z(s))$ and the cumulative flux $G_\xi(s)$, defined as

$$G_\xi(s) = \int_0^s F_\xi(\sigma) r(\sigma) \sqrt{r'(\sigma)^2 + z'(\sigma)^2}\,\mathrm{d}\sigma. \tag{3.4.1}$$

Note that if $\partial\Omega$ is parametrized by pathlength, which for example is the case in the fixed point of the Schauder map, then this definition is equivalent to (3.2.12).

3.4.1 The domain Ω

Lemma 3.4.1 *If the boundary $\partial\Omega$ is given by $C^{1,\alpha}$ Hölder continuous functions $r(s)$ and $z(s)$ as described previously, then the enclosed domain Ω is of class $C^{1,\alpha}$.*

Proof For the purposes of this proof, we extend the functions r and z to the interval $[0, 2s_{max}]$ by reflection, so for $s > s_{max}$, $r(s) = r(2s_{max} - s)$ and $z(s) = 2z(s_{max}) - z(2s_{max} - s)$. Now $r'(s_{max}) = 0$ and $z'(s_{max}) = -1$ so the derivatives are continuous. For $s_1 < s_{max} < s_2$,

$$\begin{aligned} |r'(s_2) - r'(s_1)| &\leq |r'(s_2) - r'(s_{max})| + |r'(s_{max}) - r'(s_1)| \\ &\leq \|r\|_{1,\alpha} |s_2 - s_{max}|^\alpha + \|r\|_{1,\alpha} |s_{max} - s_1|^\alpha \\ &\leq 2 \|r\|_{1,\alpha} |s_2 - s_1|^\alpha , \end{aligned} \tag{3.4.2}$$

and similar for the Hölder quotient of z', therefore these functions are Hölder continuous. We now need to prove that each point of $\partial\Omega$ has a neighbourhood which can be described as the graph of a $C^{1,\alpha}$ function. We examine the point x^* at pathlength s^* and angle θ^*. Without loss of generality we can assume that $\theta^* = 0$ due to the rotational symmetry. A point x given by the parameters s and θ in the neighbourhood of x^* has Euclidian coordinates $(x_1, x_2, x_3)^T = (r(s)\cos\theta, r(s)\sin\theta, z(s))^T$. We now introduce new coordinates ξ such that the origin lies on x^*, rotated such that the direction ξ_1 lies tangent to the curve $r(s), z(s)$ and the direction ξ_2 lies in the direction of rotation by θ. Then

$$\begin{pmatrix} \xi_1 \\ \xi_2 \\ \xi_3 \end{pmatrix} = \begin{bmatrix} -z'(s^*) & 0 & r'(s^*) \\ 0 & 1 & 0 \\ -r'(s^*) & 0 & -z'(s^*) \end{bmatrix} \begin{pmatrix} r(s)\cos\theta - r(s^*) \\ r(s)\sin\theta \\ z(s) \end{pmatrix}. \tag{3.4.3}$$

Now at $(s, \theta) = (s^*, 0)$ we have $\frac{\partial\xi}{\partial s} = (0, 0, -1)^T$ and $\frac{\partial\xi}{\partial\theta} = (0, r(s^*), 0)^T$. Therefore, if $s^* \neq 0$ then $r(s^*) \neq 0$ and by the implicit function theorem, there is a neighbourhood around x^* where we can write ξ_3 (and s and θ) as a $C^{1,\alpha}$ function of ξ_1 and ξ_2.

If, on the other hand, $s^* = 0$ then since $r'(0) = 1$, $r(s)$ is invertible in a neighbourhood of zero, and its inverse is $C^{1,\alpha}$. The tip can now be described as the graph $x_3 = z(r^{-1}(\sqrt{x_1^2 + x_2^2}))$.

■

This lemma implies that the domain Ω is of class $C^{1,\alpha}$, this ensures us (see for example [12] Theorem 8.34) that there is a unique solution to the Dirichlet problem (3.2.13) which is $C^{1,\alpha}$. Since $\partial\Omega$ is not C^2, it does not satisfy an interior sphere condition everywhere, and we cannot use the boundary point lemma to conclude that $F_\xi > 0$ everywhere. This motivates the following Lemma for less smooth domains.

Lemma 3.4.2 *Let Ω be a (not necessarily rotationally symmetric) domain sufficiently smooth that the maximum principle and divergence theorem hold and a*

normal direction $\hat{n}$ to the boundary can be defined almost everywhere. Let $u > 0$ be a weak solution of

$$\begin{aligned} \Delta u &= f(x) \quad && \text{in } \Omega, \\ u &= 0 && \text{on } \partial\Omega, \end{aligned} \tag{3.4.4}$$

where f has compact support away from the boundary. Then there is no open subset $\Gamma \subset \partial\Omega$ such that $F_u = -\frac{\partial u}{\partial \hat{n}} = 0$ on Γ.

Proof Assume such a $\Gamma \subset \partial\Omega$ exists. Let B_R be a ball of radius R centred on a point in the interior of Γ. Then R can be chosen sufficiently small such that $(\partial\Omega \cap B_R) \subset \Gamma$ and $B_R \cap \text{supp } f = \emptyset$. Let v solve

$$\begin{aligned} \Delta v &= 0 \quad && \text{in } B_R, \\ v &= u && \text{on } \partial B_R \cap \Omega, \\ v &= 0 && \text{on } \partial B_R \setminus \Omega, \end{aligned} \tag{3.4.5}$$

then by the maximum principle $v > 0$ on B_R and $u \leq v$ on $B_R \cap \Omega$. Since $u = v$ on $\partial B_R \cap \Omega$, $F_u \leq F_v$ on $\partial B_R \cap \Omega$. The ball B_R satisfies an interior sphere condition, so by the boundary point lemma, $F_v > 0$ on $\partial B_R \setminus \Omega$. By the divergence theorem, the total flux of v over ∂B_R must be zero, so $\int_{\partial B_R \cap \Omega} F_v \mathrm{d}S < 0$. This implies that $\int_{\partial B_R \cap \Omega} F_u \mathrm{d}S < 0$. By the divergence theorem, the total flux of u over $\partial(B_R \cap \Omega)$ must be zero, so $\int_{\partial\Omega \cap B_R} F_u \mathrm{d}S > 0$. This is in contradiction with our assumption that $F_u = 0$ on Γ.

■

This Lemma implies that $G_\xi(s)$ is strictly monotone in s, even though its derivative might occasionally be zero.

3.4.2 Bounds on $F_\xi(s)$

The uniform upper bound on the curvature allows us to touch a sphere of radius $R = \frac{1}{4A}$ to any point on $\partial\Omega$ such that this sphere lies outside of Ω. This together with the bounds for the distances to the VSC allows us to establish an uniform upper bound for the flux.

Lemma 3.4.3 *For sufficiently large s_{max}, the flux $F_\xi(s) = -\frac{\partial u}{\partial \hat{n}}$ passing through the point $(r(s), z(s))$ on the boundary is bounded,*

$$F_\xi(s) \leq F_{max}(\xi_{min}, \xi_{max}, A, C). \tag{3.4.6}$$

This implies that we can estimate $G'_\xi(s) \leq F_{max} s$ and $G'_\xi(s) \leq 2F_{max}$.

Proof Let B_R be a sphere of radius $R = \frac{1}{4A}$ touching $\partial\Omega$ at the point $(r(s), z(s))$, we now solve

$$\begin{aligned} \Delta v &= -4\pi\delta(r, z+\xi) - 4\pi\delta(r, z+\eta) \quad && \text{outside of } B_R, \\ v &= 0 && \text{on } \partial B_R. \end{aligned} \tag{3.4.7}$$

Since B_R lies outside of Ω, $u \leq v$ and the boundaries touch at $(r(s), z(s))$, the flux of v at this point gives us an upper bound for $F_\xi(s)$. We can determine v using reflection techniques. For simplicity we consider the sources at $z = -\xi$ and $z = -\eta$ separately and write $v = v_1 + v_2$ with v_1 and v_2 the individual contributions from these two sources. For $\frac{1}{2}\pi \leq \theta \leq \pi$ let,

$$\cos\theta = \frac{z'(s)}{\sqrt{r'(s)^2 + z'(s)^2}}, \qquad \sin\theta = \frac{r'(s)}{\sqrt{r'(s)^2 + z'(s)^2}}. \tag{3.4.8}$$

Let ρ be the distance from the VSC to the centre of B_R,

$$\rho^2 = d_\xi(s)^2 + R^2 + 2R((z(s) + \xi)\sin\theta - r(s)\cos\theta), \tag{3.4.9}$$

where $d_\xi(s)$ is the distance from the VSC to the point $(r(s), z(s))$. Let $(\tilde{r}, \tilde{z})$ be the point, on the line from the VSC to the centre of B_R, at a distance $\tilde{\rho} = \frac{R^2}{\rho}$ from the centre the sphere. Then

$$\begin{aligned} r(s) - \tilde{r} &= \frac{R^2}{\rho^2} r(s) + (1 - \frac{R^2}{\rho^2}) R\cos\theta, \\ z(s) - \tilde{z} &= \frac{R^2}{\rho^2}(z(s) + \xi) - (1 - \frac{R^2}{\rho^2}) R\sin\theta. \end{aligned} \tag{3.4.10}$$

This point acts as a reflected source of strength $-4\pi\frac{R}{\rho}$. The contribution of the source at the VSC to v is given by

$$v_1(r, z) = \frac{1}{d_1(r, z)} - \frac{R}{\rho}\frac{1}{\tilde{d}_1(r, z)} \tag{3.4.11}$$

where $d_1(r, z)$ is the distance from the point (r, z) to the VSC, and $\tilde{d}_1(r, z)$ is the distance from (r, z) to the reflected point $(\tilde{r}, \tilde{z})$ inside B_R. Note that $d_1(r(s), z(s)) = d_\xi(s)$. If we denote the VSC as the point O, $(\tilde{r}, \tilde{z})$ as P, $(r(s), z(s))$ as X and the centre of the sphere B_R as C, then the triangles OXC and XPC are similar. Thus $\frac{d_\xi(s)}{\tilde{d}_1(s)} = \frac{R}{\tilde{\rho}} = \frac{\rho}{R}$. The contribution to the flux at $(r(s), z(s))$ is then given by

$$\begin{aligned} F_1(s) &= \frac{(z(s) + \xi)\sin\theta - r(s)\cos\theta}{d_\xi(s)^3} - \frac{R}{\rho}\frac{(z(s) - \tilde{z})\sin\theta - (r(s) - \tilde{r})\cos\theta}{\tilde{d}_1(r(s), z(s))^3} \\ &= \frac{\rho^2 - R^2}{R d_\xi(s)^3} = 2\frac{(z(s) + \xi)\sin\theta - r(s)\cos\theta}{d_\xi(s)^3} + \frac{1}{R d_\xi(s)} \\ &\leq 2\frac{\xi_{max} + 2}{d_\xi^3} + \frac{1}{R d_\xi}. \end{aligned} \tag{3.4.12}$$

By Lemma 3.3.3 we can estimate d_ξ in terms of C and ξ_{min} while R can be expressed in terms of A. We treat the source at $z = -\eta$ similarly to obtain,

$$v_2(r, z) = \frac{1}{d_2(r, z)} - \frac{R}{\rho}\frac{1}{\tilde{d}_2(r, z)}, \tag{3.4.13}$$

and,

$$\begin{aligned} F_2(s) &= 2\frac{(z(s)+\eta)\sin\theta - r(s)\cos\theta}{d_\eta(s)^3} + \frac{1}{Rd_\eta(s)} \\ &\leq 6\frac{s_{max}}{d_\eta(s)} + \frac{1}{Rd_\eta(s)}. \end{aligned} \tag{3.4.14}$$

where $d_2(r,z)$ and $\tilde{d}_2(r,z)$ are the distances from the point (r,z) to the source at $z=-\eta$ respectively the reflection of this source inside B_R and $d_\eta(s) = d_2(r(s),z(s))$. Note that $d_\eta(s) \geq s_{max} - 2 - \xi_{max}$. Combining these contributions yields that $F_\xi(s) \leq F_1(s) + F_2(s) \leq F_{max}$. Since $\frac{s_{max}}{d_\eta(s)} \to 1$ and $\frac{1}{d_\eta(s)} \to 0$ as $s_{max} \to \infty$ this term can be bounded independently of s_{max} assuming s_{max} is sufficiently large. Thus F_{max} depends on A, C, ξ_{min} and ξ_{max}.

■

3.4.3 Bounds on $G_\xi(s)$

By using the upper bound on the flux derived in the previous section and then integrating we can obtain estimates for the cumulative flux G_ξ. However, it will be important to have estimates on G_ξ which do not depend on the parameter A. In order to do this we will use the following comparison principle.

Theorem 3.4.4 Comparison principle. *Let Ω and $\tilde{\Omega}$ be domains with $0 \in \Omega \cap \tilde{\Omega}$, with boundaries sufficiently smooth that the divergence theorem and the strong maximum principle hold. Let u and $\tilde{u}$ solve*

$$\begin{aligned} \Delta u &= -\delta(x) \quad \text{in } \Omega, & u &= 0 \quad \text{on } \partial\Omega, \\ \Delta \tilde{u} &= -\delta(x) \quad \text{in } \tilde{\Omega}, & \tilde{u} &= 0 \quad \text{on } \partial\tilde{\Omega}. \end{aligned}$$

Then,

$$\int\limits_{\partial\Omega\setminus\tilde{\Omega}} F_u \mathrm{d}S \leq \int\limits_{\partial\tilde{\Omega}\cap\Omega} F_{\tilde{u}} \mathrm{d}S, \qquad \int\limits_{\partial\tilde{\Omega}\setminus\Omega} F_{\tilde{u}} \mathrm{d}S \leq \int\limits_{\partial\Omega\cap\tilde{\Omega}} F_u \mathrm{d}S.$$

If $\partial\Omega$ and $\partial\tilde{\Omega}$ satisfy an interior sphere condition, then the inequalities are strict.

Proof Let v solve

$$\Delta v = -\delta(x) \quad \text{in } \Omega\cap\tilde{\Omega}, \qquad v = 0 \quad \text{on } \partial(\Omega\cap\tilde{\Omega}).$$

Then by the maximum principle, $0 \leq v \leq u$ and $0 \leq v \leq \tilde{u}$ on $\Omega\cap\tilde{\Omega}$. Moreover, since $v = u$ on $\partial\Omega\cap\tilde{\Omega}$, $F_v \leq F_u$ on $\partial\Omega\cap\tilde{\Omega}$. Similarly, $F_v \leq F_{\tilde{u}}$ on $\partial\tilde{\Omega}\cap\Omega$. By the divergence theorem,

$$\int\limits_{\partial\Omega\cap\tilde{\Omega}} F_u \mathrm{d}S + \int\limits_{\partial\Omega\setminus\tilde{\Omega}} F_u \mathrm{d}S = \int\limits_{\partial\Omega\cap\tilde{\Omega}} F_v \mathrm{d}S + \int\limits_{\partial\tilde{\Omega}\cap\Omega} F_v \mathrm{d}S.$$

Substituting the inequalities for F_v yields the first inequality. The second inequality follows by symmetry. If the boundaries satisfy an interior sphere condition, then by the boundary point lemma, $F_v < F_u$ on $\partial\Omega \cap \tilde{\Omega}$ and $F_v < F_{\tilde{u}}$ on $\partial\tilde{\Omega} \cap \Omega$ yielding strict inequalities. ■

Corollary 3.4.5 *The result also holds if the source $\delta(x)$ is replaced by several sources $\sum_i w_i \delta(x - x_i)$ of different positive weights w_i for $x_i \in \Omega \cap \tilde{\Omega}$. Similarly we can replace the point source $\delta(x)$ by a positive function $f(x)$ with compact support within $\Omega \cap \tilde{\Omega}$.*

This Lemma allows us to compare the integrated flux on $\partial\Omega$ to that of domains for which the solution of the Dirichlet problem is exactly known, for example spheres and half planes. In this way we establish the following bounds on $G_\xi(s)$.

Lemma 3.4.6 *If $\xi \leq \frac{3}{40}$ then there exists a s^* such that $G(s^*) \geq s^*$.*

Proof The reflected source at $z = -\eta$ contributes positively to the flux. Since we are interested in a lower bound, we can safely ignore it. For some R, $\xi < R < 2$ let B_R be a ball of radius R centred around the VSC. The surface of the ball may intersect $\partial\Omega$ in multiple points, let s^* identify the coordinate of the point furthest from the tip where $\partial\Omega$ intersects the surface of this ball,

$$s^* = \max\{s | (r(s), z(s)) \in \partial\Omega \cap \partial B_R\}. \tag{3.4.15}$$

Let ∂B_R^+ be that part of ∂B_R which lies in the positive z halfspace. Note that since $z(s) \leq 0$ and $R > \xi$, ∂B_R^+ is non empty and lies outside of Ω. The comparison principle, Theorem 3.4.4, now states that

$$\begin{aligned} 2\pi G_\xi(s^*) &\geq \int_{\partial\Omega \cap B_R} F_u \mathrm{d}S \geq \int_{\partial B_R \setminus \Omega} \frac{1}{R^2} \mathrm{d}S \geq \int_{\partial B_R^+} \frac{1}{R^2} \mathrm{d}S \\ &\geq \pi \frac{R^2 - (R - \xi)^2}{R^2}. \end{aligned} \tag{3.4.16}$$

We now set $R = 2\xi$ to obtain that $G(s^*) \geq \frac{3}{8}$. The point $(r(s^*), z(s^*))$ lies on ∂B_R, so $r(s^*) \leq 2\xi$ and $z(s^*) \geq -3\xi$. By integrating (3.3.2), $s^* \leq r(s^*) - z(s^*) \leq 5\xi$ and so if $\xi \leq \frac{3}{40}$ then $s^* \leq \frac{3}{8} \leq G_\xi(s^*)$.

■

Lemma 3.4.7 *If s_{max} is chosen large enough that $s_{max} \geq \xi_{max} + 2$ then*

$$G_\xi(s) \leq 8 \left(\frac{s}{\xi}\right)^2 \qquad \textit{for} \qquad 0 \leq s \leq \min\left(C^{-1}, \sqrt{\xi_{min} C^{-1}}\right). \tag{3.4.17}$$

Proof We wish to use the estimates at the tip derived in Section 3.3.2 so we must require that $s \leq C^{-1}$. Furthermore if $s \leq \sqrt{\xi_{min} C^{-1}}$, then by (3.3.7), $z(s) \geq -\frac{1}{2}\xi$. Also, if $s_{max} \geq \xi_{max} + 2$, then by (3.3.8), $z(s_{max}) \leq -\xi_{max}$, so

$\eta = -2z(s_{max}) - \xi \geq 2\xi_{max} - \xi$. This enables us to estimate the difference in the z coordinate between the point at pathlength s, the source at the VSC and the reflected source:

$$z(s) + \xi \geq \frac{1}{2}\xi \qquad \text{and,} \qquad z(s) + \eta \geq \frac{1}{2}\xi. \tag{3.4.18}$$

We define $\tilde{\Omega}$ to be the half space $\{(r,z)|z \leq z(s)\}$. Let

$$\begin{aligned}\tilde{u}(r,z) = &\left(r^2 + (z+\xi)^2\right)^{-\frac{1}{2}} - \left(r^2 + (z - 2z(s) - \xi)^2\right)^{-\frac{1}{2}} \\ &+ \left(r^2 + (z+\eta)^2\right)^{-\frac{1}{2}} - \left(r^2 + (z - 2z(s) - \eta)^2\right)^{-\frac{1}{2}}.\end{aligned} \tag{3.4.19}$$

Then $\tilde{u}$ solves the Dirichlet problem on $\tilde{\Omega}$ with sources at $z = -\xi$ and $z = -\eta$. The comparison principle for integrated fluxes now states that

$$2\pi G_\xi(s) = \int\limits_{\partial\Omega\setminus\tilde{\Omega}} F_u \mathrm{d}S \leq \int\limits_{\partial\tilde{\Omega}\cap\Omega} F_{\tilde{u}} \mathrm{d}S \tag{3.4.20}$$

$$= 4\pi\left[1 - \left(1 + \left(\frac{r(s)}{\xi + z(s)}\right)^2\right)^{-\frac{1}{2}} + 1 - \left(1 + \left(\frac{r(s)}{\eta + z(s)}\right)^2\right)^{-\frac{1}{2}}\right] \tag{3.4.21}$$

now using the inequality $1 - 1/\sqrt{1+x} \leq \frac{1}{2}x$, the upper bound $r(s) \leq s$, and the estimates (3.4.18), we obtain

$$G_\xi(s) \leq \left(\frac{r(s)}{\xi + z(s)}\right)^2 + \left(\frac{r(s)}{\eta + z(s)}\right)^2 \leq 8\left(\frac{s}{\xi}\right)^2. \tag{3.4.22}$$

■

3.4.4 Monotonicity of G_ξ in ξ

We wish to know how the cumulative flux G_ξ changes as the distance ξ between the tip and the VSC is varied while the domain Ω remains fixed. We can write the Dirichlet problem as follows, let $\tilde{u}_\xi(r,z)$ solve

$$\begin{aligned}\Delta\tilde{u}_\xi &= 0 && \text{in } \Omega, \\ \tilde{u}_\xi &= -\frac{1}{(r^2 + (z+\xi)^2)^{\frac{1}{2}}} - \frac{1}{(r^2 + (z+\eta)^2)^{\frac{1}{2}}} && \text{on } \partial\Omega\end{aligned} \tag{3.4.23}$$

then

$$u_\xi(r,z) = \tilde{u}_\xi(r,z) + \frac{1}{(r^2 + (z+\xi)^2)^{\frac{1}{2}}} + \frac{1}{(r^2 + (z+\eta)^2)^{\frac{1}{2}}} \tag{3.4.24}$$

solves (3.2.13). We now differentiate with respect to ξ; note that $\frac{\mathrm{d}\eta}{\mathrm{d}\xi} = -1$. Let $\tilde{v}_\xi(r,z)$ solve

$$\begin{aligned} \Delta\tilde{v}_\xi &= 0 && \text{in } \Omega, \\ \tilde{v}_\xi &= \frac{z+\xi}{(r^2+(z+\xi)^2)^{\frac{3}{2}}} - \frac{z+\eta}{(r^2+(z+\eta)^2)^{\frac{3}{2}}} && \text{on } \partial\Omega \end{aligned} \tag{3.4.25}$$

By Lemma 3.3.3, $\tilde{v}_\xi$ is bounded on $\partial\Omega$, and so by the maximum principle it is bounded in Ω. We define $v_\xi(r,z)$ as

$$v_\xi(r,z) = \tilde{v}_\xi(r,z) - \frac{z+\xi}{(r^2+(z+\xi)^2)^{\frac{3}{2}}} + \frac{z+\eta}{(r^2+(z+\eta)^2)^{\frac{3}{2}}}, \tag{3.4.26}$$

then $v_\xi = \frac{\partial}{\partial\xi}u_\xi$, essentially v_ξ solves a Dirichlet problem with zero boundary condition and two dipoles of opposite orientation at $z = -\xi$ and $z = -\eta$ as sources. We will first show that Ω can be divided into two connected subsets, where v_ξ is positive or negative. We will then show that this also divides the boundary $\partial\Omega$ into two connected subsets, bordering the respective subsets of Ω. Lastly we will examine the cumulative flux of v_ξ and prove a monotonicity result for $G_\xi(s)$.

Near the dipole source, Ω is divided into two regions where v_ξ is positive or negative with a surface separating these two. The following Lemma states this division can be extended to the whole domain.

Lemma 3.4.8 *Let v_ξ be defined as in (3.4.26) on a domain Ω sufficiently smooth that the maximum principle holds and such that the points $(0,-\xi)$ and $(0,-\eta)$ lie in the interior of Ω. Let*

$$\begin{aligned} \Omega^+ &= \{(r,z,\theta) \in \Omega | v(r,z) > 0 \text{ and } z > z(s_{max})\}, \\ \Omega^- &= \{(r,z,\theta) \in \Omega | v(r,z) < 0 \text{ and } z > z(s_{max})\}, \end{aligned} \tag{3.4.27}$$

then for sufficiently large s_{max}, Ω^- and Ω^+ are connected sets.

Proof Let B be a ball centred around the point $(0,-\xi)$, such that $d = \mathrm{dist}(\partial B, \partial\Omega) > 0$. The boundary condition imposed on $\tilde{v}_\xi$ in (3.4.25) is bounded and continuous, and thus by the maximum principle, $\tilde{v}_\xi$ is bounded in Ω. By [12] Theorem 2.10 the derivatives of $\tilde{v}_\xi$ are bounded in B, $\sup_B \left|\frac{\partial\tilde{v}_\xi}{\partial z}\right| \leq \frac{3}{d}\sup_\Omega |\tilde{v}_\xi|$. We now examine $v_\xi(r,z)$ on the cylinder defined by $r \leq R$ and $|z+\xi| \leq Z$ for some sufficiently small R and $Z = \frac{1}{\sqrt{3}}R$. Since $\eta = O(s_{max})$, the contribution of the reflected source to v_ξ in this cylinder is $O(s_{max}^{-2})$ and its contribution to $\frac{\partial v_\xi}{\partial z} = O(s_{max}^{-3})$, so we can choose s_{max} sufficiently large that

$$\left|\frac{z+\eta}{(r^2+(z+\eta)^2)^{\frac{3}{2}}}\right| \leq 1, \qquad \text{and} \qquad \left|\frac{\partial}{\partial z}\left(\frac{z+\eta}{(r^2+(z+\eta)^2)^{\frac{3}{2}}}\right)\right| \leq 1. \tag{3.4.28}$$

We now estimate v_ξ on the caps of the cylinder,

$$\begin{aligned} v_\xi(r, Z-\xi) &\le \sup_\Omega |\tilde{v}_\xi| + 1 - \frac{Z}{(R^2+Z^2)^{\frac{3}{2}}} \\ &\le \sup_\Omega |\tilde{v}_\xi| + 1 - \frac{9}{8}\frac{1}{R^2}, \\ v_\xi(r, -Z-\xi) &\ge -(\sup_\Omega |\tilde{v}_\xi| + 1) + \frac{Z}{(R^2+Z^2)^{\frac{3}{2}}} \\ &\ge -(\sup_\Omega |\tilde{v}_\xi| + 1) + \frac{9}{8}\frac{1}{R^2}, \end{aligned} \tag{3.4.29}$$

while on the cylinder,

$$\frac{\partial v_\xi}{\partial z}(R,z) \le \sup_B \left|\frac{\partial \tilde{v}_\xi}{\partial z}\right| + 1 - \frac{R^2-2Z^2}{(R^2+Z^2)^{\frac{5}{2}}} \le \sup_B \left|\frac{\partial \tilde{v}_\xi}{\partial z}\right| + 1 - \frac{3\sqrt{3}}{32}\frac{1}{R^3}. \tag{3.4.30}$$

Therefore we can choose an R_{max} such that for all $R < R_{max}$, $v_\xi(R, Z-\xi) < 0$, $v_\xi(R, -Z-\xi) > 0$ and $\frac{\partial v_\xi}{\partial z}(R,z) < 0$. Thus $z \to v_\xi(R,z)$ has a unique zero z_0. In other words, there exists a function $z_0(r)$ defined on the interval $[0, R_{max}]$ such that $|z_0(r) + \xi| \le \frac{1}{\sqrt{3}} r$ and $v_\xi(r, z_0(r) = 0$. By the implicit function theorem, z_0 is continuous and so this function defines a surface Σ which is part of the interface between Ω^+ and Ω^-. By continuity, $\partial\Omega^+ \cap \Sigma$ and $\partial\Omega^- \cap \Sigma$ are both non empty and both boundaries contain the dipole at $z = -\xi$. Let Ω_1 and Ω_2 be two connected components of Ω^+ or Ω^-. Assume $(0, -\xi) \notin \partial\Omega_{1,2}$, then v_ξ is harmonic in $\Omega_{1,2}$ (note that we excluded the singularity in $(0, -\eta)$ by demanding that $z > z(s_{max}),$) and $v_\xi = 0$ on $\partial\Omega_{1,2}$. The maximum principle then implies that $v_\xi = 0$ on $\Omega_{1,2}$ which is a contradiction. However, since all points in the neighbourhood of $(0, -\xi)$ for which $v_\xi = 0$ are contained in a subset $\tilde{\Sigma}$ of Σ, $\tilde{Sigma} \subset \partial\Omega_{1,2}$ so Ω_1 and Ω_2 are connected and must be equal to one another. ■

The division of Ω into two regions of positive and negative v_ξ similarly divides the boundary into two parts.

Lemma 3.4.9 *Let Ω be a domain sufficiently smooth such that the maximum principle holds, let Ω^+, Ω^- and v_ξ be defined as in the previous lemma. Then $\partial\Omega^+ \cap \partial\Omega$ and $\partial\Omega^- \cap \partial\Omega$ are closed connected sets.*

Proof This is essentially a 2D argument, since we assume radial symmetry we restrict ourselves to some plane at $\theta = 0$. We examine the region on the boundary with positive or negative flux. Let $I^\pm = \{s \in [0, s_{max}] | (r(s), z(s)) \in \partial\Omega^\pm \cap \partial\Omega\}$ be the set of parameter values whose respective points on the boundary border Ω^+ respectively Ω^-. Clearly these are closed sets. Let R_{max} be as in the proof of Lemma 3.4.8 and let $z^\pm = -\xi \pm \frac{1}{\sqrt{3}} R_{max} - \xi$. By the arguments of the previous Lemma, $(0, z^+) \in \tilde{\Omega}^-$ and $(0, z^-) \in \tilde{\Omega}^+$.

Let $s^- \in I^-$ and $s^+ \in I^+$, we will first show that $s^- \leq s^+$. Assume $s^- > s^+$, since Ω^+ and Ω^- are connected, there exist paths connecting $r(s^-), z(s^-)$ to $(0, z^+)$ and $(r(s^+), z(s^+))$ to $(0, z^-)$, such that these paths lie completely inside Ω^- respectively Ω^+. Since $z(s^+) > z(s^-)$ by the monotonicity of z, clearly these paths must intersect, which is a contradiction. Thus for $s^- \in I^-$, all points $s < s^-$ are also in I^-, similarly for $s^+ \in I^+$ all points $s > s^+$ are in I^+. Thus I^+ and I^- are closed intervals.

■

We now have enough information on v_ξ near the boundary to prove the following monotonicity result.

Lemma 3.4.10 *For sufficiently large s_{max} the cumulative flux G_ξ is strictly monotone and differentiable in ξ,*

$$\frac{\partial G_\xi}{\partial \xi}(s) < 0, \tag{3.4.31}$$

furthermore, this derivative is $C^{1,\alpha}$ Hölder continuous.

Proof We wish to examine the cumulative flux $H_\xi(s)$ of v_ξ,

$$H_\xi(s) = \frac{\partial}{\partial \xi} G_\xi(s) = \int_0^s F_v(\sigma) r(\sigma) \mathrm{d}\sigma, \tag{3.4.32}$$

where $F_v(\sigma) = -\frac{\partial v_\xi}{\partial \hat{n}}(r(s), z(s))$. By Lemmas 3.4.2 and 3.4.9 there are two closed intervals I^+ and I^- such that the flux F_v is positive, respectively negative, everywhere on these intervals and cannot be zero on an open subinterval. If $s^* \in [0, s_{max}] \setminus (I^+ \cup I^-)$ then there would exist a $R > 0$ such that a ball of radius R around $(r(s^*), z(s^*))$ lies neither in Ω^+ nor in Ω^- (where $\Omega^\pm$ is defined as in Lemma 3.4.8.) This is a contradiction since v_ξ cannot be zero on an open subset of Ω. Therefore the union of I^+ and I^- is the whole interval $[0, s_{max}]$. The flux must be zero on the intersection of these two intervals, and so this intersection must be either empty or be equal to a singleton $\{s_0\}$. It cannot be empty since the union of two disjoint closed intervals cannot be an interval. Therefore $I^- = [0, s_0]$ and $I^+ = [s_0, s_{max}]$. The cumulative flux $H_\xi(s)$ is strictly decreasing for $s \in I^-$ and strictly increasing for $s \in I^+$, by the divergence theorem $H_\xi(s_{max}) = 0$ so $H_\xi(s) < 0$ for $s \in (0, s_{max})$.

■

3.5 The travelling wave ODE

In this section we will assume we are given a family of functions $G_\xi(s)$ parametrized by ξ with

$$\begin{aligned} 0 < G_\xi(s) < 2 \qquad & \text{for } 0 < s < s_{max}, \\ G_\xi(s_{max}) = 2, & \\ G'_\xi(s) \geq 0, & \\ G_\xi(s) \leq \frac{1}{2}\tilde{C}(\xi) s^2 \quad & \text{for } 0 \leq s \leq \tilde{C}(\xi)^{-1}, \end{aligned} \tag{3.5.1}$$

where the constant $\tilde{C}(\xi)$ is given in Lemma 3.4.7. Using this we will solve the travelling wave ODE for each ξ,

$$r'_\xi(s) = \sqrt{1 - \left(\frac{G_\xi(s)}{r_\xi(s)}\right)^2}, \qquad r_\xi(0) = 0, \qquad r'_\xi(0) = 1 \tag{3.5.2}$$

and show that there exists a ξ^* such that $r_{\xi^*}(s_{max}) = 2$. Since this differential equation is not Lipschitz, we cannot use standard arguments for existence and uniqueness of solutions. In fact, there are many solutions satisfying $r_\xi(0) = 0$, in subsection 3.5.1 we will use a contraction argument to show that there is a unique solution $r_{f,\xi}$ which also satisfies $r'_{f,\xi}(0) = 1$. In subsection 3.5.3 we then show there is a unique solution $r_{b,\xi}$ satisfying $r_{b,\xi}(s_{max}) = 2$. Finally in subsection 3.5.4 we show that for $\xi = \xi^*$ these two solutions match, giving the desired solution.

3.5.1 The forward solution

In this section we show that, for each ξ there exists a solution starting at $s = 0$. We substitute $r_\xi(s) = s - s^3 x(s)$, a function $x(s)$ solving the ODE must then be a fixed point of the integral operator Φ.

$$\Phi[x](s) = \frac{1}{s^3}\int_0^s 1 - \sqrt{1 - h(x(\sigma), \sigma)}\mathrm{d}\sigma, \tag{3.5.3}$$

where

$$h(x, s) = \left(\frac{G_\xi(s)}{s - s^3 x}\right)^2. \tag{3.5.4}$$

We examine Φ on the ball B of radius $\frac{1}{9}\tilde{C}(\xi)^2$ in the space of continuous bounded functions on the interval $[0, \tilde{C}(\xi)^{-1}]$ equipped with the supremum norm.

Lemma 3.5.1 *The integral operator Φ has a unique fixed point on B.*

Proof First of all $\Phi : B \to B$. To see this, assume $x(s) \le a\tilde{C}(\xi)^2$ for some value of a. If $a \le \frac{1}{2}$ then for $s \le \tilde{C}(\xi)^{-1}$, $\frac{G_\xi(s)}{s - s^3 x(s)} \le \frac{1}{2}\frac{\tilde{C}(\xi)}{1-a}s \le \frac{1}{2(1-a)} \le 1$. Now for $h \le 1$, $1 - \sqrt{1-h} \le h$ and so $\Phi[x](s) \le \frac{1}{12}\frac{\tilde{C}(\xi)^2}{(1-a)^2}$. If we set $a = \frac{1}{9}$ then $\Phi[x](s) \le a\tilde{C}(\xi)^2$.

Furthermore, Φ is a contraction on B. Let $\|\cdot\|$ be the supremum norm on B,

$$\|\Phi[x_2] - \Phi[x_1]\| \le \frac{1}{s^3}\int_0^s \sup_{x\in[x_1,x_2]} \left|\frac{\partial}{\partial x}\left(1 - \sqrt{1 - h(x,\sigma)}\right)\right| \cdot |x_2(\sigma) - x_1(\sigma)|\,\mathrm{d}\sigma. \tag{3.5.5}$$

Now,

$$\begin{aligned} \frac{\partial}{\partial x}\left(1 - \sqrt{1 - h(x,s)}\right) &= \frac{G_\xi(s)^2}{(1 - s^2x)^3\sqrt{1 - h(x,s)}} \\ \le \frac{1}{4(1-a)^3\sqrt{1 - \frac{1}{4(1-a)^2}}}s^2 &\le \frac{1}{2}s^2 \qquad \text{for } a = \frac{1}{9}. \end{aligned} \tag{3.5.6}$$

Therefore, $\|\Phi[x_2] - \Phi[x_1]\| \leq \frac{1}{6}\|x_2 - x_1\|$. By the Banach fixed point theorem, Φ must have a fixed point.

■

We will denote this fixed point as $r_{f,\xi}$.

3.5.2 Determination of ξ_{min} and ξ_{max}

We wish to find a value ξ^* such that r_{f,ξ^*} can be continued to the interval $(0, s_{max}]$ with $r_{f,\xi^*}(s_{max}) = 2$. Clearly, since $r_{f,\xi}(s) \leq s$, if at some point s^*, $G_\xi(s^*) \geq s^*$ then we cannot continue the solution at this value of ξ since $r'_{f,\xi}(s^*)$ would not be defined. By Lemma 3.4.6 such a value of s^* exists, and so $\xi^* \geq \xi_{min} = \frac{3}{40}$.

If there exists an $s^* \leq s_{max}$ such that $r_{f,\xi}(s^*) \geq 2$, the solution can be continued till infinity, however, due to the monotonicity of $r_{f,\xi}$ it will be impossible to meet the requirement that $r_{f,\xi}(s_{max}) = 2$. By Lemma 3.5.1, $r_{f,\xi}(\tilde{C}(\xi)^{-1}) \geq \frac{8}{9}\tilde{C}(\xi)^{-1}$, so if $\tilde{C}(\xi) \leq \frac{4}{9}$ and $\tilde{C}(\xi)^{-1} < s_{max}$ then the continuation of r_ξ will grow too large. By Lemma 3.4.7, $\tilde{C}(\xi) = \frac{16}{\xi^2}$ and so $\xi^* \leq \xi_{max} = 6$.

3.5.3 The backwards solution

In this section we will show that there exists a unique solution from $s = s_{max}$ with $r_\xi(s_{max}) = 2$ extending backwards till $s = 0$.

Lemma 3.5.2 *Given $\xi \in (\xi_{min}, \xi_{Max})$ and $s^* \in (0, s_{max})$. Then any two functions r_1 and r_2 solving (3.5.2) on an interval $(s_0, s^*]$ having equal endpoints, $r_1(s^*) = r_2(s^*)$, must be equal over the entire interval.*

Proof We write the ODE as $r' = f(r(s), s)$ and examine the derivative to r,

$$\frac{\partial f}{\partial r} = \frac{1}{f(r,s)}\frac{G_\xi(s)^2}{r^3} > 0. \tag{3.5.7}$$

Now assume r_1 and r_2 are two different solutions to (3.5.2) on an interval $I = (s^* - \delta, s^*)$ such that $r_1(s^*) = r_2(s^*)$. We will show that there is a contradiction. If r_1 and r_2 are different, there exists an $s_0 \in I$ such that $r_2(s_0) \neq r_1(s_0)$. Without loss of generality, assume that $r_2(s_0) > r_1(s_0)$. The difference between r_2 and r_1 satisfies the differential equation

$$\frac{\mathrm{d}}{\mathrm{d}s}\left(r_2(s) - r_1(s)\right) = \int_{r_1(s)}^{r_2(s)} \frac{\partial f}{\partial r}\mathrm{d}r > 0. \tag{3.5.8}$$

and so $r_2(s) - r_1(s) > r_2(s_0) - r_1(s_0) > 0$ for all $s > s_0$, specifically at $s = s^*$.

■

Lemma 3.5.3 *Given $\xi \in (\xi_{min}, \xi_{max})$ and $s^* \in (0, s_{max}]$ then there exists a unique solution $r : (0, s^*] \to [0, 2]$ to the differential equation (3.5.2) satisfying $r(s^*) = G_\xi(s^*)$.*

Proof We examine the differential equation

$$r'(s) = f(s, r(s)), \tag{3.5.9}$$

where

$$f(s,r) = \begin{cases} \sqrt{1 - \left(\dfrac{G_\xi(s)}{r}\right)^2} & \text{if } r \geq G_\xi(s) \text{ and } s \leq s_{max}, \\ 0 & \text{if } r \leq G_\xi(s) \text{ and } s \leq s_{max}, \\ \sqrt{1 - \left(\dfrac{2}{r}\right)} & \text{if } r \geq 2 \text{ and } s \geq s_{max}, \\ 0 & \text{if } r \leq 2 \text{ and } s \geq s_{max}. \end{cases} \tag{3.5.10}$$

The function f is continuous, so by Peano's existence theorem there exist solutions $s \mapsto r(s)$ satisfying $r(s^*) = G(s^*)$ defined in a neighbourhood of s^*. Assume there is an $s_0 < s^*$ in this neighbourhood such that $r(s_0) < G_\xi(s_0)$. Let $s_1 = \min\{s \in (s_0, s^*] | r(s) \geq G_\xi(s)\}$, this definition makes sense since r and G_ξ are continuous and $r(s^*) = G_\xi(s^*)$. By the mean value theorem there exists an $s_2 \in (s_0, s_1)$ such that

$$r'(s_2) = \frac{r(s_1) - r(s_0)}{s_1 - s_0} > \frac{G_\xi(s_1) - G_\xi(s_0)}{s_1 - s_0} > 0, \tag{3.5.11}$$

since $G_\xi(s)$ is strictly monotone. Thus by (3.5.9), $r(s_2) \geq G_\xi(s_2)$ which is in contradiction with our definition of s_1. Therefore $r(s) \geq G_\xi(s)$ for $s \leq s^*$ and the restriction of our solution to $s \leq s_{max}$ solves (3.5.2), repeating this argument enables us to extend this solution until $s = 0$. Uniqueness then follows from Lemma 3.5.2. ■

Setting $s^* = s_{max}$ in Lemma 3.5.3 we obtain a unique solution on $(0, s_{max}]$.

3.5.4 Matching

In the previous sections we have constructed solutions to the travelling wave ODE. The forward solution, which we denote as $r_{f,\xi}$, exists on an interval $[0, \tilde{C}(\xi)]$ while the backward solution $r_{b,\xi}$, exists on the interval $(0, s_{max}]$. We will examine both solutions at the point $s = \bar{C}^{-1}$, where

$$\bar{C}^{-1} = \min_{\xi \in [\xi_{min}, \xi_{max}]} \{\tilde{C}(\xi)^{-1}\}. \tag{3.5.12}$$

If we examine the solutions at $\xi = \xi_{min}$ we see that at some point s^*, $r_{f,\xi_{min}}(s^*) = G_{\xi_{min}}(s^*) \leq r_{b,\xi min}(s^*)$. Since solutions to the same ODE cannot intersect,

$$r_{f,\xi_{min}}(\bar{C}^{-1}) \leq r_{b,\xi min}(\bar{C}^{-1}). \tag{3.5.13}$$

Similarly, examining the solution at $\xi = \xi_{max}$ we see that $r_{f,\xi_{max}}(\bar{C}(\xi_{max})^{-1}) \geq 2 \geq r_{b,\xi_{max}}(\bar{C}(\xi_{max})^{-1})$ and so

$$r_{f,\xi_{max}}(\bar{C}^{-1}) \geq r_{b,\xi max}(\bar{C}^{-1}). \tag{3.5.14}$$

Lemma 3.5.4 *The forwards and backwards solutions $r_{f,\xi}$ and $r_{b,\xi}$ are strict monotone in ξ for $s > 0$,*

$$\frac{\partial r_{f,\xi}}{\partial \xi} > 0, \qquad \frac{\partial r_{b,\xi}}{\partial \xi} < 0. \tag{3.5.15}$$

Proof If we differentiate the ODE (3.5.2) to ξ we see that $u = \frac{\partial r_\xi}{\partial \xi}$ satisfies the differential equation

$$\frac{\mathrm{d}u}{\mathrm{d}s}(s) = f(s)u(s) + g(s), \tag{3.5.16}$$

where

$$f(s) = \frac{G_\xi(s)^2}{r'_\xi(s) r_\xi(s)^3}, \quad g(s) = -\frac{G_\xi(s)}{r'_\xi(s) r_\xi(s)^2} \frac{\partial G_\xi}{\partial \xi}. \tag{3.5.17}$$

Since r_ξ, r'_ξ and G_ξ are positive, $f(s) > 0$ for $s > 0$ and by Lemma 3.4.10, $g(s) > 0$ for $s > 0$.

To study the forward solution, we examine the solution of this ODE with initial condition $u(0) = 0$. By (3.3.5) and Lemma 3.4.7 its clear that f and g remain bounded as $s \to 0$, so by the variation of constants formula

$$\frac{\partial r_{f,\xi}}{\partial \xi}(s) = e^{-\mu(s)} \int_0^s e^{\mu(\sigma)} g(\sigma) \mathrm{d}\sigma > 0 \tag{3.5.18}$$

where

$$\mu(s) = \int_0^s f(\sigma) \mathrm{d}\sigma. \tag{3.5.19}$$

For the backwards solution, $r_{b,\xi}(s_{max}) = G_\xi(s_{max}) = 2$ for all ξ. So a similar variations of constants arguments, with $u(s_{max}) = 0$ yields that $\frac{\partial r_{b,\xi}}{\partial \xi} < 0$.

■

The inequalities for the forward and backward solutions at $s = \tilde{C}^{-1}$, together with the strict monotonicity established in the above Lemma yield that there must exist an unique $\xi^* \in [\xi_{min}, \xi_{max}]$ such that

$$r_{f,\xi^*}(\tilde{C}^{-1}) = r_{b,\xi^*}(\tilde{C}^{-1}). \tag{3.5.20}$$

We now define $r_{\xi^*}(s)$ to be equal to r_{f,ξ^*} if $s \leq \tilde{C}^{-1}$ and equal to r_{b,ξ^*} otherwise. Thus r_{ξ^*} solves (3.5.2) with the desired boundary conditions at $s = 0$ and $s = s_{max}$.

3.6 Fixed point of the Schauder map

In Sections 3.4 and 3.5 we defined a map from $\Xi(M, A, C; s_{max})$ to $C^{1,\alpha} \times C^{0,\alpha}$. In this section we will choose the constants C, A and M such that the image of this map is a subset of the original domain. We will then show that both domain and image are compact and the map is continuous in the $C^{1,\beta}$ topology for any $\beta < \alpha$, and thereby satisfies all the requirements of Schauder's fixed point theorem.

3.6.1 Determination of C

From Lemma 3.4.7 we have that

$$G_{\xi^*}(s) \leq \frac{1}{2}\tilde{C}s^2 \qquad \text{for } 0 \leq s \leq \tilde{C}^{-1}, \tag{3.6.1}$$

where $\tilde{C} = \max(\frac{16}{\xi_{min}^2}, \sqrt{\frac{C}{\xi_{min}}}, C)$. From Lemma 3.5.1 and the monotonicity of r_{ξ^*} we then have that

$$\begin{aligned} s - \frac{1}{9}\tilde{C}^2 s^3 \leq r_{\xi^*}(s) \leq 2 \quad &\text{for} \qquad 0 \leq s \leq \tilde{C}^{-1}, \\ \frac{8}{9}\tilde{C}^{-1} \leq r_{\xi^*}(s) \leq 2 \quad &\text{for} \quad \tilde{C}^{-1} \leq s \leq s_{max}, \end{aligned} \tag{3.6.2}$$

If we choose $C \geq \frac{16}{\xi_{min}^2} = \frac{25600}{9}$ then $\tilde{C} = C$.

3.6.2 Determination of A

If one were to differentiate (3.5.2) to s we would obtain

$$r''_{\xi^*} = \frac{G_{\xi^*}^2}{r_{\xi^*}^3} - \frac{G_{\xi^*}}{r_{\xi^*}^2}\frac{G'_{\xi^*}}{r'_{\xi^*}} \quad z''_{\xi^*} = \frac{G_{\xi^*}}{r_{\xi^*}^2}r'_{\xi^*} - \frac{G'_{\xi^*}}{r_{\xi^*}}. \tag{3.6.3}$$

Since r'_{ξ^*} might be equal to zero, the negative contribution to r''_{ξ^*} may be infinite and we cannot say that r is twice differentiable. The difference quotients of the first derivatives are however always defined, and equal to

$$r'_{\xi^*}(s_2) - r'_{\xi^*}(s_1) = \int_{s_1}^{s_2} \frac{G_{\xi^*}^2}{r_{\xi^*}^3} - \frac{G_{\xi^*}}{r_{\xi^*}^2}\frac{G'_{\xi^*}}{r'_{\xi^*}}\mathrm{d}s \quad \leq \int_{s_1}^{s_2} \frac{G_{\xi^*}^2}{r_{\xi^*}^3}\mathrm{d}s, \tag{3.6.4}$$

where without loss of generality we can assume that $s_2 \geq s_1$. Now using (3.6.1), (3.6.2) and the fact that by the divergence theorem, $G_{\xi^*}(s) \leq 2$ one can estimate

$$\begin{aligned} \frac{G_{\xi^*}^2}{r_{\xi^*}^3} \leq \frac{1}{4}\frac{C^2}{(1-\frac{1}{9}C^2s^2)^3}s \leq \frac{1}{4}\left(\frac{9}{8}\right)^3 C \quad &\text{for} \qquad 0 \leq s \leq C^{-1}, \\ \frac{G_{\xi^*}^2}{r_{\xi^*}^3} \leq 4\left(\frac{9}{8}\right)^3 C^3 \quad &\text{for} \quad C^{-1} \leq s \leq s_{max}, \\ \frac{G_{\xi^*}}{r_{\xi^*}^2} \leq \frac{1}{2}\frac{C}{(1-\frac{1}{9}C^2s^2)^2} \leq \frac{1}{4}\left(\frac{9}{8}\right)^2 C \quad &\text{for} \qquad 0 \leq s \leq C^{-1}, \\ \frac{G_{\xi^*}}{r_{\xi^*}^2} \leq 2\left(\frac{9}{8}\right)^2 C^2 \quad &\text{for} \quad C^{-1} \leq s \leq s_{max}. \end{aligned} \tag{3.6.5}$$

All four of these estimates are bounded and only depend on the constant C determined previously, and so we can choose a suitable A such that we can estimate

$$r'_{\xi^*}(s_2) - r'_{\xi^*}(s_1) \leq A(s_2 - s_1). \tag{3.6.6}$$

Similar arguments yield the estimate for the difference quotient on z'_{ξ^*}.

3.6.3 Hölder continuity

We have now established enough bounds on r_{ξ^*} and G_{ξ^*} to establish an uniform $C^{1,\alpha}$ Hölder norm. Since r'_{ξ^*} is the square root of a C^1 function, we expect it to be bounded for Hölder exponent $\alpha \leq \frac{1}{2}$.

Lemma 3.6.1 *There is an M, independent of s_{max}, such that the solutions r_{ξ^*} and z'_{ξ^*} have the following Hölder norms for Hölder exponent $\alpha \leq \frac{1}{2}$:*

$$\begin{aligned} \|r_{\xi^*}\|_{1,\alpha} &\leq M, \\ \left\|z'_{\xi^*}\right\|_{0,\alpha} &\leq M. \end{aligned} \tag{3.6.7}$$

Proof We estimate the difference in first derivatives at points s_1 and s_2,

$$\begin{aligned} \left|r'_{\xi^*}(s_2) - r'_{\xi^*}(s_1)\right| &= \left| \sqrt{1 - \left(\frac{G_{\xi^*}(s_2)}{r_{\xi^*}(s_2)}\right)^2} - \sqrt{1 - \left(\frac{G_{\xi^*}(s_1)}{r_{\xi^*}(s_1)}\right)^2} \right| \\ &\leq \sqrt{\left| \left(\frac{G_{\xi^*}(s_2)}{r_{\xi^*}(s_2)}\right)^2 - \left(\frac{G_{\xi^*}(s_1)}{r_{\xi^*}(s_1)}\right)^2 \right|} \\ &\leq \left| \max\left(\frac{\mathrm{d}}{\mathrm{d}s}\left(\frac{G_{\xi^*}^2}{r_{\xi^*}^2}\right)\right)\right|^{\frac{1}{2}} \cdot |s_2 - s_1|^{\frac{1}{2}}. \end{aligned} \tag{3.6.8}$$

Now,

$$\frac{\mathrm{d}}{\mathrm{d}s}\left(\frac{G_{\xi^*}(s)^2}{r_{\xi^*}(s)^2}\right) = \frac{2G_{\xi^*}G'_{\xi^*}}{r_{\xi^*}^2} - \frac{2G_{\xi^*}^2 r'_{\xi^*}}{r_{\xi^*}^3}, \tag{3.6.9}$$

and using Lemma 3.4.3 and estimates (3.6.5) we see all these terms are uniformly bounded by constants depending only on C, A, ξ_{min}, and ξ_{max}. Similarly, by (3.6.3) and (3.6.5), z'' can be bounded from above by A, and below by a constant depending only on C, A and F_{max}, and so the Hölder norm of z' can be bound similarly. The constants C, A, ξ_{max} and ξ_{min} have been determined in the previous sections, F_{max} depends only on these constants, thus M can be expressed in terms of these known constants. Specifically, M does not depend on s_{max}.

■

3.6.4 Continuity of $(r, z) \to G_\xi$

We wish to show that, for a sequence $(r_n, z'_n) \in C^{1,\alpha} \times C^{0,\alpha}$ uniformly, describing boundaries $\partial\Omega_n$ such that $(r_n, z_n) \to (\bar{r}, \bar{z})$ in the $C^{1,\beta}$ topology, the associated fluxes $F_n \to \bar{F}$ in the $C^{0,\beta}$ topology. In order to do this we need to create bijections between the domains Ω_n and $\bar{\Omega}$.

Lemma 3.6.2 *There exist surjective mappings $\phi_n : \bar{\Omega} \to \Omega_n \subset \mathbb{R}^3$ such that $\phi_n \in C^{1,\alpha}$ uniformly, and $\phi_n \to \mathrm{Id}$ in the $C^{1,\beta}$ topology.*

Proof We first define ϕ_n on the boundary $\partial\bar{\Omega}$ by mapping the point at pathlength s on $\partial\bar{\Omega}$ to the point at the same pathlength on $\partial\Omega_n$. For $x = (x_1, x_2, x_3) = (\bar{r}(s)\cos\theta, \bar{r}(s)\sin\theta, \bar{z}(s)) \in \partial\bar{\Omega}$,

$$\begin{aligned} \phi_n^{(1)}(x) &= r_n(s)\cos\theta, \\ \phi_n^{(2)}(x) &= r_n(s)\sin\theta, \\ \phi_n^{(3)}(x) &= z_n(s). \end{aligned} \tag{3.6.10}$$

We treat these as boundary conditions and extend $\phi_n^{(i)}$ to the interior by solving $\Delta\phi_n^{(i)} = 0$ for $i = 1, 2, 3$. By Schauder's boundary estimates for $C^{1,\alpha}$ domains ([12], Thm 8.33) $\left\|\phi_n^{(i)}\right\|_{1,\alpha} \leq C(\|r_n\|_{1,\alpha} + \|z_n\|_{1,\alpha})$ where the constant C depends only on the boundary $\partial\bar{\Omega}$. As such, the functions $\phi_n^{(i)}$ are uniformly bounded in the $C^{1,\alpha}$ Hölder norm. Furthermore, $\phi_n(\bar{\Omega}) = \Omega_n$, if there were a point in Ω_n which was not mapped to, the image would have a different topological class than $\bar{\Omega}$ which is impossible for a continuous map. If we were to apply the same procedure to construct a map $\bar{\phi} : \bar{\Omega} \to \bar{\Omega}$ then on the boundary $\bar{\phi}^{(1)}(x)|_{\partial\Omega} = \bar{r}(s)\cos\theta = x_1$. The harmonic extension of this boundary would be $\bar{\phi}^{(1)}(x) = x_1$ and similar for the x_2 and x_3 coordinates, so $\bar{\phi}$ is the identity mapping Id. We now examine $\phi_n^{(1)} - x_1$, this function is harmonic and assumes values $(r_n(s) - \bar{r}(s))\cos\theta$ on the boundary. We apply Schauder's boundary estimates again to see that $\|\phi_n - Id\|_{1,\beta} \leq C(\|r_n - \bar{r}\|_{1,\beta} + \|r_n - \bar{z}\|_{1,\beta})$ with the constant C depending only on $\partial\bar{\Omega}$. Since $r_n \to \bar{r}$ and $z_n \to \bar{z}$ in $C^{1,\beta}$, $\phi_n \to Id$ in $C^{1,\beta}$. ∎

We now examine the Dirichlet problem on Ω_n and $\bar{\Omega}$. For simplicity we place the source at the origin, the tip of each domain lies at $(r, z) = (0, z_n(0))$. We write $u_n(x) = \frac{1}{|x|} - w_n$, $\bar{u} = \frac{1}{|x|} - \bar{w}$ where w_n and $\bar{w}$ are the solutions of

$$\begin{aligned} \Delta w_n = 0 \quad &\text{in } \Omega_n, \quad w_n = \frac{1}{|x|} \quad \text{for } x \in \partial\Omega_n, \\ \Delta \bar{w} = 0 \quad &\text{in } \bar{\Omega}, \qquad \bar{w} = \frac{1}{|x|} \quad \text{for } x \in \partial\bar{\Omega}. \end{aligned} \tag{3.6.11}$$

Now $\frac{1}{|x|}$ is smooth away from the origin, and all it's derivatives can be bounded by a function of d_{min}, the minimal distance between $\partial\Omega_n$ and the origin for all n. So $\left\|\frac{1}{|x|}\right\|_{1,\alpha;\partial\Omega_n} \leq C(\|r_n\|_{1,\alpha} + \|z_n\|_{1,\alpha})$ where the constant C depends only on d_{min}. By the boundary estimates, $\|w_n\|_{1,\alpha;\Omega_n} \leq C(\left\|\frac{1}{|x|}\right\|_{1,\alpha;\partial\Omega_n})$ where the constant C depends on the $C^{1,\alpha}$ norms of r_n and z_n. Since these are uniformly bounded, there is a C independent of n such that $\|w_n\|_{1,\alpha;\Omega_n} \leq C$. We now examine the compositions $w_n \circ \phi_n : \bar{\Omega} \to \mathbb{R}$. Since, by the above Lemma, the maps ϕ_n are uniformly bounded in $C^{1,\alpha}$, these compositions are uniformly bounded in $C^{1,\alpha}$. On the boundary $w_{n_j} \circ \phi_{n_j}|_{\partial\bar{\Omega}} = \frac{1}{|\phi_{n_j}|}$ and clearly converges to $\bar{w}|_{\partial\Omega}$.

Lemma 3.6.3 *Let $\phi_n : \bar{\Omega} \to \Omega_n \subset \mathbb{R}^3$ be a sequence of mappings, $w_n : \Omega_n \to \mathbb{R}$ be a sequence of harmonic functions, and let $\bar{w} : \bar{\Omega} \to \mathbb{R}$ be a harmonic function, such that:*

- *The mappings $\phi_n \to Id$ in the $C^{1,\beta}(\bar{\Omega}; \mathbb{R}^3)$ norm.*
- *The compositions $w_n \circ \phi_n$ are uniformly bounded in the $C^{1,\alpha}(\bar{\Omega}; \mathbb{R})$ norm.*
- *On the boundary, $w_n \circ \phi_n|_{\partial\bar{\Omega}} \to \bar{w}|_{\partial\bar{\Omega}}$ in the $C^{1,\beta}(\partial\bar{\Omega}; \mathbb{R})$ norm.*

Then we have convergence on the full set $\bar{\Omega}$, the compositions $w_n \circ \phi_n \to \bar{w}$ in the $C^{1,\beta}(\bar{\Omega}; \mathbb{R})$ norm.

Proof Since $w_n \circ \phi_n$ is uniformly bounded in $C^{1,\alpha}$ it has a convergent subsequence in $C^{1,\beta}$. Let us examine such a convergent subsequence, which we will also denote as $w_{n_j} \circ \phi_{n_j}$ and let the limit be denoted as $\tilde{w}$. Each w_{n_j} is a weak solution of the Dirichlet problem, so for all $v_{n_j} \in C_0^1(\Omega_{n_j}; \mathbb{R})$

$$\int_{\Omega_{n_j}} \nabla w_{n_j} \cdot \nabla v_{n_j} \mathrm{d}x = 0 \tag{3.6.12}$$

Now $\Omega_{n_j} = \phi_{n_j}(\bar{\Omega})$ and so we can perform a coordinate transform. Furthermore, for sufficiently large n the Jacobian $D\phi_{n_j}$ is sufficiently close to the identity matrix that it can be inverted, and ϕ_{n_j} is a bijection. So writing $v_{n_j} = v \circ \phi_{n_j}^{-1}$, the above statement holds for all $v \in C_0^1(\bar{\Omega}; \mathbb{R})$. Now

$$\begin{aligned}
\int_{\phi_{n_j}(\bar{\Omega})} \nabla w_{n_j} \cdot \nabla v_{n_j} &= \int_{\bar{\Omega}} ((\nabla w_{n_j}) \circ \phi_{n_j}) \cdot ((\nabla v_{n_j}) \circ \phi_{n_j}) \left|\det D\phi_{n_j}\right| \mathrm{d}x \\
&= \int_{\bar{\Omega}} (D\phi_{n_j})^{-1} \nabla (w_{n_j} \circ \phi_{n_j}) \cdot (D\phi_{n_j})^{-1} \nabla v \left|\det D\phi_{n_j}\right| \mathrm{d}x \\
&= 0.
\end{aligned} \tag{3.6.13}$$

We now take the limit as $n \to \infty$, and see that for all v

$$\int_{\bar{\Omega}} \nabla \tilde{w} \cdot \nabla v \mathrm{d}x = 0, \tag{3.6.14}$$

and so $\tilde{w}$ is weakly harmonic. Since $w_n \circ \phi_n|_{\partial\bar{\Omega}} \to \bar{w}|_{\partial\bar{\Omega}}$ and there is only one harmonic function with a given boundary value, $\tilde{w} = \bar{w}$.

Now assume that $w_n \circ \phi_n$ does not converge to $\bar{w}$, then there exist ϵ and N such that for all $n \geq N$, $\|w_n - \bar{w}\|_{1,\beta} \geq \epsilon$. This is in contradiction with the fact that there is a subsequence such that $w_{n_j} \to \bar{w}$.

■

We can now prove the convergence of the fluxes F_n. We consider each flux to be a function on $\partial\bar{\Omega}$ parametrized by s. Then

$$F_n = |(\nabla u_n) \circ \phi_n| = \left| (D\phi_n)^{-1} \left(\nabla \left(\frac{1}{|\phi_n|} \right) - \nabla (w_n \circ \phi_n) \right) \right|, \tag{3.6.15}$$

and clearly

$$F_n \to \left| \nabla \left(\frac{1}{|x|} \right) - \nabla \bar{w} \right| = \bar{F}, \tag{3.6.16}$$

in $C^{0,\beta}$.

3.6.5 Continuity of $G_\xi \to (\xi^*, r_{\xi^*}, z'_{\xi^*})$

We wish to show that for a sequence, $G_{n,\xi}$ of families of cumulative fluxes parametrized by ξ, uniformly bounded in $C^{1,\alpha}$ and converging to $\bar{G}_\xi$ in $C^{1,\beta}$ for each value of ξ, the associated solutions (r_n, z'_n, ξ^*_n) converge to $(\bar{r}, \bar{z}', \bar{\xi}^*)$. Each r_n satisfies

$$\begin{aligned} \int_0^s \sqrt{r_n(\sigma)^2 - G_{n,\xi^*_n}(\sigma)^2} \mathrm{d}\sigma &= \frac{1}{2} r_n(s)^2, \\ \int_0^{s_{max}} \sqrt{r_n(\sigma)^2 - G_{n,\xi^*_n}(\sigma)^2} \mathrm{d}\sigma &= 2. \end{aligned} \tag{3.6.17}$$

Since r_n is uniformly bounded in $C^{1,\alpha}$ and $\xi_n \in [\xi_{min}, \xi_{max}]$ we examine a subsequence of solutions r_{n_j} and ξ_{n_j}, such that $r_{n_j} \to \tilde{r}$ and $\xi^*_{n_j} \to \tilde{\xi}^*$. Now

$$\begin{aligned} \left\| G_{n_j,\xi^*_{n_j}} - \bar{G}_{\tilde{\xi}^*} \right\|_{1,\beta} &\leq \left\| G_{n,\xi^*_{n_j}} - G_{n,\tilde{\xi}^*} \right\|_{1,\beta} + \left\| G_{n_j,\tilde{\xi}^*} - \bar{G}_{\tilde{\xi}^*} \right\|_{1,\beta}, \\ &\leq \left\| \frac{\partial G_{n_j,\xi}}{\partial \xi} \right\|_{1,\beta} \left| \xi_{n_j} - \tilde{\xi} \right| + \left\| G_{n_j,\tilde{\xi}^*} - \bar{G}_{\tilde{\xi}^*} \right\|_{1,\beta}. \end{aligned} \tag{3.6.18}$$

By Lemma 3.4.10 the derivative of the flux to ξ is uniformly bounded in $C^{1,\alpha}$, so $G_{n_j,\xi^*_{n_j}} \to \bar{G}_{\tilde{\xi}^*}$ in $C^{1,\beta}$. Therefore we can pass through the limit and see that $\tilde{r}$, $\tilde{\xi}^*$ and $\bar{G}_{\tilde{\xi}^*}$ satisfy (3.6.17). Since, given a family of cumulative fluxes, solutions to the travelling wave ODE are unique, $\tilde{r} = \bar{r}$ and $\tilde{\xi}^* = \bar{\xi}^*$. Now assume that r_n and ξ^*_n do not converge to $\bar{r}$ and $\bar{\xi}$, then there exist ϵ and N such that for all $n \geq N$, $\|r_n - \bar{r}\|_{1,\beta} \geq \epsilon$ or $\left|\xi^*_n - \bar{\xi}^*\right| \geq \epsilon$. This is in contradiction with the fact that there is a subsequence such that $r_{n_j} \to \bar{r}$ and $\xi^*_{n_j} \to \bar{\xi}^*$.

The quotients $z'_n = \frac{G_{n,\xi^*_n}}{r_{n,\xi^*_n}}$ are uniformly bounded in $C^{1,\alpha}$ and thus have a convergent subsequence z'_{n_j} which converges to $\tilde{z}'$. Now clearly $\tilde{z}'(0) = \bar{z}'(0)$ and for $s > 0$,

$$|\tilde{z}'(s) - \bar{z}'(s)| \leq \left| \tilde{z}'(s) - z'_{n_j}(s) \right| + \frac{1}{r_{n_j}(s)} \left| G_{n_j,\xi^*_{n_j}}(s) - \bar{G}_{\bar{\xi}^*}(s) \right| + \frac{\bar{z}'(s)}{r_{n_j}(s)} \left| \bar{r}(s) - r_{n_j}(s) \right|. \tag{3.6.19}$$

Since the right hand side converges to zero, $\tilde{z}'(s) = \bar{z}'(s)$ for all s. A similar argument as used for the convergence of r_n and ξ_n now yields that $z'_n \to \bar{z}'$ in $C^{0,\beta}$.

3.6.6 Fixed point

We now have all the ingredients to use Schauder's fixed point theorem. The necessary constants C, A, M ξ_{min} and ξ_{max} have been determined in Sections 3.6.1, 3.6.2, 3.6.3, and Section 3.5.2. Since $\Xi(M, A, C; s_{max})$ is bounded in the $C^{1,\alpha} \times C^{0,\alpha}$ norm, its compact in the $C^{1,\beta} \times C^{0,\beta}$ norm. In Sections 3.4 and 3.5 we define a map from $\Xi(M, A, C; s_{max})$ to itself, in 3.6.4 and 3.6.5 we prove this map is continuous in the $C^{1,\beta} \times C^{0,\beta}$ norm. Therefore this map has a fixed point, this fixed point solves the bounded travelling wave problem as defined in Section 3.2.6.

3.7 The limit as $s_{max} \to \infty$

In the previous sections we have shown that, given a sufficiently large value of s_{max} one can find a solution to the travelling wave problem with a bounded domain, as described in Section 3.2.6. In this section we will show that as $s_{max} \to \infty$ the solution profiles approach a limit profile which solves the travelling wave problem on an unbounded domain.

3.7.1 The limit profile r_∞, z_∞

We examine a sequence $s_{max,n}$ such that $s_{max,n} \to \infty$ as $n \to \infty$ and such that $s_{max,n+1} - s_{max,n} > 2$. The estimates established in (3.3.8) then imply that $|z(s_{max})|$ increases monotonically to infinity. Previously we showed that for each value of $s_{max,n}$ one can find a distance ξ_n^* and two functions $r_n : [0, s_{max,n}] \to [0, 2]$ and $z_n : [0, s_{max,n}] \to \mathbb{R}^-$ solving the travelling wave problem on a bounded domain. Since $\xi_n^* \in [\xi_{min}, \xi_{max}]$, it is possible to choose our sequence $s_{max,n}$ such that ξ_n^* converges to some value ξ_∞^* in the same interval.

Since the functions $r_{\xi_n^*}, z'_{\xi_n^*}$ are uniformly bound in $C^{1,\alpha} \times C^{0,\alpha}$, by the Arzela-Ascoli theorem it is always possible to find a subsequence such that the restrictions to a compact interval converge in $C^{1,\beta} \times C^{0,\beta}$. We use this to construct r_∞ and z'_∞.

Let $n_j^{(0)}$ be the sequence $1, 2, 3, \ldots$. For each $i \geq 1$ we define the subsequence $n_j^{(i)}$ of $n_j^{(i-1)}$ such that the restrictions of $r_{n_j^{(i)}}$ and $z'_{n_j^{(i)}}$ to the interval $[0, s_{max,i}]$ converge. We now examine the diagonal sequence $n_j^{(j)}$. Let $I \subset \mathbb{R}^+$ be an arbitrary compact interval. For sufficiently large j, $r_{n_j^{(j)}}$ and $z'_{n_j^{(j)}}$ are defined on this interval and their restrictions converge to functions r_∞ and z'_∞. Since I was arbitrary, the functions r_∞ and z'_∞ are defined on $\mathbb{R}^+$. Integrating z'_∞ with respect to s yields the function z_∞. To simplify notation, for the remainder of Section 3.7 we will denote the sequences of functions $r_{n_j^{(j)}}$ and $z_{n_j^{(j)}}$ as r_n and z_n.

3.7.2 The cumulative flux G_∞

The functions r_∞ and z_∞ define a boundary $\partial\Omega_\infty$ of a domain Ω_∞ in the same manner as described previously. In this case, the domain is unbounded and there is no zero flux boundary condition at $z = z(s_{max})$. We place a source at a distance ξ_∞ from the tip and solve the Dirichlet problem (3.2.1) to obtain a vesicle density u_∞ and the associated flux F_∞ and cumulative flux G_∞. By Lemma 3.4.1, Ω_∞ is of class $C^{1,\alpha}$ and so $G_\infty \in C^{1,\alpha}(\mathbb{R})$. By the divergence theorem, $G_\infty(s) \to 2$ as $s \to \infty$.

The curvature of the limit profile $\partial\Omega_\infty$ has the same upper bound as for the bounded profiles. This again gives an outer sphere condition which enables us to give an upper bound for the flux F_∞.

Lemma 3.7.1 *The flux F_∞ passing though the point $(r_\infty(s), z_\infty(s))$ on the boundary is bounded,*

$$F_\infty \leq F_{max}, \tag{3.7.1}$$

where F_{max} is the same as in Lemma 3.4.3. This implies we can estimate $G'_\infty(s) \leq sF_{max}$ and $G'_\infty(s) \leq 2F_{max}$.

Proof The proof is essentially the same as the first part of the proof of Lemma 3.4.3. In that proof, the reflected source gives a positive contribution and thus can be neglected. ∎

The comparison principle established in Theorem 3.4.4 allows us to calculate the asymptotics of G_∞ as $s \to \infty$.

Lemma 3.7.2 *The cumulative flux G_∞ approaches its limit value of 2 algebraically. For sufficiently large s,*

$$0 < 2 - G_\infty(s) \leq \frac{4}{(s - 2 - \xi_\infty)^2}. \tag{3.7.2}$$

Proof We assume $s > \xi_\infty + 2$, then $z(s) < -\xi$. We use similar arguments as in Lemma 3.4.7 except we compare with a halfspace at the other side of the VSC. Let $\tilde{\Omega}$ be the halfspace $\{(r, z) | z \geq z(s)\}$. Let

$$\tilde{u}(r, z) = (r^2 + (z + \xi)^2)^{-\frac{1}{2}} - (r^2 + (z - 2z(s) - \xi)^2)^{-\frac{1}{2}}, \tag{3.7.3}$$

then $\tilde{u}$ solves the Dirichlet problem on $\tilde{\Omega}$ with a source at $z = -\xi_\infty$. The comparison principle now states that

$$\begin{aligned} 2\pi(2 - G_\infty(s)) &= \int_{\partial\Omega \setminus \tilde{\Omega}} F_u \mathrm{d}S \leq \int_{\partial\tilde{\Omega} \cap \Omega} F_{\tilde{u}} \mathrm{d}S \\ &\leq 4\pi \left[1 - \left(1 + \left(\frac{r(s)}{z(s) + \xi_\infty} \right)^2 \right)^{-\frac{1}{2}} \right], \\ &\leq 2\pi \left(\frac{r(s)}{z(s) + \xi_\infty} \right)^2 \leq 2\pi \left(\frac{2}{s - 2 - \xi_\infty} \right)^2, \end{aligned} \tag{3.7.4}$$

where we used the inequalities $r(s) < 2$ and $-s < z(s) < -s + 2$. ∎

In fact it is possible, by comparing with a capped cylinder instead of a half plane, to show that G_∞ approaches 2 exponentially fast, however the above result is sufficient for our purposes.

3.7.3 The limit of G_n

Let $I \subset \mathbb{R}^+$ be an arbitrary compact interval. For sufficiently large n, G_n is defined on I. In this section we wish to show that, restricted to I, $G_n \to G_\infty$ in the $C^{1,\beta}(I)$ topology. It is sufficient to show this in the case that $I = [0, s^*]$ for some arbitrary, but sufficiently large value of s^*. This can be shown using arguments similar to those used in Section 3.6.4 when showing the continuity of the Schauder map.

Lemma 3.7.3 *Let $I = [0, s^*]$ for some arbitrary but sufficiently large value of s^*. Then,*

$$G_n|_I \to G_\infty|_I \tag{3.7.5}$$

in the $C^{1,\beta}(I)$ norm.

Proof We cut off Ω_∞ at the plane $z = z_\infty(s^*)$. Let $\bar{\Omega}_\infty = \{(r, z) \in \Omega_\infty | z > z_\infty(s^*)\}$. Similarly we cut off Ω_n at the plane $z = z_n(s^*)$, so $\bar{\Omega}_n = \{(r, z) \in \Omega_n | z > z_n(s^*)\}$. Since the restrictions of r_n and z_n to I approach r_∞ and z_∞ in $C^{1,\beta}$ and are uniformly bounded in $C^{1,\alpha}$, by Lemma 3.6.2 there exist mappings $\phi_n : \bar{\Omega} \to \Omega_n \subset \mathbb{R}^3$ which are uniformly bounded in $C^{1,\alpha}$ and converge to the identity in the $C^{1,\beta}$ norm. Let u_n be the solution of the Dirichlet problem (with a zero flux condition at the plane $z = z_n(s_{max,n})$ on Ω_n, restricted to $\bar{\Omega}_n$. Similarly, let u_∞ be the solution to the (unbounded) Dirichlet problem, restricted to $\bar{\Omega}_n$. On $\bar{\Omega}_n$ respectively $\bar{\Omega}_\infty$ we define

$$\begin{aligned} w_n(r, z) &= \frac{1}{\sqrt{r^2 + (z + \xi_n)^2}} - u_n, \\ w_\infty(r, z) &= \frac{1}{\sqrt{r^2 + (z + \xi_\infty)^2}} - u_\infty. \end{aligned} \tag{3.7.6}$$

We examine the compositions $w_n \circ \phi_n$ viewed as functions of s and restricted to I. So $w_n \circ \phi_n|_I(s) = w_n(r_n(s), z_n(s))$. By Lemma 3.3.3 the terms in the square roots are bounded from below. Since $r_n \to r_\infty$, $z_n \to z_\infty$ in $C^{1,\beta}$ and $\xi_n \to \xi_\infty$, the compositions $w_n \circ \phi_n|_I \to w_\infty(r_\infty, z_\infty)|_I$ in the $C^{1,\beta}$ norm. By Lemma 3.6.2, $w_n \circ \phi_n \to w_\infty$ on $\bar{\Omega}$. The same arguments as used at the end of section 3.6.4 now yield that $G_n \to G_\infty$ in $C^{1,\beta}$.

■

3.7.4 Solution to the unbounded travelling wave problem

For sufficiently large n, r_n is defined on the interval I, and for $s \in I$,

$$r_n(s)^2 = 2 \int_0^s \sqrt{r_n(\sigma)^2 - G_n(\sigma)^2} \mathrm{d}\sigma. \tag{3.7.7}$$

Since $r_n \to r_\infty$ and $G_n \to G_\infty$, we pass through the limit to see that r_∞ and G_∞ satisfy the same equation. Differentiating to s and dividing by $r_\infty(s)$ shows that r_∞ satisfies the travelling wave ODE on any arbitrary interval I and thus it satisfies it for all s. Hence r_∞, z'_∞ and ξ^*_∞ solve the unbounded travelling wave problem. Scaling back, as described in Section 3.2.4 results in a solution for arbitrary values of the parameters P and c yielding the proof of our main result, theorem 3.2.1.

3.8 Conclusions

Using a Schauder fixed point argument, we have shown the existence of travelling solutions to the diffusive Vesicle Supply Centre model. Note that Schauder's fixed point theorem does not guarantee uniqueness, and we have not been able to show that this solution is unique by other means. However, we conjecture that this solution is indeed unique, as is the case in the ballistic model in [17]. Possibly one can prove this using the comparison principle (Theorem 3.4.4) along with the equation for travelling solutions (3.2.11). This is a direction for future research.

Since the equations in Section 3.2.5 hold for any flux, not only for the diffusive case, the Schauder map Ψ defined in Section 3.3.1 will have the same form for many models. Therefore the method described in this article should yield an existence proof for various related models, provided similar estimates as those in Sections 3.4 through 3.6 can be derived.

Chapter 4

Asymptotics and other properties of the solution to the diffusive model

The results in this chapter were mainly obtained in an attempt to define a Schauder map, in a similar fashion as in the previous chapter, but in a Hölder $C^{2,\alpha}$ space so that we could use Schauder's fixed point theorem to prove the existence of a $C^{2,\alpha}$ Hölder continuous travelling wave solution to the Diffusive VSC Model. However, as we were incapable of finding a uniform bound on the second derivative of $r(s)$, we abandoned this approach in favour of the $C^{1,\alpha}$ method described in the previous chapter. Attempts to bootstrap the solution from the previous chapter to higher regularity also fail due to various difficulties, however many of the results presented in this chapter still hold for the $C^{1,\alpha}$ solution, while other results hold if one assumes the solution from the previous chapter is $C^{2,\alpha}$ and has certain asymptotics.

We will begin by showing why attempts to bootstrap the $C^{1,\alpha}$ solution do not succeed. We then proceed to prove some properties, mainly asymptotics as $s \to \infty$, for the $C^{1,\alpha}$ solution. Finally we will prove some further properties of this solution, under the assumption of higher regularity.

4.1 The $C^{1,\alpha}$ solution

Our starting point is the solution $r_\infty \in C^{1,\alpha}$ with $0 < \alpha \leq \frac{1}{2}$, z_∞ (the integral of $z'_\infty \in C^{0,\alpha}$) and a constant $\xi^*_\infty \in [\xi_{min}, \xi_{max}]$, and all associated functions found at the end of the previous chapter. To simplify notation we will be dropping all sub and superscripts. We first summarize some of the main equations, estimates and results from the previous chapter.

4.1.1 The ODE and bounds on derivatives

The functions $r : \mathbb{R}^+ \mapsto [0, r_{max})$ and $z : \mathbb{R}^+ \mapsto (-\infty, 0]$ parametrise a curve $\{(r(s), z(s)) | 0 \leq s \leq \infty\}$, which when rotated around the z axis forms the boundary $\partial\Omega$ of a domain Ω. These functions satisfy

$$\begin{aligned} r'(s) &= \sqrt{1 - \left(\frac{G(s)}{r(s)}\right)^2}, \quad r(0) = 0, \quad r'(0) = 1, \quad \lim_{s\to\infty} r(s) = r_{max} = 2, \\ z'(s) &= -\frac{G(s)}{r(s)}, \qquad\qquad z(0) = 0, \quad z'(0) = 0, \quad \lim_{s\to\infty} z(s) = -\infty, \end{aligned} \tag{4.1.1}$$

where G is the cumulative flux of u

$$\begin{aligned} G(s) &= \int_0^s F(\sigma) r(\sigma) \mathrm{d}\sigma, \\ F(s) &= -\frac{\partial u}{\partial \hat{n}}(r(s), z(s)), \end{aligned} \tag{4.1.2}$$

where $\hat{n}$ is the outward normal to $\partial\Omega$, and $u \in C^{1,\alpha}(\bar{\Omega}; \mathbb{R})$ solves

$$\begin{aligned} \Delta u &= -4\pi\delta(r, z + \xi), && \text{in } \Omega, \\ u &= 0, && \text{on } \partial\Omega. \end{aligned} \tag{4.1.3}$$

Here the constant ξ is the distance from the VSC to the tip, and lies between $\xi_{min} = 3/40$ and $\xi_{max} = 6$. Directly from the ODEs we have the following properties

$$\begin{aligned} r'(s)^2 + z'(s)^2 &= 1 && 0 \leq r'(s) \leq 1, \\ r'(s) - z'(s) &\geq 1, && -1 \leq z'(s) \leq 0, \end{aligned} \tag{4.1.4}$$

while from the definition of the domain of the Schauder map in Section 3.3.1 we have

$$\begin{aligned} \|r\|_{1,\alpha} &\leq M, && \frac{r'(s_2) - r'(s_1)}{s_2 - s_1} \leq A && \text{for } s_1 < s_2, \\ \|z'\|_{0,\alpha} &\leq M, && \frac{z'(s_2) - z'(s_1)}{s_2 - s_1} \leq A && \text{for } s_1 < s_2. \end{aligned} \tag{4.1.5}$$

Here A is the constant determined in Section 3.6.2 and M is the constant determined in Lemma 3.6.3.

4.1.2 Estimates in the tip

For $0 \leq s \leq C^{-1}$, where $C = \frac{25600}{9}$ was determined in Section 3.6.1, we have

$$\begin{aligned} s - \frac{1}{9}C^2 s^3 \leq r(s) \leq s, \\ -\frac{1}{2}Cs^2 \leq z(s) \leq 0, \\ 0 \leq G(s) \leq \frac{1}{2}Cs^2. \end{aligned} \tag{4.1.6}$$

4.2 Attempts at C^2 regularity

Differentiating the ODE for the hyphoid solution to s we obtain the following expression for $r''(s)$,

$$r''(s) = \frac{G(s)}{r(s)^2}\Big(\frac{G(s)}{r(s)} - \frac{G'(s)}{r'(s)}\Big). \tag{4.2.1}$$

From (3.6.5) we see that the terms G/r^2 and G/r remain bounded as $s \to 0$, the solution is twice differentiable in the tip. The only reason why r'' might be undefined is if there is some $s^* > 0$ with $r'(s^*) = 0$. From the ODE for the hyphoid solution, we see that this implies that $r(s^*) = G(s^*)$. Furthermore, if $G'(s^*) > 0$ then the solution couldn't exist for $s > s^*$ since the ODE implies that $r(s) \geq G(s)$. Now if $\partial\Omega$ were C^2 we could use the boundary point lemma to conclude that $G'(s) > 0$ everywhere. Since $r(s)$ exists for all s we would have to conclude that $r'(s) > 0$ and thus r is twice differentiable for all s. Unfortunately this is not the case, as far as we know our boundary is $C^{1,\alpha}$. Therefore we have to examine the possibility that there is an s^* such that

$$\begin{aligned} r(s^*) &= G(s^*), \qquad \text{and} \\ r'(s^*) &= G'(s^*) = 0. \end{aligned} \tag{4.2.2}$$

In this section we will examine solutions to the initial (or final) value problem

$$r'(s) = \sqrt{1 - \left(\frac{G(s)}{r(s)}\right)^2}, \tag{4.2.3}$$

with boundary values given by (4.2.2) and various assumptions on $G(s)$. In order to try to prove C^2 regularity we will examine three possibilities:

- Solutions to the ODE with boundary condition (4.2.2) do not exist for $s < s^*$. Since the hyphoid solution exists for all s it could not have passed through such a point. This possibility can immediately be excluded due to Lemma 3.5.3.

- All solutions to the ODE around (4.2.2) still satisfy an interior sphere condition. If this were the case, we could still use the boundary point lemma to conclude that $G'(s^*) > 0$. This contradiction would yield that $r \in C^2$.

  Now since $r'(s^*) = 0$ and $r'(s) \geq 0$ the boundary curves upward for $s > s^*$ (the hyphoid solution is not convex) so Ω satisfies an interior hemisphere condition: for some ball B touching $\partial\Omega$ at $(r(s^*), z(s^*)$ the left half $\{(r,z) \in B | z < z(s^*)\} \subset \bar{\Omega}$. As such we only need to show that the right hemisphere of B lies in $\bar{\Omega}$. This is the case if we can show that $r(s)$ has quadratic bounds for $s < s^*$. We will examine this possibility in Section 4.2.1.

- Solutions to the ODE with initial condition (4.2.2) do not exist for $s > s^*$. Since the hyphoid solution exists for all s it could not have passed through such a point. We will examine this possibility in Section 4.2.2 and give some requirements on $G(s)$ for which this approach will, or will not, work.

We will show that in all the above cases, under various assumptions on G which are consistent with everything we have proved in the previous chapter, it is possible to construct solutions to (4.2.3) around $s = s^*$ which fail to satisfy the requirements described above. In other words, simply knowing the ODE, knowing that $G \in C^{1,\alpha}$ and knowing $C^{1,\alpha}$ hyphoid solutions exist is not sufficient to prove that these solutions are C^2 using local arguments around potentially singular points. Additional information, presumably improved bounds for the flux and better bounds for $G(s)$ are needed.

4.2.1 The backward solution

In this section we will examine possible solutions to the travelling wave ODE for $s < s^*$. Under some extra assumptions on G which are consistent with what we already know about the cumulative flux, we will show that there exist solutions with boundary condition (4.2.2) which are not C^2 and for which the boundary curve does not satisfy an interior sphere condition. This implies that if one wishes to prove the hyphoid solution is C^2, extra information about the flux is needed in order to exclude the possibility described in this section.

Let

$$y(x) = r(s^*)^2 - r(s^* - x)^2, \tag{4.2.4}$$

then

$$\begin{aligned} y'(x) &= 2r(s^* - x)r'(s^* - x) \\ &= 2\sqrt{r(s^* - x)^2 - G(s^* - x)^2} \\ &= 2\sqrt{G(s^*)^2 - G(s^* - x)^2 - y(x)} \\ &= 2\sqrt{f(x) - y(x)}, \end{aligned} \tag{4.2.5}$$

where

$$f(x) = G(s^*)^2 - G(s^* - x)^2. \tag{4.2.6}$$

Now, since $G \in C^{1,\alpha}$ we know there is some constant $C_1 > 0$ such that $f(x) \leq C_1 x^{1+\alpha}$. Furthermore, since G is an increasing function of x, f is increasing as well. If we now assume that $f(x)$ increases sufficiently fast, that it has a lower bound of the form $f(x) \geq C_2 x^{1+\beta}$ for some $\beta \in [\alpha, (1+\alpha)/2)$, then the ODE (4.2.5) has solutions for which we can calculate the asymptotics as $x \to 0^+$.

Lemma 4.2.1 *If*

$$C_2 x^{1+\beta} \leq f(x) \leq C_1 x^{1+\alpha}$$

with $\alpha \leq \beta < (1+\alpha)/2$ *then the differential equation*

$$y'(x) = 2\sqrt{f(x) - y(x)}$$

has a solution satisfying

$$\frac{2\sqrt{2C_2}}{3+\beta}x^{(3+\beta)/2} \le y(x) \le \frac{4\sqrt{C_1}}{3+\alpha}x^{(3+\alpha)/2}$$

for x in a suitably small interval $[0, x_{max}]$.

Proof To simplify notation we define $A = 4\sqrt{C_1}/(3+\alpha)$ and $\gamma = (1+\alpha)/2-\beta > 0$. Now for a suitable value of $x_{max} > 0$ to be determined later, we consider the integral operator Φ on a subset D of the continuous functions on $[0, x_{max}]$,

$$D = \{y \in C([0, x_{max}]) \quad | \quad 0 \le y(x) \le Ax^{(3+\alpha)/2}\}$$
$$\Phi[y](x) = \int_0^x 2\sqrt{f(\xi) - y(\xi)}\mathrm{d}\xi.$$

Clearly a fixed point of Φ is a solution of the differential equation. We will use a contraction argument to show that Φ has a unique fixed point on D.

First, if $y \in D$ then

$$y(x) \le Ax^{(3+\alpha)/2} \le Ax^{1+\beta}x_{max}^{\gamma},$$

so if we choose x_{max} sufficiently small such that $Ax_{max}^{\gamma} \le \frac{1}{2}C_2$ then $y(x) \le f(x)$ and Φ is well defined. Furthermore, if $y \ge 0$ then

$$\Phi[y](x) \le \int_0^x 2\sqrt{C_1}\xi^{(1+\alpha)/2}\mathrm{d}\xi \le Ax^{(3+\alpha)/2},$$

so Φ maps from D to D. We now define a weighted supremum norm $\|\cdot\|_D$ on D,

$$\|y\|_D = \sup_{0\le x\le x_{max}} \frac{y(x)}{x^{(3+\alpha)/2}}.$$

If $y_1, y_2 \in D$ then

$$\begin{aligned}
|\Phi[y_2](x) - \Phi[y_1](x)| &\le \int_0^x 2\left|\sqrt{f(\xi) - y_2(\xi)} - \sqrt{f(\xi) - y_1(\xi)}\right|\mathrm{d}\xi \\
&\le \int_0^x 2\frac{|y_2(\xi) - y_1(\xi)|}{\sqrt{f(\xi) - y_2(\xi)} + \sqrt{f(\xi) - y_1(\xi)}}\mathrm{d}\xi \\
&\le \int_0^x \frac{|y_2(\xi) - y_1(\xi)|}{\sqrt{C_2\xi^{1+\beta} - A\xi^{(3+\alpha)/2}}}\mathrm{d}\xi \\
&\le \|y_2 - y_1\|_D \int_0^x \frac{\xi^{(2+\alpha-\beta)/2}}{\sqrt{C_2 - Ax_{max}^{\gamma}}}\mathrm{d}\xi \\
&\le \|y_2 - y_1\|_D \frac{2}{4+\alpha-\beta}\sqrt{\frac{2}{C_2}}x^{(4+\alpha-\beta)/2} \\
&\le q\,\|y_2 - y_1\|_D\, x^{(3+\alpha)/2},
\end{aligned}$$

where

$$q = \frac{2}{4+\alpha-\beta}\sqrt{\frac{2}{C_2}}x_{max}^{(1-\beta)/2}.$$

Therefore we can choose x_{max} sufficiently small that $q < 1$ and Φ is a contraction on D. By the Banach fixed point theorem, Φ must have a unique fixed point $y_{fix} \in D$. Now for this fixed point,

$$\begin{aligned} y_{fix}(x) &\geq \int_0^x 2\sqrt{C_2\xi^{1+\beta} - A\xi^{(3+\alpha)/2}}\mathrm{d}\xi \\ &\geq \int_0^x 2\xi^{(1+\beta)/2}\sqrt{C_2 - Ax_{max}^{\gamma}}\mathrm{d}\xi \\ &\geq \frac{2\sqrt{2C_2}}{3+\beta}x^{(3+\beta)/2}. \end{aligned}$$

■

Corollary 4.2.2 *If $G(s)$ satisfies a bound $G(s^*)^2 - G(s)^2 \geq C_2(s^* - s)^{1+\beta}$ for $s < s^*$ then there is a solution to the travelling wave ODE around $s = s^*$ of the form $r(s) = \sqrt{r(s^*)^2 - y(s^* - s)}$. Since $(3+\beta)/2 < 2$ this solution does not have the quadratic bounds required to satisfy an interior sphere condition.*

4.2.2 The forward solution

Let

$$y(x) = r(s^* + x)^2 - G(s^* + x)^2, \tag{4.2.7}$$

then y satisfies the differential equation

$$y'(x) = 2\sqrt{y(x)} - 2G(s^* + x)G'(s*+x). \tag{4.2.8}$$

We first examine the toy problem where $2G(s^* + x)G'(s*+x) = Cx$ for some constant $C > 0$. This implies that $G(s) = \sqrt{G(s^*)^2 + Cx^2/2}$ which is consistent with G being an increasing $C^{1,\alpha}$ function.

If we now substitute $y = ax^2$ then we can solve for the constant a,

$$a = \frac{1 - C \pm \sqrt{1-2C}}{2}. \tag{4.2.9}$$

This toy problem, while overly simplified, tells us one thing: simply knowing that $G \in C^{1,\alpha}$ is not sufficient to prevent a solution from leaving a problematic point at $s = s^*$. However, the square root in (4.2.9) suggests that if C is sufficiently large, or in other words if the rate of increase of G is sufficiently large, then solutions might not exist. In order to derive conditions for which these solutions cease to exist, we first rewrite (4.2.8) as the integral equation

$$y(x) = \int_0^x 2\sqrt{y(\xi)}\mathrm{d}\xi - g(x), \tag{4.2.10}$$

where

$$g(x) = G(s^* + x)^2 - G(s^*)^2. \tag{4.2.11}$$

Lemma 4.2.3 *Let $y(x)$ be a solution to the integral equation*

$$y(x) = \int_0^x 2\sqrt{y(\xi)}\mathrm{d}\xi - g(x),$$

for some positive function $g(x)$ and let there be positive constants y_0 and x_{max} such that $0 \le y(x) \le y_0$ for $0 \le x \le x_{max}$. Then for all $n \ge 0$ these solutions have upper bounds

$$y(x) \le y_n x^{\alpha_n},$$

where the constants y_n and α_n satisfy

$$\alpha_n = 2 - 2^{1-n},$$

and

$$y_{n+1} = \frac{2}{2 - 2^{-n}}\sqrt{y_n}.$$

The constants α_n are bounded $0 \le \alpha_n < 2$ and the constants y_n are bounded $y_n \le \max(y_0, 4)$.

Proof Assume that $y(x)$ satisfies $y(x) \le y_n x^{\alpha_n}$ for some positive constants y_n and α_n. If we substitute this estimate into the integral equation, from the positivity of $g(x)$ we obtain

$$y(x) \le \int_0^x 2\sqrt{y_n}\xi^{\alpha_n/2}\mathrm{d}\xi \le \frac{2\sqrt{y_n}}{\alpha_n/2+1}x^{\alpha_n/2+1} \le y_{n+1}x^{\alpha_{n+1}},$$

where

$$\alpha_{n+1} = \alpha_n/2 + 1, \qquad \text{and} \qquad y_{n+1} = \frac{2}{\alpha_n/2+1}\sqrt{y_n}.$$

Now if $\alpha_0 = 0$ then the recurrence relation for α_n has as solution $\alpha_n = 2 - 2^{1-n}$, substituting this we obtain

$$y_{n+1} = \frac{2}{(2-2^{1-n})/2+1}\sqrt{y_n} = \frac{2}{2-2^{-n}}\sqrt{y_n}.$$

Clear $0 \le \alpha_n < 2$. To establish the bounds on y_n we first note that $y_{n+1} \le 2\sqrt{y_n}$. Now if $y_n \le 4$ then $y_{n+1} \le 4$ and the sequence remains bounded below 4. If $y_n > 4$, then $4y_n < y_n^2$ so $y_{n+1} \le 2\sqrt{y_n} < y_n$ and the sequence is strictly decreasing and must be bounded by its initial value y_0. ■

Corollary 4.2.4 *If there is a lower bound for the cumulative flux such that* $g(x) \geq Cx^{1+\beta}$ *for constants* $C > 0$ *and* $\beta < 1$ *then, since* $\alpha_n \to 2$*, if* n *is sufficiently large* $\alpha_n > 1 + \beta$*. Substituting this again into* (4.2.10) *we obtain that* $y(x) \leq y_{n+1}x^{\alpha_{n+1}} - Cx^{1+\beta}$ *and so* $y(x) < 0$ *for sufficiently small* x*. As a result of this contradiction, if* G *satisfies such a lower bound then* (4.2.10) *has no solutions for* $x > 0$*.*

4.2.3 Concavity

Showing that the hyphoid solution is concave, or showing that $r'(s)$ is a decreasing function of s, is a problem closely associated with the problem of showing C^2 regularity. Earlier we showed that that C^2 regularity can only fail if there is an $s^* > 0$ such that $r'(s^*) = 0$. Since $r'(s) \geq 0$ for all s, if such an s^* exists then the solution is not concave. Equivalently, if the hyphoid solution is concave then it must be twice differentiable. Unfortunately, when attempting to prove concavity we encounter the same problems as when attempting to prove C^2 regularity. Clearly, from (4.2.1) if we wish to show $r''(s) \leq 0$ we need a lower bound on $G'(s)$ similar to what we required in Corollary 4.2.2.

However, observations of fungal hyphae show that the tip is concave, furthermore numerical simulations of the diffusive VSC model, in Chapter 5 show no signs that the solution to the model is not concave. Thus, even though we cannot prove it, it seems not unreasonable to assume that r is in fact concave and thus twice differentiable. We will assume this, or the stronger assumption of $C^{2,\alpha}$ regularity, for many of the results in the remainder of this chapter.

4.3 Asymptotic upper bounds away from the tip

In this section we will consider asymptotics of r, z, G and u as $s \to \infty$, or equivalently, $z \to -\infty$. Many of the results in this section rely on harmonic functions or solutions to the Dirichlet problem, on cylinders. For this we first introduce some notation which will be used throughout this section.

We consider the Dirichlet problem on capped cylinders of radius r_{max}. Let

$$\Omega_{(a,b)} = \{(r, z) \quad | \quad 0 < r < r_{max}, \quad a < z < b\} \tag{4.3.1}$$

be a cylinder with caps at $z = a$ and $z = b$ (possibly $\pm\infty$.) For $a < -\xi < b$ we consider the solutions $u_{(a,b)}$ to the Dirichlet problem

$$\begin{aligned} \Delta u_{(a,b)} &= -4\pi\delta(r, z + \xi) \qquad \text{in } \Omega_{(a,b)}, \\ u_{(a,b)} &= 0 \qquad\qquad\qquad\quad \text{on } \partial\Omega_{(a,b)}. \end{aligned} \tag{4.3.2}$$

4.3.1 Bounds on u and $u_{(a,b)}$

The following two lemmas establish some upper bounds for the solutions $u_{(a,b)}$.

Lemma 4.3.1 *There is a constant $C > 0$ such that for the hyphoid solution $u(r,z)$ and all solutions $u_{(a,b)}(r,z)$ with $a < -2\xi$ and $-\xi < b$*

$$u(r,z) \le CJ_0(\lambda_1 r)e^{\lambda_1 z},$$
$$u_{(a,b)}(r,z) \le CJ_0(\lambda_1 r)e^{\lambda_1 z}.$$

for all $z \le -2\xi$.

Here J_α are the Bessel functions of the first kind, k_n is the n-th zero of J_0 and $\lambda_n = k_n/r_{max}$ (specifically $\lambda_1 \approx 1.2$.)

Proof We first consider $u_{(-\infty,0)}$. At $z = -2\xi$, $u_{(-\infty,0)}(r,-2\xi)$ and all its derivatives to r are bounded, and so there is a sufficiently large constant $C > 0$ such that

$$u_{(-\infty,0)}(r,-2\xi) \le CJ_0(\lambda_1 r).$$

Now $CJ_0(\lambda_1 r)e^{\lambda_1 z}$ and $u_{(-\infty,0)}(r,z)$ are harmonic on $\Omega_{(-\infty,-2\xi)}$ and $u_{(-\infty,0)}(r,z) \le CJ_0(\lambda_1 r)e^{\lambda_1 z}$ on $\partial\Omega_{(-\infty,-2\xi)}$ so the maximum principle yields that

$$u_{(-\infty,0)}(r,z) \le CJ_0(\lambda_1 r)e^{\lambda_1 z},$$

for $z \le -2\xi$. Now $u_{(-\infty,0)} \ge 0$ on $\partial\Omega$ and $\partial\Omega_{(a,b)}$ so the maximum principle (the difference between functions is harmonic) again yields that $u(r,z) \le u_{(-\infty,0)}(r,z)$ and $u_{(a,b)}(r,z) \le u_{(-\infty,0)}$ in Ω respectively $\Omega_{(a,b)}$. ∎

Lemma 4.3.2 *For $z^* \le -2\xi$ we consider the function $u_{(z^*,0)}$. If $z^* \le z \le -2\xi$, then*

$$u_{(z^*,0)}(r,z) \le C\frac{e^{\lambda_1(z+2\xi)} - e^{-\lambda_1(z-2z^*-2\xi)}}{1 - e^{2\lambda_1(z^*+2\xi)}}J_0(\lambda_1 r).$$

Proof By Lemma 4.3.1 $u_{(z^*,0)}(r,-2\xi) \le u_{(-\infty,0)}(r,-2\xi) \le CJ_0(\lambda_1 r)$. Let

$$v(r,z) = C\frac{e^{\lambda_1(z+2\xi)} - e^{-\lambda_1(z-2z^*-2\xi)}}{1 - e^{2\lambda_1(z^*+2\xi)}}J_0(\lambda_1 r).$$

This function is harmonic in $\Omega_{(z^*,-2\xi)}$ and satisfies $v(r_{max},z) = 0$ for all z, $v(r,z^*) = 0$ and $v(r,-2\xi) = CJ_0(\lambda_1 r)$ for $0 \le r \le r_{max}$. Thus $u_{(z^*,0)} \le v$ on $\partial\Omega_{(z^*,-2\xi)}$ and by the maximum principle, $u_{(z^*,0)} \le v$ in $\Omega_{(z^*,-2\xi)}$. ∎

Note that it is also possible to obtain an exact Fourier-Bessel series solutions for $u_{(a,b)}$, however those expressions are rather cumbersome and the above estimates are sufficient for our purposes.

4.3.2 Bounds on Du

We can use the bounds on u established in the previous section to establish upper bounds on the first partial derivatives of u.

Lemma 4.3.3 *There is a constant $C > 0$ and a $z^* < -2\xi$ such that*

$$|Du(r,z)| \leq Ce^{\lambda_1 z}$$

for $z < z^*$.

Proof Choose some $d > 0$ and set $z^* = -2\xi - 3d$. If $z < z^*$ and $0 \leq r \leq r_{max}(z)$ there are two possibilities, either $\text{dist}((r,z), \partial\Omega) > 2d$ or $\text{dist}((r,z), \partial\Omega) \leq 2d$.

In the first case, let B_1 and B_2 be open balls of radius d and $2d$ around (r,z). Then $B_1 \subset\subset B_2 \subset \Omega$. Let β be any multi-index, then by the interior estimates for harmonic functions ([12] Theorem 2.10) and the upper bound on u we have that

$$\sup_{B_1} \left|D^\beta u(r,z)\right| \leq \left(\frac{3\,|\beta|}{d}\right)^{|\beta|} \sup_{B_2} |u(r,z)| \leq \left(\frac{3\,|\beta|}{d}\right)^{|\beta|} Ce^{\lambda_1(z+2d)},$$

specifically for $|\beta| = 1$ we get bounds on the first derivatives,

$$|Du(r,z)| \leq \frac{3}{d} Ce^{\lambda_1(z+2d)}.$$

In the second case, let B_2 be as above, let B_3 be an open ball of radius $3d$ around (r,z) and let $T = \partial\Omega \cap B_3$. Then the Hölder estimates for first derivatives ([12] Corollary 8.36) yield that

$$\|u\|_{1,\alpha;B_2} \leq C(T,d)\,\|u\|_{0;B_3} \leq Ce^{\lambda_1(z+3d)}.$$

■

Corollary 4.3.4 *The exponential bound on Du also implies that the flux $F(s) = O(e^{-\lambda_1 s})$.*

Corollary 4.3.5 *If $\partial\Omega$ is $C^{2,\alpha}$ (except possibly in some neighbourhood of the tip) we could have used [12] Corollary 6.7 to see that also the second derivatives D^2u and the derivative $F'(s)$ of the flux are $O(e^{\lambda_1 z})$ respectively $O(e^{-\lambda_1 s})$.*

4.3.3 Asymptotics of $G(s)$ as $s \to \infty$

In Lemma 3.7.2 we showed that $G(s) \to 2$ algebraically as $s \to \infty$. Since u decays exponentially, one might expect the cumulative flux $G(s)$ to approach its limit value in the same manner. This is in fact the case.

Theorem 4.3.6 *The cumulative flux $G(s)$ approaches its limit value of 2 exponentially. For $s > 3\xi + 2$, there is a constant $C > 0$ such that*

$$0 < 2 - G(s) \leq Ce^{-\lambda_1 s},$$

where $\lambda_1 = k_1/r_{max}$ as defined above.

Proof For some $z^* < -3\xi$ we consider $u_{(z^*,0)}$ and the function v as described in the proof of Lemma 4.3.2. From that lemma, $u_{(z^*,0)} \leq v$ for $z^* \leq z \leq -2\xi$. Moreover since both $u_{(z^*,0)}$ and v are zero at $z = z^*$, the outward flux of $u_{(z^*,0)}$ at this left cap must be less than the outward flux of v,

$$0 \leq \frac{\partial u_{(z^*,0)}}{\partial z}(r, z^*) \leq \frac{\partial v}{\partial z}(r, z^*) = \frac{2\lambda_1 C J_0(\lambda_1 r)}{e^{-\lambda_1(z^*+2\xi)} - e^{\lambda_1(z^*+2\xi)}}.$$

Integrating this from 0 to r_{max} we can now estimate the total flux arriving at the left cap at $z = z^*$. By Bessel's equation, $J_0(\lambda_1 r) = -\frac{1}{\lambda_1^2}\frac{\mathrm{d}}{\mathrm{d}r}(\lambda_1 r J_0'(\lambda_1 r)) = \frac{1}{\lambda_1^2}\frac{\mathrm{d}}{\mathrm{d}r}(\lambda_1 r J_1(\lambda_1 r)$ so

$$\begin{aligned}
G_{cap}(z^*) &= \int_0^{r_{max}} \frac{\partial u_{(z^*,0)}}{\partial z}(r, z^*) r \mathrm{d}r \\
&\leq \frac{2\lambda_1 C}{e^{-\lambda_1(z^*+2\xi)} - e^{\lambda_1(z^*+2\xi)}} \int_0^{r_{max}} J_0(\lambda_1 r) r \mathrm{d}r \\
&\leq \frac{2C}{\lambda_1(e^{-\lambda_1(z^*+2\xi)} - e^{\lambda_1(z^*+2\xi)})} \int_0^{r_{max}} \frac{\mathrm{d}}{\mathrm{d}r}\Big[\lambda_1 r J_1(\lambda_1 r)\Big] \mathrm{d}r \\
&\leq \frac{2C r_{max} J_1(k_1)}{e^{-\lambda_1(z^*+2\xi)} - e^{\lambda_1(z^*+2\xi)}} \leq \tilde{C} e^{\lambda_1 z^*},
\end{aligned}$$

where

$$\tilde{C} = \frac{2C r_{max} J_1(k_1) e^{2\lambda_1 \xi}}{1 - e^{-2\lambda_1 \xi}} e^{\lambda_1 z^*}.$$

We now use similar arguments as in Lemma 3.7.2. If $s > 3\xi + 2$ then from (3.3.8) we see that $z(s) \leq -(s-2) < -3\xi$, we now let $z^* = z(s)$. Using the comparison principle to compare the flux through the hyphoid solution with the capped cylinder $\Omega_{(z^*,0)}$ we obtain

$$2 - G(s) \leq G_{cap}(z^*) \leq \tilde{C} e^{\lambda_1 z^*} \leq \tilde{C} e^{-\lambda_1(s-2)}.$$

■

Note that we could also have obtained the same result by integrating the estimate in Corollary 4.3.4.

4.3.4 Asymptotics for r as $s \to \infty$

Theorem 4.3.7 *For $s > 3\xi + 2$, there is a constant $C > 0$ such that,*

$$\begin{aligned}
0 < 2 - r(s) &\leq C e^{-\lambda_1 s}, \\
0 \leq r'(s) &\leq C^{-\lambda_1 s/2}.
\end{aligned}$$

Proof Since $G(s) \leq r(s) \leq 2$, the asymptotics for $r(s)$ follow immediately from

Theorem 4.3.6. Now

$$\begin{aligned} r'(s) &= \sqrt{1-\left(\frac{G(s)}{r(s)}\right)^2} \\ &= \frac{1}{r(s)}\sqrt{((2-G(s))-(2-r(s)))(G(s)+r(s))} \\ &\leq \frac{2}{r(s)}\sqrt{2-G(s)} \\ &\leq \frac{2}{2-Ce^{-\lambda_1(3\xi+2)}}\sqrt{C}e^{-\lambda_1 s/2}. \end{aligned}$$

■

These estimates yield one of the main differences between the Ballistic VSC Model, described in chapters 1 and 2, with the Diffusive VSC Model described in this and the previous chapter. The solution to the diffusive model reaches its maximal width r_{max} exponentially fast, while the solution to the ballistic model only approaches r_{max} algebraically. This means that for the diffusive model, the growth is more focussed in the tip, resulting in a blunter tip shape.

4.3.5 Fourier-Bessel series expansion of $u(r,z)$

The function $z(s)$ is invertible, we denote its inverse as z^{-1} and define $r_{max}(z) = r(z^{-1}(z))$. At fixed $z < -2\xi$, $u(r,z)$ is bounded and can be expressed as as a Fourier-Bessel series on the disc of radius $r_{max}(z)$.

$$u(r,z) = \sum_{n=1}^{\infty} c_n(z) J_0\left(k_n \frac{r}{r_{max}(z)}\right). \tag{4.3.3}$$

Using the orthogonality of Bessel functions,

$$\begin{aligned} \int_0^{r_{max}(z)} J_0\left(k_i\frac{r}{r_{max}(z)}\right) J_0\left(k_j\frac{r}{r_{max}(z)}\right) r\mathrm{d}r &= r_{max}(z)^2 \int_0^1 J_0(k_i x)J_0(k_j x)x\mathrm{d}x \\ &= \frac{1}{2}\delta_{ij} r_{max}(z)^2 J_1(k_i)^2, \end{aligned} \tag{4.3.4}$$

so

$$\begin{aligned} \int_0^{r_{max}(z)} u(r,z) J_0\left(k_n\frac{r}{r_{max}(z)}\right) r\mathrm{d}r &= c_n(z)\int_0^{r_{max}(z)} J_0\left(k_n\frac{r}{r_{max}(z)}\right)^2 r\mathrm{d}r \\ &= \frac{1}{2}c_n(z) r_{max}(z)^2 J_1(k_i)^2, \end{aligned} \tag{4.3.5}$$

and the coefficients $c_n(z)$ can be calculated

$$\begin{aligned} c_n(z) &= \frac{2}{r_{max}(z)^2 J_1(k_n)^2}\int_0^{r_{max}(z)} u(r,z) J_0\left(k_n\frac{r}{r_{max}(z)}\right) r\mathrm{d}r \\ &= \frac{2}{J_1(k_n)^2}\int_0^1 u(x r_{max}(z), z) J_0(k_n x) x\mathrm{d}x. \end{aligned} \tag{4.3.6}$$

Lemma 4.3.8 *The first coefficient $c_1(z)$ is positive, furthermore there are constants $C_n > 0$ such that*

$$|c_n(z)| \leq C_n e^{\lambda_1 z},$$

for all n and $z < -2\xi$.

Proof We fix $z < -2\xi$ and first examine $c_1(z)$. Positivity of $c_1(z)$ follows from the fact that both $u(r_{max}(z)x, z)$ and $J_0(k_1 x)$ are positive for $0 \leq x \leq 1$. We define $a = r_{max}(z)/r_{max} \leq 1$, since $J_0(k_1 x)$ is decreasing we have $J_0(k_1 x) \leq J_0(k_1 a x)$. So after substituting the upper bound for u found in Lemma 4.3.1 we obtain

$$\begin{aligned}
c_1(z) &\leq \frac{2Ce^{\lambda_1 z}}{J_1(k_1)^2} \int_0^1 J_0(k_1 a x) J_0(k_1 x) x \mathrm{d}x \\
&\leq \frac{2Ce^{\lambda_1 z}}{J_1(k_1)^2} \int_0^1 J_0(k_1 a x)^2 x \mathrm{d}x \\
&\leq \frac{2Ce^{\lambda_1 z}}{a^2 J_1(k_1)^2} \int_0^a J_0(k_1 \rho)^2 \rho \mathrm{d}\rho \\
&\leq \frac{2Ce^{\lambda_1 z}}{a^2 J_1(k_1)^2} \int_0^1 J_0(k_1 \rho)^2 \rho \mathrm{d}\rho \\
&\leq \frac{C}{a^2} e^{\lambda_1 z}.
\end{aligned}$$

Similarly for $n \geq 2$, since $|J_0| \leq 1$ we have

$$\begin{aligned}
|c_n(z)| &\leq \frac{2Ce^{\lambda_1 z}}{J_1(k_n)^2} \int_0^1 |J_0(k_n a x)| \, |J_0(k_1 x)| \, x \mathrm{d}x \\
&\leq \frac{Ce^{\lambda_1 z}}{J_1(k_n)^2}
\end{aligned}$$

■

4.3.6 Asymptotic bounds for the coefficients c_n

Since the constant a in the proof of Lemma 4.3.8 is nearly equal to one one would expect from the orthogonality of Bessel functions that the constants C_n would be small for $n \geq 2$. Proving this however requires additional assumptions on r. Under these assumptions, we can show that the constants C_n are uniformly bounded in n and coefficients c_n decay faster than c_1 for $n > 1$.

Theorem 4.3.9 *If $r \in C^{2,\alpha}([s^*, \infty))$ for some sufficiently large s^* and there exist constants $C > 0$ and $\mu > 0$ such that*

$$\begin{aligned}
0 \leq r'(s) &\leq Ce^{-\mu s}, \qquad \textit{and} \\
|r''(s)| &\leq Ce^{-\mu s},
\end{aligned}$$

for all $s \geq s^*$, then there exist constants $z^* < -2\xi$ and $\tilde{C} > 0$ such that

$$\begin{aligned} |c_n(z)| &\leq \tilde{C} e^{\lambda_n z} && \text{if } \lambda_n < \mu + \lambda_1, \\ |c_n(z)| &\leq \tilde{C} e^{(\lambda_1+\mu)z} && \text{if } \lambda_n > \mu + \lambda_1, \\ |c_n(z)| &\leq \tilde{C}\,|z|\, e^{(\lambda_1+\mu)z} && \text{if } \lambda_n = \mu + \lambda_1. \end{aligned}$$

for all $n \geq 1$ and all $z < z^*$. Specifically this implies that if $n \geq 2$, c_n decays faster than $e^{\lambda_1 z}$.

Note that Theorem 4.3.7 gives a suitable bound on r', however we have not been able to prove that r'' exists, let alone that it decays exponentially. We will prove Theorem 4.3.9 at the end of this section, however we first require some intermediate results.

Lemma 4.3.10 *If the assumptions of Theorem 4.3.9 hold, then there are positive constants $C_1, \ldots, C_4$ and a negative constant $z^* < -2\xi$ such that*

$$\begin{aligned} |r'_{max}(z)| &\leq C_1 e^{\mu z}, \\ |r''_{max}(z)| &\leq C_2 e^{\mu z}, \\ |Du(r,z)| &\leq C_3 e^{\lambda_1 z}, \qquad \text{and} \\ \left|D^2 u(r,z)\right| &\leq C_4 e^{\lambda_1 z}, \end{aligned}$$

Proof First, since $r'^2 + z'^2 = 1$, we see that $r'r'' + z'z'' = 0$ and $z'' = -r'r''/z'$. From the asymptotics for r' we see that $z' \to -1$ exponentially, so for sufficiently large s, $z'(s)$ is bounded away from zero. Thus $z'' \in C^{2,\alpha}$ and $\partial\Omega$ is $C^{2,\alpha}$ sufficiently far away from the tip. Now writing $s = z^{-1}(z)$,

$$r'_{max}(z) = \frac{r'(s)}{z'(s)} = -\frac{r'(s)}{\sqrt{1 - r'(s)^2}}$$

and so

$$\begin{aligned} r''_{max}(z) &= \Big(\frac{r''(s)}{\sqrt{1 - r'(s)^2}} + \frac{r'(s)^2 r''(s)}{(1 - r'(s)^2)^{(3/2)}} \Big) / z'(s) \\ &= \frac{r''(s)}{z'(s)^4}. \end{aligned}$$

The bounds on r' and r'', together with $-s < z < -s + 2$ now give the bound on r'_{max} and r''_{max} while Corollary 4.3.5 yields the bounds on Du and D^2u for some sufficiently large negative $z^* < -2\xi$. ∎

We now write $c_n(z) = 2w_n(z)/J_1(k_n)^2$ with

$$w_n(z) = \int_0^1 u(x r_{max}(z), z) J_0(k_n x) x \mathrm{d}x. \tag{4.3.7}$$

Then

$$w_n''(z) = \int_0^1 \Big[\frac{\partial^2 u}{\partial r^2} x^2 r'_{max}(z)^2 + \frac{\partial u}{\partial r} x r''_{max}(z) + 2\frac{\partial^2 u}{\partial r \partial z} x r'_{max}(z)\Big] J_0(k_n x) x \mathrm{d}x + \int_0^1 \frac{\partial^2 u}{\partial z^2} J_0(k_n x) x \mathrm{d}x. \tag{4.3.8}$$

Now by Lemma 4.3.10,

$$\left|\int_0^1 \Big[\frac{\partial^2 u}{\partial r^2} x^2 r'_{max}(z)^2 + \frac{\partial u}{\partial r} x r''_{max}(z) + 2\frac{\partial^2 u}{\partial r \partial z} x r'_{max}(z)\Big] J_0(k_n x) x \mathrm{d}x\right| \leq C_1^2 C_4 e^{(\lambda_1+2\mu)z} + C_2 C_3 e^{(\lambda_1+\mu)z} + 2C_1 C_4 e^{(\lambda_1+\mu)z}, \tag{4.3.9}$$

so we can write

$$w_n''(z) = e^{(\lambda_1+\mu)z} f_n(z) + \int_0^1 \frac{\partial^2 u}{\partial z^2} J_0(k_n x) x \mathrm{d}x, \tag{4.3.10}$$

where $f_n(z)$ is uniformly bounded in n and z. Since u is harmonic,

$$\frac{\partial^2 u}{\partial z^2}(r_{max}(z)x, z) = -\frac{1}{r_{max}(z)^2 x}\frac{\partial}{\partial x}\Big(x\frac{\partial}{\partial x}\Big(u(r_{max}(z)x, z)\Big)\Big), \tag{4.3.11}$$

so after two partial integrations we see that

$$\begin{aligned}
&\int_0^1 \frac{\partial^2 u}{\partial z^2}(r_{max}(z)x, z) J_0(k_n x) x \mathrm{d}x \\
&\quad = -\frac{1}{r_{max}(z)^2}\int_0^1 u(r_{max}(z)x, z)\frac{\partial}{\partial x}\Big(x\frac{\partial}{\partial x}\Big(J_0(k_n x)\Big)\Big)\mathrm{d}x, \\
&\quad = \frac{k_n^2}{r_{max}(z)^2}\int_0^1 u(r_{max}(z)x, z) J_0(k_n x) x \mathrm{d}x, \\
&\quad = \frac{k_n^2}{r_{max}(z)^2} w_n(z).
\end{aligned} \tag{4.3.12}$$

If we now define

$$\begin{aligned}
e^{\lambda_1 z}\rho(z) &= \frac{1}{r_{max}(z)^2} - \frac{1}{r_{max}^2} \\
&= \frac{(r_{max} - r_{max}(z))}{r_{max}(z)^2} \cdot \frac{(r_{max} + r_{max}(z))}{r_{max}^2} \\
&\leq \frac{C}{(2 - Ce^{-2\lambda_1 \xi})^2} e^{\lambda_1 z},
\end{aligned} \tag{4.3.13}$$

then $\rho(z)$ is positive and bounded for all z, and w_n satisfies the second order ordinary differential equation

$$w_n''(z) - \lambda_n^2 w_n(z) = f_n(z)e^{(\lambda_1+\mu)z} + k_n^2 \rho(z) w_n(z) e^{\lambda_1 z}. \tag{4.3.14}$$

We are interested in finding solutions to this ODE satisfying $\lim_{z\to-\infty} w_n(z) = 0$.

Lemma 4.3.11 *There is an $a < z^*$ and a constant $C > 0$ (both not depending on n) such that for each n there exists a solution to the ODE (4.3.14) on $(-\infty, a)$ with the following upper bounds for $z < a$,*

$$|w_n(z)| \le \Big(2\,|w_n(a)|\,e^{-\lambda_n a} \quad + \quad C\Big)e^{\lambda_n z} \qquad \text{if } \lambda_n < \mu + \lambda_1,$$

$$|w_n(z)| \le \Big(2\,|w_n(a)|\,e^{-(\lambda_1+\mu)a} \quad + \quad \frac{C}{\lambda_n^2}\Big)e^{(\lambda_1+\mu)z} \qquad \text{if } \lambda_n > \mu + \lambda_1,$$

$$|w_n(z)| \le \Big(2\,|w_n(a)|\,e^{-\lambda_n a}/|a| \quad + \quad C\Big)\,|z|\,e^{(\lambda_1+\mu)z} \qquad \text{if } \lambda_n = \mu + \lambda_1.$$

Proof Both $f_n(z)$ and $\rho(z)$ are bounded, we define

$$F = \sup_{n\ge 1, z<z^*} |f_n(z)|\,, \qquad P = \sup_{z<z^*} \rho(z).$$

We substitute $w_n = \phi_n(z)e^{\lambda_n z}$ to get the following ODE for ϕ_n

$$\begin{aligned} 2\lambda_n\phi_n'(z) + \phi_n''(z) &= e^{-2\lambda_n z}\frac{\mathrm{d}}{\mathrm{d}z}\Big(e^{2\lambda_n z}\phi_n'(z)\Big) \\ &= f_n(z)e^{(\mu+\lambda_1-\lambda_n)z} + k_n^2\rho(z)\phi_n(z)e^{\lambda_1 z}. \end{aligned}$$

For boundary values α_n, and a constant a to be determined later, we consider the integral operators

$$\begin{aligned} \Phi_n[\phi](z) &= \alpha_n e^{-\lambda_n a} \\ &\quad - \int_z^a e^{-2\lambda_n\tilde{z}} \int_{-\infty}^{\tilde{z}} \Big(f_n(\tilde{\tilde{z}})e^{(\lambda_1+\mu+\lambda_n)\tilde{\tilde{z}}} + k_n^2\rho(\tilde{\tilde{z}})\phi(\tilde{\tilde{z}})e^{(\lambda_1+2\lambda_n)\tilde{\tilde{z}}}\Big)\,\mathrm{d}\tilde{\tilde{z}}\mathrm{d}\tilde{z}. \end{aligned}$$

If this operator were to have a fixed point ϕ_n^{fix}, differentiating twice to z would yield that this fixed point is a solution to the ODE for ϕ_n. Furthermore, if $\phi_n^{fix}(z)$ were $o(e^{-\lambda_n z})$ then $w_n(z) = e^{\lambda_n z}\phi_n^{fix}(z)$ would be a solution to (4.3.14) with boundary values $w_n(a) = \alpha_n$ and $\lim_{z\to-\infty} w_n(z) = 0$.

We now define the norms

$$\begin{aligned} \|\phi\|_0 &= \sup_{z<a} |\phi(z)|\,, \\ \|\phi\|_\gamma &= \sup_{z<a} |e^{\gamma z}\phi(z)|\,, \\ \|\phi\|_z &= \sup_{z<a} \left|\frac{\phi(z)}{z}\right|, \end{aligned}$$

and let X^0, X^γ and respectively X^z be the subspaces of the continuous function with the corresponding norms. Let n_1 be the maximal n such that $\lambda_n < \lambda_1 + \mu$, since λ_n are strictly increasing, n_1 is well defined and $n_1 \ge 1$. Let n_2 be the minimal n such that $\lambda_n > \lambda_1 + \mu$, then $n_2 \ge n_1 + 1$ (specifically, it's either equal to $n_1 + 1$ unless $\lambda_{n_1+1} = \lambda_1 + \mu$, in which case $n_2 = n_1 + 2$.) We will examine three cases, $\lambda_n < \lambda_1 + \mu$ (or equivalently, $1 \le n \le n_1$), $\lambda_n > \lambda_1 + \mu$ (or equivalently $n \ge n_2$) and the special case $\lambda_n = \lambda_1 + \mu$. Note that since λ_n are strictly increasing and unbounded last case will occur for at most one value of n.

- Case 1 : $\lambda_n < \lambda_1 + \mu$. If $|\phi| \leq \|\phi\|_0$, then

$$\begin{aligned}
|\Phi_n[\phi](z)| &\leq |\alpha_n| e^{-\lambda_n a} \\
&\quad + \int_z^a e^{-2\lambda_n \tilde{z}} \int_{-\infty}^{\tilde{z}} \left(F e^{(\lambda_1+\mu+\lambda_n)\tilde{\tilde{z}}} + k_n^2 P \|\phi\|_0 e^{(\lambda_1+2\lambda_n)\tilde{\tilde{z}}} \right) \mathrm{d}\tilde{\tilde{z}} \mathrm{d}\tilde{z} \\
&\leq |\alpha_n| e^{-\lambda_n a} + \int_z^a \left[\frac{F e^{(\lambda_1+\mu-\lambda_n)\tilde{z}}}{\lambda_1+\mu+\lambda_n} + \frac{k_n^2 P e^{\lambda_1 \tilde{z}}}{\lambda_1+2\lambda_n} \|\phi\|_0 \right] \mathrm{d}\tilde{z} \\
&\leq |\alpha_n| e^{-\lambda_n a} + \frac{F e^{(\lambda_1+\mu-\lambda_n)a}}{(\lambda_1+\mu)^2 - \lambda_n^2} + \frac{k_n^2 P e^{\lambda_1 a}}{(\lambda_1+2\lambda_n)\lambda_1} \|\phi\|_0 ,
\end{aligned}$$

  and Φ_n maps from X^0 to X^0. Furthermore,

$$|\Phi_n[\phi_2](z) - \Phi_n[\phi_1](z)| \leq \frac{k_n^2 P e^{\lambda_1 a}}{(\lambda_1+2\lambda_n)\lambda_1} \|\phi_2 - \phi_1\|_0 ,$$

  so if $|a|$ is chosen sufficiently large such that $\frac{k_n^2 P e^{\lambda_1 a}}{(\lambda_1+2\lambda_n)\lambda_1} \leq \frac{1}{2}$ for all $1 \leq n \leq n_1$ then Φ_n is a contraction and by the Banach fixed point theorem, it has a fixed point ϕ_n^{fix}. The estimate on $\left|\Phi_n[\phi_n^{fix}]\right|$ then yields that

$$\left\|\phi_n^{fix}\right\|_0 \leq 2 |\alpha_n| e^{-\lambda_n a} + 2 \frac{F e^{(\lambda_1+\mu-\lambda_n)a}}{(\lambda_1+\mu)^2 - \lambda_n^2}.$$

  Since $\lambda_n < \lambda_1 +' mu$ for only a finite amount of values of n, we can choose C_1 such that $\left\|\phi_n^{fix}\right\|_0 \leq 2\alpha_n e^{-\lambda_n a} + C_1$ for $1 \leq n \leq n_1$. So

$$|w_n(z)| \leq \left\|\phi_n^{fix}\right\|_0 e^{\lambda_n z} \leq \left(2 |w_n(a)| e^{-\lambda_n a} + C_1\right) e^{\lambda_n z}.$$

- Case 2 : $\lambda_n > \lambda_1 + \mu$. Since this will be the case for infinitely many $n \geq n_2$ we have to make certain our estimates stay bounded as $n \to \infty$. Let $\gamma_n = \lambda_n - \lambda_1 - \mu$, by assumption γ_n is positive. If $|\phi(z)| \leq \|\phi\|_{\gamma_n} e^{-\gamma_n z}$ then

$$\begin{aligned}
|\Phi_n[\phi](z)| &\leq |\alpha_n| e^{-\lambda_n a} \\
&\quad + \int_z^a e^{-2\lambda_n \tilde{z}} \int_{-\infty}^{\tilde{z}} \left(F + k_n^2 P \|\phi\|_{\gamma_n} e^{\lambda_1 \tilde{\tilde{z}}} \right) e^{(\lambda_1+\lambda_n+\mu)\tilde{\tilde{z}}} \mathrm{d}\tilde{\tilde{z}} \mathrm{d}\tilde{z} \\
&\leq |\alpha_n| e^{-\lambda_n a} + \int_z^a \frac{F + k_n^2 P \|\phi\|_{\gamma_n} e^{\lambda_1 a}}{\lambda_1+\lambda_n+\mu} e^{-\gamma_n \tilde{z}} \mathrm{d}\tilde{z} \\
&\leq |\alpha_n| e^{-\lambda_n a} + \frac{F + k_n^2 P \|\phi\|_{\gamma_n} e^{\lambda_1 a}}{\lambda_n^2 - (\lambda_1+\mu)^2} e^{-\gamma_n z},
\end{aligned}$$

  so,

$$\|\Phi_n[\phi]\|_{\gamma_n} \leq |\alpha_n| e^{-(\lambda_1+\mu)a} + \frac{F + k_n^2 P \|\phi\|_{\gamma_n} e^{\lambda_1 a}}{\lambda_n^2 - (\lambda_1+\mu)^2},$$

and Φ_n maps from X^{γ_n} to X^{γ_n}. Furthermore,

$$|\Phi_n[\phi_2](z) - \Phi_n[\phi_1](z)|e^{\gamma_n z} \leq \frac{k_n^2 P e^{\lambda_1 a}}{\lambda_n^2 - (\lambda_1+\mu)^2} \left\|\phi_2 - \phi_1\right\|_{\gamma_n}.$$

Now, as $n \to \infty$, k_n, λ_n and γ_n are all $O(n)$. Therefore there is a constant k such that $\frac{k_n^2}{\lambda_n^2-(\lambda_1+\mu)^2} \leq k$ for all $n \geq n_2$. Now

$$\left\|\Phi_n[\phi_2] - \Phi_n[\phi_1]\right\|_{\gamma_n} \leq kPe^{\lambda_1 a} \left\|\phi_2 - \phi_1\right\|_{\gamma_n},$$

and if $|a|$ is chosen sufficiently large such that $kPe^{\lambda_1 a} \leq \frac{1}{2}$ then Φ_n is a contraction and by the Banach fixed point theorem, it has a unique fixed point ϕ_n^{fix}. The estimate on $\left\|\Phi_n[\phi_n^{fix}]\right\|_{\gamma_n}$ then yields that

$$\begin{aligned}\left\|\phi_n^{fix}\right\|_{\gamma_n} &\leq 2\left(|\alpha_n|\, e^{-(\lambda_1+\mu)a} + \frac{F}{\lambda_n^2 - (\lambda_1+\mu)^2}\right) \\ &\leq 2\,|\alpha_n|\, e^{-(\lambda_1+\mu)a} + \frac{2F}{\lambda_n^2\left(1 - \left(\frac{\lambda_1+\mu}{\lambda_{n_2}}\right)^2\right)^2}.\end{aligned}$$

We let $C_2 = 2F/(1-(\lambda_1+\mu)^2/\lambda_{n_2}^2)$, then

$$|w_n(z)| \leq \left\|\phi_n^{fix}\right\|_{\gamma_n} e^{(\lambda_n-\gamma_n)z} \leq \left(2\,|w_n(a)|\, e^{-(\lambda_1+\mu)a} + \frac{C_2}{\lambda_n^2}\right) e^{(\lambda_1+\mu)z}.$$

- Case 3 : $\lambda_n = \lambda_1 + \mu$. If $|\phi(z)| \leq \|\phi\|_z\,|z|$, then

$$\begin{aligned}|\Phi_n[\phi](z)| &\leq |\alpha_n|\, e^{-\lambda_n a} \\ &\quad + \int_z^a e^{-2\lambda_n \tilde{z}} \int_{-\infty}^{\tilde{z}} \left(Fe^{2\lambda_n \tilde{\tilde{z}}} + k_n^2 P \left\|\phi\right\|_z \left|\tilde{\tilde{z}}\right| e^{(\lambda_1+2\lambda_n)\tilde{\tilde{z}}}\right) \mathrm{d}\tilde{\tilde{z}}\mathrm{d}\tilde{z} \\ &\leq |\alpha_n|\, e^{-\lambda_n a} \\ &\quad + \int_z^a \left[\frac{F}{2\lambda_n} + k_n^2 P \left\|\phi\right\|_z \left(\frac{|\tilde{z}|}{\lambda_1+2\lambda_n} + \frac{1}{(\lambda_1+2\lambda_n)^2}\right) e^{\lambda_1 \tilde{z}}\right] \mathrm{d}\tilde{z} \\ &\leq |\alpha_n|\, e^{-\lambda_n a} + \frac{F}{2\lambda_n}(a-z) \\ &\quad + k_n^2 P \left\|\phi\right\|_z \left(\frac{|z|}{\lambda_1(\lambda_1+2\lambda_n)} + 2\frac{\lambda_1+\lambda_n}{\lambda_1^2(\lambda_1+2\lambda_n)^2}\right) e^{\lambda_1 a} \\ &\leq \left(\frac{|\alpha_n|\, e^{-\lambda_n a}}{|a|} + \frac{F}{2\lambda_n} \right. \\ &\quad \left. + k_n^2 P \left\|\phi\right\|_z \left(\frac{1}{\lambda_1(\lambda_1+2\lambda_n)} + 2\frac{\lambda_1+\lambda_n}{\lambda_1^2(\lambda_1+2\lambda_n)^2|a|}\right)\right) e^{\lambda_1 a}|z|,\end{aligned}$$

and Φ maps from X^z to X^z. Furthermore,

$$\begin{aligned}
&|\Phi_n[\phi_2](z) - \Phi_n[\phi_1](z)| \\
&\quad \le k_n^2 P \left\|\phi_2 - \phi_1\right\|_z \int_z^a e^{-2\lambda_n \tilde{z}} \int_{-\infty}^{\tilde{z}} e^{2\lambda_n \tilde{\tilde{z}}} |\tilde{\tilde{z}}| e^{\lambda_1 \tilde{\tilde{z}}} \mathrm{d}\tilde{\tilde{z}} \mathrm{d}\tilde{z} \\
&\quad \le k_n^2 P \left\|\phi_2 - \phi_1\right\|_z \left(\frac{1}{\lambda_1(\lambda_1 + 2\lambda_n)} + 2\frac{\lambda_1 + \lambda_n}{\lambda_1^2(\lambda_1 + 2\lambda_n)^2 |a|} \right) e^{\lambda_1 a} |z|
\end{aligned}$$

and so, if we choose $|a|$ sufficiently large such that

$$k_n^2 P \left(\frac{1}{\lambda_1(\lambda_1 + 2\lambda_n)} + 2\frac{\lambda_1 + \lambda_n}{\lambda_1^2(\lambda_1 + 2\lambda_n)^2 |a|} \right) e^{\lambda_1 a} \le \frac{1}{2},$$

then Φ_n is a contraction on X^z and by the Banach fixed point theorem, it has a unique fixed point ϕ_n^{fix}. The estimate on $\left\|\Phi_n[\phi_n^{fix}]\right\|_z$ then yields that

$$\left\|\phi_n^{fix}\right\|_z \le 2\frac{|\alpha_n| e^{-\lambda_n a}}{|a|} + \frac{F}{\lambda_n}.$$

We let $C_3 = F/\lambda_n$, then

$$|w_n(z)| \le \left\|\phi_n^{fix}\right\|_z |z|\, e^{\lambda_n z} \le \left(2\frac{|w_n(a)|\, e^{-\lambda_n a}}{|a|} + C_3 \right) |z|\, e^{(\lambda_1 + \mu)z}.$$

We now define $C = \max(C_1, C_2, C_3)$ proving this Lemma. ∎

Lemma 4.3.12 *Given a boundary condition α_n the solution found in Lemma 4.3.11 is the only solution to* (4.3.14) *satisfying $w_n(a) = \alpha_n$ and $\lim_{z\to-\infty} w_n(z) = 0$.*

Proof Let $w_{n,1}(z)$ and $w_{n,2}(z)$ be two solutions to (4.3.14) satisfying $w_{n,i}(a) = \alpha_n$ and $\lim_{z\to-\infty} w_{n,i}(z) = 0$, then the difference $w_{n,d}(z) = w_{n,2}(z) - w_{n,1}(z)$ satisfies the homogeneous ODE,

$$w_{n,d}''(z) = \lambda_n^2 w_{n,d}(z) + k_n^2 \rho(z) w_{n,d}(z) e^{\lambda_1 z}.$$

with boundary conditions

$$w_{n,d}(a) = 0, \qquad \text{and} \qquad \lim_{z\to-\infty} w_{n,d}(z) = 0.$$

We will show that $w_{n,d}(z) = 0$.

First, assume that $w_{n,d}(z) > 0$ for some $z \in (-\infty, a)$, then there must be some $z_+ \in (-\infty, a)$ such that $w_{n,d}(z)$ reaches an absolute maximum $w_+ = w_{n,d}(z_+) > 0$. Now the above ODE states that $w_{n,d}''(z_+) = \lambda_n^2 w_+ + k_n^2 \rho(z_+) w_+ e^{\lambda_1 z_+} > 0$ since $\rho(z) > 0$. This is in contradiction with the fact that w_+ is a maximum, so $w_{n,d}(z) \le 0$ for all z.

A similar argument yields that $w_{n,d}(z) \ge 0$ and so $w_{n,d}(z) = 0$ for all z. ∎

Before we can translate the bounds on w_n to bounds on c_n we need to show that factors $1/(k_n J_1(k_n))$ remain bounded. The following Lemma shows that they approach zero as $n \to \infty$.

Lemma 4.3.13 *There is a constant $C > 0$ such that*

$$a_n = \left| \frac{1}{\sqrt{k_n} J_1(k_n)} \right| \leq C,$$

for all $n \geq 1$.

Proof By Bourget's hypothesis we know that $J_1(k_n)$ is nonzero for all n, so a_n is finite for all n. For large x, the asymptotic expansion for J_1 ([28], Chapter VII) states that

$$J_1(x) = \sqrt{\frac{2}{\pi x}} \left(\cos\left(x - \frac{3}{4}\pi \right) + O\left(\frac{1}{x} \right) \right),$$

while k_n lies in the interval $(n\pi + \frac{3}{4}\pi, n\pi + \frac{7}{8}\pi)$ ([28], Chapter XV) so the cosine term in the expansion above is bounded away from zero. Thus a_n remains bounded as $n \to \infty$.

■

This allows us to calculate the following estimate for $c_n(z)$.

Lemma 4.3.14 *Assume the assumptions of Theorem 4.3.9 hold, then there is a $C > 0$ such that*

$$\sum_{n=1}^{\infty} k_n^3 c_n(z)^2 \leq C e^{2\lambda_1 z},$$

for all $z < z^*$.

Proof For fixed z we let D be the intersection of Ω with the plane at coordinate z, and let Δ_D be the radial Laplacian on D. Since u is twice differentiable, we can apply Parseval's theorem to $\Delta_D u$,

$$\sum_{n=1}^{\infty} \frac{1}{2} \left(\frac{k_n}{r_{max}(z)} \right)^4 c_n(z)^2 J_1(k_n)^2 = \left\| \Delta_D u \right\|_{L^2(D)}.$$

Now using Lemma 4.3.13 we obtain

$$\begin{aligned} \sum_{n=1}^{\infty} k_n^3 c_n(z)^2 &\leq \sum_{n=1}^{\infty} k_n^3 c_n(z)^2 \frac{k_n J_1(k_n)^2}{k_n J_1(k_n)^2} \\ &\leq C \sum_{n=1}^{\infty} k_n^4 c_n(z)^2 J_1(k_n)^2 \\ &\leq 2C r_{max}^4 \left\| \Delta_D u \right\|_{L^2(D)}. \end{aligned}$$

From the asymptotics for $D^2 u$ in Lemma 4.3.10 we see that $\left\| \Delta_D u \right\|_{L^2(D)} \leq C e^{2\lambda_1 z}$ for $z < z^*$. ■

We can now prove Theorem 4.3.9.

Proof of Theorem 4.3.9 Since $w_n(z) \to 0$ as $z \to -\infty$, Lemma 4.3.12 states that the functions w_n must have the asymptotics described in Lemma 4.3.11. Now, from Lemma 4.3.14 we see that $c_n(a)$ is uniformly bounded. Thus there is a constant $W > 0$ such that $|w_n(a)| \leq J_1(k_n)^2 W/2$ for all n. So

$$\begin{aligned}
|c_n(z)| &\leq \Big(2We^{-\lambda_n a} + \frac{2C}{J_1(k_n)^2}\Big)e^{\lambda_n z} && \text{if } \lambda_n < \mu + \lambda_1,\\
|c_n(z)| &\leq \Big(2We^{-(\lambda_1+\mu)a} + \frac{2C}{\lambda_n^2 J_1(k_n)^2}\Big)e^{(\lambda_1+\mu)z} && \text{if } \lambda_n > \mu + \lambda_1,\\
|c_n(z)| &\leq \Big(2We^{-\lambda_n a}/|a| + \frac{2C}{J_1(k_n)^2}\Big)\,|z|\,e^{(\lambda_1+\mu)z} && \text{if } \lambda_n = \mu + \lambda_1.
\end{aligned}$$

Now since there are only a finite amount of terms where $\lambda_n \leq \mu + \lambda_1$ and $J_1(k_n)$ is nonzero, we can choose $\tilde{C}$ sufficiently large that $\tilde{C} \geq 2We^{-\lambda_n a} + 2C/J_1(k_n)^2$ and $\tilde{C} \geq 2We^{-\lambda_n a}/|a| + 2C/J_1(k_n)^2$. Furthermore, since by Lemma 4.3.13 $1/(k_n J_1(k_n))$ is bounded, we can also choose $\tilde{C}$ sufficiently large that $\tilde{C} \geq 2We^{-(\lambda_1+\mu)a} + 2C/(\lambda_n^2 J_1(k_n)^2)$. Finally since c_n are bounded over the interval $[a, z^*]$ we can choose $\tilde{C}$ sufficiently large that the above estimates hold for $z < z^*$ instead of $z < a$. ∎

4.4 Asymptotic lower bounds away from the tip

The results from the previous section, specifically the upper bounds found for the coefficients $c_n(z)$ in combination with harmonics on cylinders inside Ω allow us to establish lower bounds for $c_1(z)$, and through this for the (cumulative) flux.

4.4.1 A lower bound for $c_1(z)$

We now define

$$\tilde{c}(z) = u(0, z) - c_1(z) = \sum_{n=2}^{\infty} c_n(z). \tag{4.4.1}$$

Clearly since both u and c_1 are $O(e^{\lambda_1 z})$, $\tilde{c}(z) = O(e^{\lambda_1 z})$. However, since each individual $c_n(z)$ decays faster for $n \geq 2$ we wish to improve this estimate.

Lemma 4.4.1 *If the assumptions of Theorem 4.3.9 hold, and if $\lambda_1 + \mu \neq \lambda_2$ then we define $\tilde{\lambda} = \min(\lambda_1 + \mu, \lambda_2)$. Thus $c_n(z) = O(e^{\tilde{\lambda} z})$ for $n \geq 2$. Now for any $\frac{1}{2} < \eta < 1$,*

$$|\tilde{c}(z)| \leq C(\eta) e^{((1-\eta)\tilde{\lambda} + \eta\lambda_1)z},$$

for all $z < z^*$.

Proof We use an interpolation inequality. For arbitrary η, and for p and q such that $1/p + 1/q = 1$,

$$\left|\sum_{n=2}^{\infty} c_n(z)\right| \leq \sum_{n=2}^{\infty} \left(k_n^{-3\eta/2} |c_n(z)|^{1-\eta}\right) \left(k_n^{3\eta/2} |c_n(z)|^{\eta}\right),$$

so using Hölder inequality

$$|\tilde{c}(z)| \leq \left(\sum_{n=2}^{\infty} k_n^{-3\eta p/2} |c_n(z)|^{(1-\eta)p}\right)^{1/p} \left(\sum_{n=2}^{\infty} k_n^{3\eta q/2} |c_n(z)|^{\eta q}\right)^{1/q}.$$

We now choose $p = 2/(2-\eta)$ and $q = 2/\eta$ and substitute the asymptotics $c_n(z) = O(e^{\tilde{\lambda} z})$ and $\sum k_n^3 c_n(z)^2 = O(e^{2\lambda_1 z})$. So

$$\begin{aligned} |\tilde{c}(z)| &\leq \left(Ce^{\tilde{\lambda} z}\right)^{1-\eta} \left(\sum_{n=2}^{\infty} k_n^{-\frac{3\eta}{2-\eta}}\right)^{(2-\eta)/2} \left(\sum_{n=2}^{\infty} k_n^3 c_n(z)^2\right)^{\eta/2} \\ &\leq C(\eta) e^{((1-\eta)\tilde{\lambda} + \eta\lambda_1)z} \left(\sum_{n=2}^{\infty} k_n^{-\frac{3\eta}{2-\eta}}\right)^{(2-\eta)/2}. \end{aligned}$$

Now $k_n = O(n)$ so if $\frac{1}{2} < \eta < 1$ then $3\eta/(2-\eta) > 1$ and the last sum converges. ■

Corollary 4.4.2 *If $\lambda_1 + \mu = \lambda_2$ the above calculations remain practically the same and*

$$|\tilde{c}(z)| \leq C(\eta) |z|^{1-\eta} e^{((1-\eta)\tilde{\lambda} + \eta\lambda_1)z}.$$

Alternatively, we could choose $\tilde{\lambda} = \lambda_2 - \epsilon$ for some sufficiently small $\epsilon > 0$ to obtain

$$|\tilde{c}(z)| \leq C(\eta, \epsilon) e^{((1-\eta)\tilde{\lambda} + \eta\lambda_1)z}.$$

Since the sum of coefficients $c_n(z)$ for $n \geq 2$ decays faster than $c_1(z)$ as $z \to -\infty$, by finding a suitable lower bound for u we can now establish a lower bound for $c_1(z)$.

Theorem 4.4.3 *If the assumptions of Theorem 4.3.9 hold, then by Lemma 4.4.1 and Corollary 4.4.2 we can choose a λ^* with $\lambda_1 < \lambda^* < \min(\lambda_1 + \mu, \lambda_2)$ such that $\tilde{c}(z) = O(e^{\lambda^* z})$. We now define $\lambda(\xi) = \xi\lambda_1 + (1-\xi)\lambda^*$ for $0 < \xi < 1$, then there exist constants $\tilde{C}(\xi) > 0$ and $\tilde{z}_\xi < z^*$ such that*

$$c_1(z) \geq \tilde{C}(\xi) e^{\lambda(\xi) z}$$

for all $z < \tilde{z}_\xi$.

Proof Fix ξ and let $r_\xi = k_1/\lambda(\xi)$. Since $\lambda_1 < \lambda(\xi)$, $r_\xi < r_{max}$ and $r_{max}(z) \to r_{max}$ as $z \to -\infty$, we can choose a $z_\xi < z^*$ such that $r_\xi < r_{max}(z_\xi)$. Let

$$\Omega_\xi = \{(r,z) \quad | \quad 0 \le r < r_\xi, \quad z < z_\xi\}$$

be the cylinder of radius r_ξ with a right cap at $z = z_\xi$. Clearly $\Omega_\xi \subset\subset \Omega$, let

$$C(\xi) = e^{-\lambda(\xi) z_\xi} \min_{0 \le r \le r_\xi} u(r, z_\xi),$$

then $C(\xi) > 0$ since $u(r, z_\xi) > 0$ for $r \le r_\xi$. On Ω_ξ we define

$$v_\xi(r,z) = C(\xi) J_0(\lambda(\xi) r) e^{\lambda(\xi) z},$$

then v_ξ is harmonic in Ω_ξ, $v_\xi \le u$ on $\partial\Omega_\xi$ and by the maximum principle $v_\xi \le u$ in Ω_ξ. If we now examine u on the central axis $r = 0$ then we obtain

$$u(0,z) = c_1(z) + \tilde{c}(z) \ge C(\xi) e^{\lambda(\xi) z},$$

for $z \le z_\xi$. Since $\tilde{c}(z) = O(e^{\lambda^* z})$ and $\lambda^* > \lambda(\xi)$ we can find $\tilde{C}(\xi) > 0$ and $\tilde{z}_\xi < z_\xi$ such that the result of this theorem holds.

■

Note that we can not let $\lambda(\xi) = \lambda_1$, as $z_\xi \to -\infty$ and subsequently $C(\xi) \to 0$ as $\lambda(\xi) \to \lambda_1$.

4.4.2 A lower bound for the flux

Differentiating (4.3.3) to r and z and evaluating this at a boundary point $(r(s), z(s))$ we obtain

$$\begin{aligned} \frac{\partial u}{\partial r}(r(s), z(s)) &= -\sum_{n=1}^{\infty} \frac{k_n}{r(s)} c_n(z(s)) J_1(k_n), \\ \frac{\partial u}{\partial z}(r(s), z(s)) &= \quad \sum_{n=1}^{\infty} \frac{k_n}{r(s)} c_n(z(s)) J_1(k_n) \frac{r'(s)}{z'(s)}, \end{aligned} \tag{4.4.2}$$

and so we have an expression for the flux $F(s)$ in terms of the coefficients c_n,

$$\begin{aligned} F(s) &= z'(s) \frac{\partial u}{\partial r}(r(s), z(s)) - r'(s) \frac{\partial u}{\partial z}(r(s), z(s)) \\ &= -\frac{1}{r(s) z'(s)} \sum_{n=1}^{\infty} k_n c_n(z(s)) J_1(k_n). \end{aligned} \tag{4.4.3}$$

Theorem 4.4.4 *If the assumptions of Theorem 4.3.9 hold, then there is a λ, with $\lambda_1 < \lambda < \min(\lambda_1 + \mu, \lambda_2)$ and a $a < z^*$ such that*

$$F(s) \ge C e^{-\lambda s},$$

for $s > a$.

Proof We now write $F(s) = F_1(s) + \tilde{F}(s)$ where

$$F_1(s) = -\frac{1}{r(s)z'(s)} k_1 c_1(z(s)) J_1(k_1),$$
$$\tilde{F}(s) = -\frac{1}{r(s)z'(s)} \sum_{n=2}^{\infty} k_n c_n(z(s)) J_1(k_n).$$

We first use similar arguments as in the proof of Lemma 4.4.1 to show that $\tilde{F}(s) = O(e^{-\lambda' s})$ for some λ' with $\lambda_1 < \lambda' < \min(\lambda_1 + \mu, \lambda_2)$. Since $J_1(x) = O(1/\sqrt{x})$, $\sqrt{k_n} J_1(k_n)$ remains bounded, furthermore, for $s > 2\xi$, $r(s) > r(2\xi)$ so there is a C such that

$$\tilde{F}(s) \leq C \sum_{n=2}^{\infty} \sqrt{k_n} c_n(z(s)).$$

For some η to be determined later, and constants p and q with $1/p + 1/q = 1$ we use Hölder's inequality and Lemma 4.3.14 to obtain bounds for the above sum,

$$\begin{aligned}\left| \sum_{n=2}^{\infty} \sqrt{k_n} c_n(z(s)) \right| &\leq \sum_{n=1}^{\infty} \left(k_n^{\frac{1-3\eta}{2}} |c_n(z(s))|^{1-\eta} \right) \left(k_n^{3\eta/2} |c_n(z(s))|^{\eta} \right) \\ &\leq \left(\sum_{n=2}^{\infty} k_n^{\frac{1-3\eta}{2} p} |c_n(z(s))|^{(1-\eta)p} \right)^{1/p} \left(k_n^{3\eta q/2} |c_n(z(s))|^{\eta q} \right)^{1/q}\end{aligned}$$

we now choose $p = 2/(2-\eta)$ and $q = 2/\eta$, then

$$\begin{aligned}\left| \sum_{n=2}^{\infty} \sqrt{k_n} c_n(z(s)) \right| &\leq \left(C e^{-\tilde{\lambda} s} \right)^{1-\eta} \left(\sum_{n=2}^{\infty} k_n^{\frac{1-3\eta}{2-\eta}} \right)^{\frac{2-\eta}{2}} \left(\sum_{n=2}^{\infty} k_n^3 c_n(z(s))^2 \right)^{\eta/2} \\ &\leq C(\eta) e^{-((1-\eta)\tilde{\lambda} + \eta\lambda_1)s} \left(\sum_{n=2}^{\infty} k_n^{\frac{1-3\eta}{2-\eta}} \right)^{\frac{2-\eta}{2}}.\end{aligned}$$

Since $k_n = O(n)$, if $\frac{3}{4} < \eta < 1$ then $\frac{1-3\eta}{2-\eta} < -1$ and the last sum converges, so by choosing a suitable η we let $\lambda' = (1-\eta)\tilde{\lambda} + \eta\lambda_1$ to obtain

$$\left| \tilde{F}(s) \right| \leq \tilde{C} e^{-\lambda' s}.$$

Now, since $r(s) < r_{max}$ and $z'(s) \geq -1$ and $-s < z(s) < -s + 2$ the lower bound on c_1 from Theorem 4.4.3 yields that we can choose a λ with $\lambda_1 < \lambda < \lambda'$, so that there is a $C_1 > 0$, and a sufficiently large a such that $F_1(s) \geq C_1 e^{-\lambda s}$ for $s > a$.

So $F(s) \geq C_1 e^{-\lambda s} - \tilde{C} e^{-\lambda' s}$ therefore if we choose a sufficiently large, $F(s) \geq C e^{-\lambda s}$ for $s > a$.

■

4.5 The $C^{2,\alpha}$ Schauder map

As stated at the start of this chapter, the calculations presented here originated from an attempt to set up a Schauder fixed point argument in a $C^{2,\alpha}$ space. The idea was to define a bounded set $\Xi \subset C^{2,\alpha}$ containing functions r satisfying conditions similar to (3.3.1) through (3.3.5) as well as satisfying the asymptotics assumed in Theorem 4.3.9.

In a manner similar to that used in Section 3.4 we would then obtain a family of cumulative fluxes $G_\xi \subset C^{2,\alpha}$ parametrized by ξ. In addition to all the properties found in Section 3.4 we would also obtain lower bounds on the (cumulative) flux from Theorem 4.4.4. This defines a map $\Psi_1 : \Xi \to C^{2,\alpha}$. Given $G_\xi \in Im(\Psi_1)$ we would then find a value of ξ such that we can find a solution to the travelling wave ODE in a similar manner as in Section 3.5. This defines a map Ψ_2 on $Im(\Psi_1)$. We will refer to the composition $\Psi = \Psi_2 \circ \Psi_1$ as the Schauder map. If we could show that Ξ is convex and compact, $Im(\Psi) \subset \Xi$ and Ψ is continuous, we could use Schauder's fixed point theorem to show the existence of a $C^{2,\alpha}$ solution to the diffusive VSC model.

In attempting this, several problems presented themselves:

- If the original function $r \in \Xi$ is $C^{2,\alpha}$ we could use the boundary point lemma to obtain that the flux was non-zero. As a result, for the solution $r \in Im(\Psi)$ of the travelling wave ODE, we have $r'(s) > 0$ for all s and so by (4.2.1) the new solution r would be twice differentiable. However a stronger lower bound on the flux is required if one wishes to show that $\|r\|_{C^2}$ is uniformly bounded for all $r \in Im(\Psi)$, proving a similar bound for the $C^{2,\alpha}$ norm is even more difficult. To illustrate, hypothetically it might be possible that by iterating the Schauder map the C^2 norm of r explodes, and the travelling wave solutions converge to some $C^{1,\alpha}$ surface that has C^2 singularities as described in Section 4.2.

- The use of interpolation inequalities in the proofs of Lemma 4.4.1 and Theorem 4.4.4 resulted in a weakening of the asymptotics for the flux: the exponent λ from Theorem 4.4.4 is larger than λ_1. As such it will probably be extremely difficult to show that the asymptotics of some $r \in Im(\Phi)$ are the same as those originally assumed in Theorem 4.3.9.

- Lastly, even if the previous two problem were overcome, if one wanted to prove the image of this Schauder map lies within its domain, we would need to show that the constants C and s^* for the asymptotics some $r \in Im(\Phi)$ are smaller than those constants as assumed in Theorem 4.3.9. This would require obtaining explicit expressions for these constants, which are very hard to obtain. As a result of this and the previous point, one cannot show that Φ maps Ξ into itself.

As a result of these difficulties, we abandoned the attempt to set up a Schauder fixed point argument in a $C^{2,\alpha}$ space in favour of the $C^{1,\alpha}$ approach used in the previous chapter. However, the results from Sections 4.3.1 through 4.3.5 are still valid, as they only assume $C^{1,\alpha}$ regularity.

Chapter 5

Numerical simulations of the Diffusive VSC model

The dynamics of the diffusive VSC model, as described in Chapter 3, was numerically simulated by adapting a code for the simulation of wound healing by Vermolen [18], [26], [27]. This numerical method consists of a finite difference method, where the boundary of the cell is calculated using a level set formulation, and a finite element method using a triangulation of the cell interior used to solve the associated Dirichlet problem in the interior.

Starting point for these calculations was a spherical cell, with a VSC moving at a constant velocity in the z direction.

In this chapter we will describe the numerical methods used and conclude with some simulations of the cell boundary. We start with a description of the various grids used for the finite difference methods and the level set formulation of the VSC model. We then describe how we form the triangulation used to solve the Dirichlet problem, and finally we conclude by showing some numerical results.

5.1 Initial condition and two dimensional formulation of the dynamics

Initially, we will start our numerical simulation assuming a spherical cell of radius four around the origin. The VSC is located at the origin, and moving with a velocity of 1 along the z-axis. Clearly the initial condition is rotationally symmetric around the z-axis, and the solution will remain so. As such we can model this problem om a rectangle in $\mathbb{R}^2$ with cartesian coordinates r and z. To avoid having to deal with boundary conditions on the line $r = 0$, we let this grid, our initial condition and hence subsequent solutions be symmetric with respect to reflections along the z-axis. When solving the Dirichlet problem on

this domain, we continue to use the radially symmetric Laplacian

$$\Delta_r = \frac{1}{r}\frac{\partial}{\partial r} r \frac{\partial}{\partial r} + \frac{\partial^2}{\partial z^2}.$$

5.2 Grids and finite differences

As described in the previous section, due to rotational symmetry around the z-axis, we can model the surrounding space $\mathbb{R}^3$ as a two dimensional plane with (r, z) coordinates symmetric with respect to reflections about the z-axis. For finite difference calculations this space modelled as several grids. The coarse grid is used mainly away from the cell boundary $\partial\Omega$. The refined grid is a rectangular grid with more grid points, points on the coarse grid are also points on the refined grid. The cartesian band is a subset of the refined grid defined around the cell boundary.

- The *coarse cartesian grid* is a rectangular grid of $n_r \times n_z$ points.
- The *refined cartesian grid* is a rectangular grid of $\tilde{n}_z \times \tilde{n}_r$ points, where $\tilde{n}_{z,r} = \alpha(n_{z,r} - 1) + 1$ and α is the refinement ratio. The grid points of the coarse grid overlap the points in the refined grid.
- The *cartesian band* is a subset of the refined grid, consisting of those grid points within a certain distance d of the cell boundary.

If we say a function f is defined on the coarse/refined grid or on the band, the function is represented by its values $f_{i,j}$ where $i \in 1 \dots n_z$, $j \in 1 \dots n_r$ for the coarse grid, or $i \in 1 \dots \tilde{n}_z$, $j \in 1 \dots \tilde{n}_r$ for the refined grid and the cartesian band. In the latter case, only those values (i, j) are considered if the corresponding grid point lies in the band. The cartesian band is implemented using a function defined on the refined grid, which is equal to one of the grid point is in the band, and zero otherwise.

If the appropriate neighbours of a grid point (i, j) are defined (the point does not lie on the boundary of the grid or band), then derivatives are calculated using central finite differences.

$$\begin{aligned} \left(\frac{\partial f}{\partial r}\right)_{i,j} &= \frac{f_{i,j+1} - f_{i,j-1}}{2\mathrm{d}r}, \\ \left(\frac{\partial f}{\partial z}\right)_{i,j} &= \frac{f_{i+1,j} - f_{i-1,j}}{2\mathrm{d}z}, \end{aligned} \tag{5.2.1}$$

where $\mathrm{d}r$ and $\mathrm{d}z$ are the distances between grid points in the r respectively the z directions in the grid used. If a point (i, j) lies of the boundary of the domain, noncentral differences are used, for example if the point $(i, j-1)$ does not exist then

$$\left(\frac{\partial f}{\partial r}\right)_{i,j} = \frac{f_{i,j+1} - f_{i,j}}{\mathrm{d}r}, \tag{5.2.2}$$

and similarly for other missing neighbours. Higher derivatives are calculated by applying the above procedure several times.

5.3 Level set formulation

The cell boundary $\partial\Omega$ is described as the zero set of a function $\psi(r, z, t)$ defined in a neighbourhood of $\partial\Omega$, where ψ is positive inside Ω and negative outside. If we choose ψ such that $|\nabla\psi| = 1$, this function represents the distance to the boundary $\partial\Omega$. In this formulation, the outward normal vector is given by

$$\hat{n} = -\nabla\psi, \tag{5.3.1}$$

the first principle curvature can be calculated by taking the divergence of the normal vector

$$\kappa_1 = \Delta\psi \tag{5.3.2}$$

and the second principal curvature is found using

$$\kappa_2 = -\frac{\frac{\partial\psi}{\partial r}}{r}. \tag{5.3.3}$$

If the boundary $\partial\Omega$ is transported by a velocity field $v = v_n\nabla\psi$, then ψ must satisfy the transport equation

$$\frac{\partial\psi}{\partial t} + v\cdot\nabla\psi = \frac{\partial\psi}{\partial t} + v_n = 0. \tag{5.3.4}$$

The normal velocity is defined on the boundary, where $\phi = 0$, and must be extended in such a way that $\nabla\psi$ remains of length one. Now

$$\frac{\partial\,|\nabla\phi|}{\partial t} = \nabla\phi\cdot\nabla\frac{\partial\phi}{\partial t} = -\nabla\psi\cdot\nabla v_n, \tag{5.3.5}$$

so if v_n is extended in such a way that its normal derivative is zero, the gradient of ψ will remain of length one. Let $\tilde{v}_n(r, z, \tau, t)$ solve

$$\begin{aligned} \frac{\partial\tilde{v}_n}{\partial\tau} + \nabla\psi\cdot\nabla\tilde{v}_n &= 0 \qquad \text{outside } \Omega, \\ \frac{\partial\tilde{v}_n}{\partial\tau} - \nabla\psi\cdot\nabla\tilde{v}_n &= 0 \qquad \text{inside } \Omega, \\ \tilde{v}_n &= v_n \qquad \text{on } \partial\Omega, \end{aligned} \tag{5.3.6}$$

then an equilibrium (in τ) of $\tilde{v}_n$ is an extension of v_n satisfying $\nabla\psi\cdot\nabla v_n = 0$.

5.4 Finite element method

5.4.1 Triangulation

A *triangulation* of a two dimensional set in $\mathbb{R}^2$ consists of a set of N_v vertices $\{x_i\}_{i=1}^{N_v} \subset \bar{\Omega}$ giving the coordinates of the vertices of the triangulation, and a set of N_t triplets of indices $\{(a_k, b_k, c_k)\}_{k=1}^{N_t}$, where each a_k, b_k or c_k is a different integer from 1 to N_v. We define the k-th triangle, $T_k \subset \mathbb{R}^2$ to be the open triangle having x_{a_k}, x_{b_k} and x_{c_k} as its vertices. The triangulation satisfies the following properties:

- Each vertex is unique, if $x_i = x_j$ then $i = j$.
- There are no overlapping triangles. If for some point x, $x \in T_k$ and $x \in T_l$ then $k = l$.
- Every point x_i is the vertex of a triangle, $\bigcup_{k=1}^{N_t} \{a_k, b_k, c_k\} = \{1 \dots N_v\}$.
- Vertices do not lie on the edges of triangles. If $x_i \in \partial T_k$ then i must be equal to either a_k, b_k or c_k for some k.

A triangulation is created by diagonally dividing grid elements of both the coarse grid and the cartesian band into an upper left and a lower right triangle. On the boundary of these two, the upper left or lower right triangle is further divided into r triangles so that the boundary of these and the triangles of the cartesian band share vertices. Triangles within the cartesian band are further divided if the cell boundary $\partial\Omega$ crosses their edges, additional vertices are created at these crossings. An example of a triangulation near the boundary $\partial\Omega$ can be see in Figure 5.1 while a triangulation of the full rectangular space can be seen in Figure 5.2.

We now define the triangulated space $\tilde{\Omega}$ as the union of the triangles with boundary

$$\tilde{\Omega} = \bigcup_{j=1}^{N_t} \bar{T}_j. \tag{5.4.1}$$

We define the following function space H of piecewise linear functions on $\tilde{\Omega}$

$$H = \{f \in C(\tilde{\Omega}; \mathbb{R}) : \forall k, f|_{T_k} \text{ is affine linear}\}. \tag{5.4.2}$$

Any function $f \in H$ is uniquely identified by giving its values on the vertices x_i of the triangulation since outside these points the function can be calculated using linearity. For $(r, z) \in \bar{T}_k$, we let

$$(r_A, z_A) = x_{a_k}, \qquad (r_B, z_B) \quad = x_{b_k}, \qquad (r_C, z_C) = x_{c_k}. \tag{5.4.3}$$

now $f|_{T_k}(r, z) = \alpha_k r + \beta_k z + \gamma_k$ and the coefficients α_k, β_k and γ_k are given by

$$\begin{pmatrix} \alpha_k \\ \beta_k \\ \gamma_k \end{pmatrix} = \begin{bmatrix} r_A & z_A & 1 \\ r_B & z_B & 1 \\ r_C & z_C & 1 \end{bmatrix}^{-1} \begin{pmatrix} f(x_{a_k}) \\ f(x_{b_k}) \\ f(x_{c_k}) \end{pmatrix}. \tag{5.4.4}$$

Now, for i from 1 to N_v we define the functions ϕ_i by $\phi_i(x_j) = \delta_{ij}$. Clearly these functions form a basis of H.

For practical purposes it will be useful to define the set of interior indices I,

$$I = \{i \in 1 \cdots N_v : x_i \notin \partial\tilde{\Omega}\}. \tag{5.4.5}$$

if we define H_0 to be those functions in H which are zero on the boundary $\partial\tilde{\Omega}$ then for $i \in I$, ϕ_i form a basis of H_0.

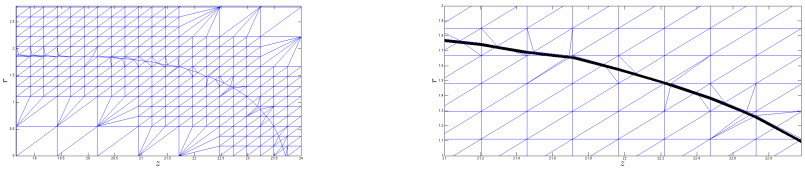

Figure 5.1: Triangulation for the hyphoid solution: left – coarse and fine grid, right – fine grid and triangulation near $\partial\Omega$.

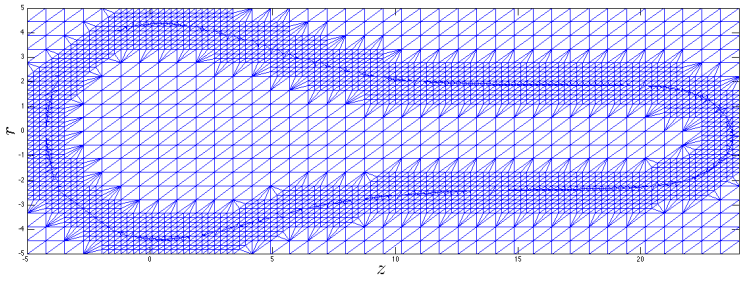

Figure 5.2: Full triangulation for the hyphoid solution and origin sphere.

5.4.2 Weak formulation of the Dirichlet problem

A solution to the Dirichlet problem on Ω,

$$\begin{aligned} -\Delta u &= f \quad \text{in } \Omega, \\ u &= 0 \quad \text{on } \partial\Omega, \end{aligned} \tag{5.4.6}$$

has as weak formulation

$$\int_\Omega (\nabla u \cdot \nabla \phi) \mathrm{d}x = \int_\Omega f\phi \mathrm{d}x \qquad \text{for all } \phi \in C_0^\infty(\Omega). \tag{5.4.7}$$

We approximate the solution u in our triangulation by finding a $u \in H_0$ such that

$$\int_{\tilde{\Omega}} (\nabla u \cdot \nabla \phi_j) \mathrm{d}x = \int_{\tilde{\Omega}} f\phi_j \mathrm{d}x \qquad \text{for all } j \in I. \tag{5.4.8}$$

note that since this the weak formulation holds for all basis functions of H_0, it holds for all test functions $\phi \in H_0$. Expressing u in terms of the basis functions, $u = \sum_{i\in I} u_i\phi_i$ we see that

$$\sum_{i\in I} u_i M_{ij} = g_j, \tag{5.4.9}$$

where

$$M_{ij} = \int_{\tilde{\Omega}} (\nabla \phi_i \cdot \nabla \phi_j) \mathrm{d}x, \qquad g_j = \int_{\tilde{\Omega}} f\phi_j \mathrm{d}x. \tag{5.4.10}$$

This is a linear system with the amount of equations and unknowns equal to the amount of elements in I, and thus it can be solved by matrix inversion. We shall refer to the matrix M with coefficients M_{ij} as the *stiffness matrix*.

Calculating the stiffness matrix

Using (5.4.4) we define $\alpha_{i,k}$, $\beta_{i,k}$ and $\gamma_{i,k}$ such that for all $i \in I$ and k from 1 to N_t

$$\phi_i|_{T_k}(r,z) = \alpha_{i,k} r + \beta_{i,k} z + \gamma_{i,k}, \tag{5.4.11}$$

note that these coefficients will be zero for most triangles T_k unless T_k has x_i as a vertex. Now the integral can be seen as a sum over all the triangles T_k,

$$M_{ij} = \sum_{k=1}^{N_t} (\alpha_{i,k}\alpha_{j,k} + \beta_{i,k}\beta_{j,k}) A_k, \tag{5.4.12}$$

where

$$A_k = \int_{T_k} 1 \mathrm{d}x. \tag{5.4.13}$$

Now in two dimensions, A_k would be the area of the triangle T_k which is given by

$$A_k^{2D} = \frac{1}{2} \left| (r_B - r_A)(z_C - z_A) - (r_C - r_A)(z_B - z_A) \right|. \tag{5.4.14}$$

For problems in three dimensions with cylindrical symmetry, A_k is the volume of the triangle T_k when it is rotated around the z axis. By Pappus' centroid theorem we obtain

$$\begin{aligned} A_k &= 2\pi \frac{r_A + r_B + r_C}{3} A_k^{2D}, \\ &= \pi \frac{r_A + r_B + r_C}{3} \left| (r_B - r_A)(z_C - z_A) - (r_C - r_A)(z_B - z_A) \right|, \end{aligned} \tag{5.4.15}$$

where $r_{A,B,C}$ and $z_{A,B,C}$ are given by (5.4.3).

5.5 Numerical simulation of the dynamics of the VSC model

We now have all the ingredients necessary to describe how we numerically simulate the evolution of the VSC model.

1. The cell boundary at time t, $\partial\Omega_t$ is formulated as a level set function on the cartesian band.

2. The space is triangulated as described in section 5.4.1.

3. The Dirichlet problem is solved on the triangulation, as described in section 5.4.2.

4. The flux (norm of ∇u), and the velocity function are calculated on grid points in the boundary and then extended to the cartesian band. This is done by solving the PDE (5.3.6) using 10 forward Euler τ steps with $\Delta\tau = \frac{1}{2}\min(\Delta r, \Delta z)$ where Δr and Δz are the grid sizes of the refined grid.

5. The level set is updated by a forward Euler time step of size Δt.

This process is repeated as long as is deemed necessary.

5.6 Results

The VSC model was numerically simulated, starting from a sphere of radius 4 around the origin and the VSC starting from the origin and moving with a speed of 1 in the z direction. Selected iterations, also showing the density $u(r, z)$ of vesicles, are shown in Figures 5.3, 5.4 and 5.5. In these figures you can see a hyphoid like solution forming from the spherical cell, eventually assuming an constant tip shape as time advances.

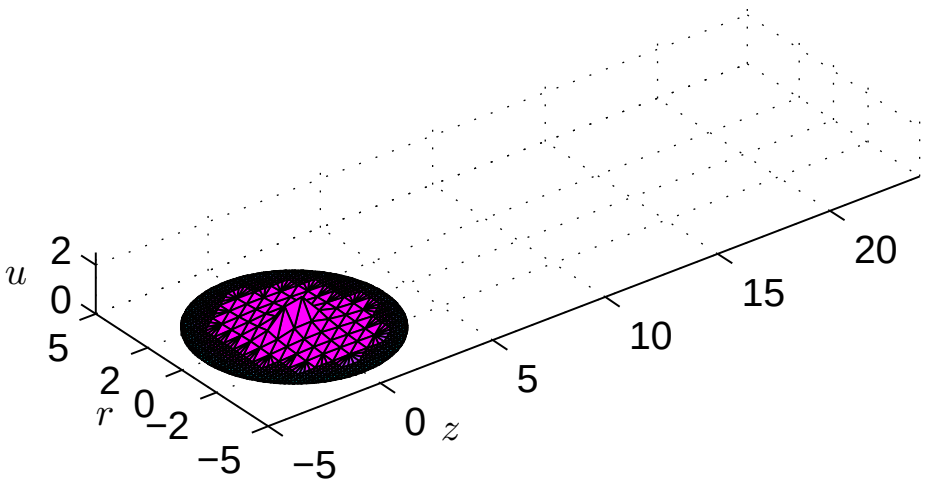

(a) Iteration 1, time = 0.00

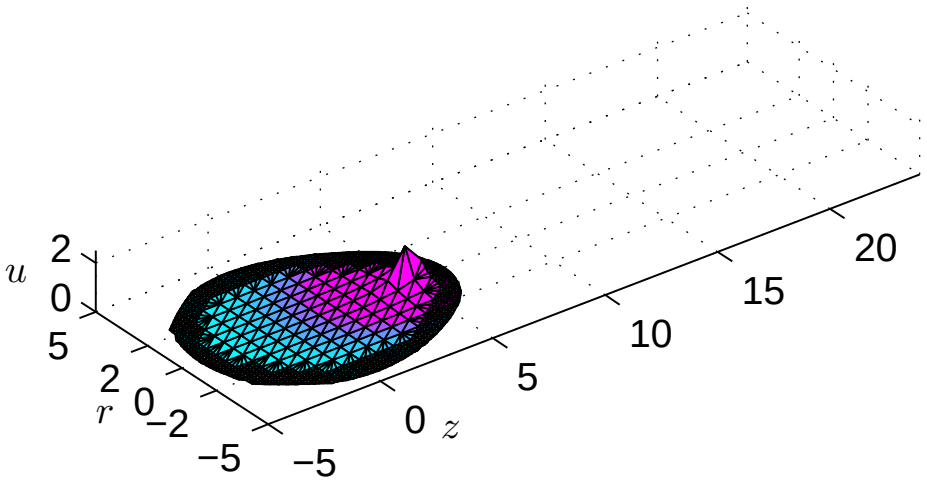

(b) Iteration 201, time = 5.01

Figure 5.3: VSC Model Simulation

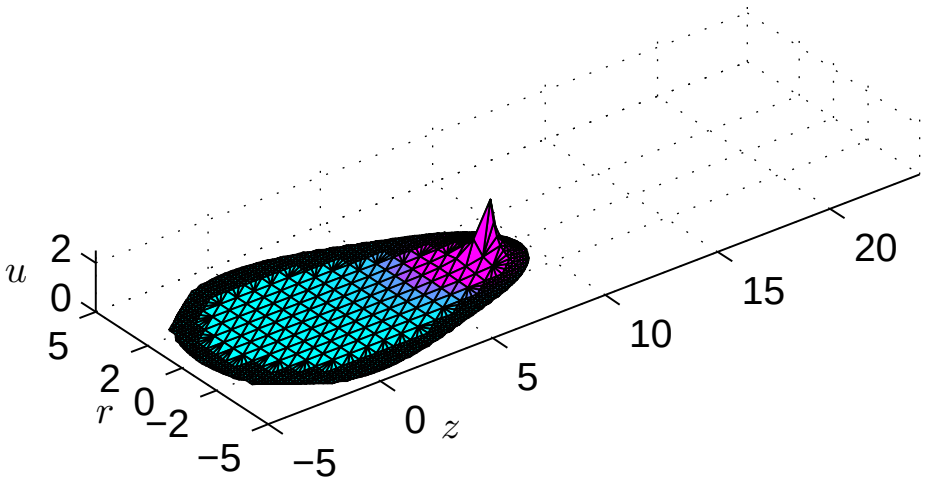

(a) Iteration 401, time = 8.55

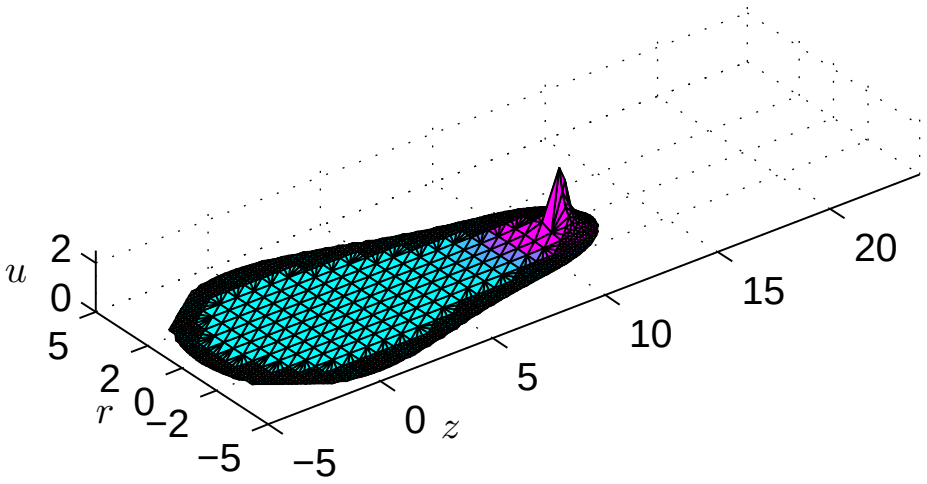

(b) Iteration 601, time = 11.8

Figure 5.4: VSC Model Simulation

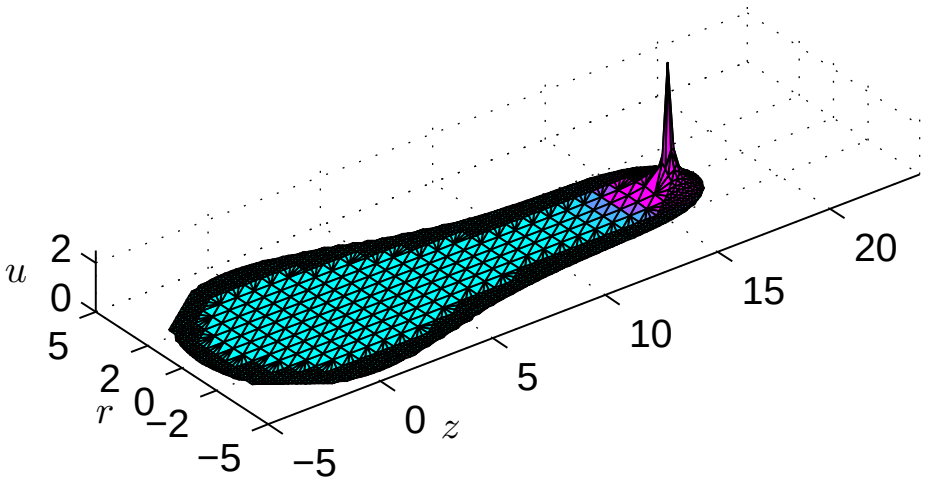

(a) Iteration 801, time = 15.0

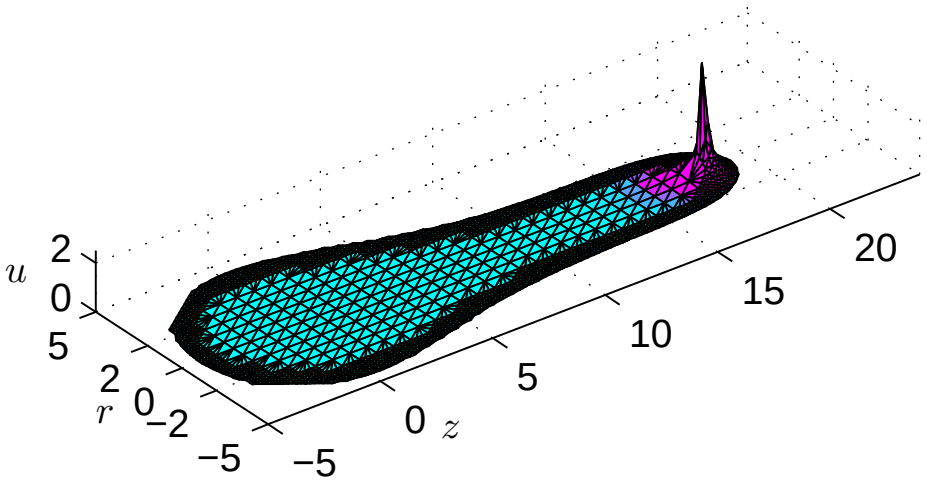

(b) Iteration 1001, time = 18.2

Figure 5.5: VSC Model Simulation

Chapter 6

Modifications to VSC type models

6.1 Introduction

When modelling the growth of hypha in the previous five chapters, we have always made the assumption that the velocity of the cell wall is orthogonal to the surface of the cell wall. This assumption is justified by observations, ink markers placed on the cell wall of growing fungal hypha appear to move in the direction of the normal to the cell surface. Moreover, this assumption greatly simplifies the mathematics involved. If the velocity is only normal to the cell surface, terms involving tangential flow of material along the cell wall disappear, and we obtain the evolution equation $v_n = -F/H$, where F is either the ballistic or diffusive flux, and H is the mean curvature.

There are several objections to this assumption. First of all, no physical argument is given for orthogonal growth aside from some hand-waving about turgor pressure. Second, whatever the model for the flux, this assumption yields that the velocity is inversely proportional to the mean curvature. These models obviously break down when the mean curvature is zero. Now in the tip of the hypha this does not occur as the tip is concave and both principal curvatures are negative. Further from the tip the hypha approximates a cylinder, so one of the principal curvatures approaches zero, while the other approaches $-1/r_{max}$ and so the mean curvature remains non-zero. However, when one looks on the scale of the mycelium, one sees a connected, often branching network of hypha. At the location of these branches, the cell surface is saddle-shaped, the two principal curvatures have differing signs and the mean curvature might well be zero or positive. Any material which arrives at such a point, no matter how small, cannot be incorporated in the cell wall by moving the wall outward. It *must* result in tangential flow.

Lastly, the purpose of models such as these is to understand the inner working of the cell by making educated guesses about the mechanics involved, and

then showing the model reproduces observations of real hyphae. When one uses one of these observations as a modelling assumption without any physical argument this starts to appear like circular logic. We are assuming that which we wish to observe. Ideally, orthogonal growth should be a result of the model, not one of its assumptions.

In this chapter we will suggest a model without the assumption of orthogonal growth. Essentially we assume that the cell wall tries to incorporate new material by moving as little as possible. We model this by minimizing the kinetic energy of the cell wall. In the environment through which the cell is growing this may make sense, the surrounding soil is relatively solid and provides a high resistance to movement. From this model we will derive the resulting evolution equation, and differential equation for the ship of a travelling wave in a similar manner as in the previous chapter. We then provide a plan, based on the existence proof from chapter 3, how one might prove the existence of travelling waves for this model.

6.2 Geometry

If one takes an arbitrary bounded region $A \subset \partial\Omega$ of the surface of the cell, with surface area $\|A\|$ and boundary curve ∂A, then the total flux of material absorbed in A is given by

$$\frac{\mathrm{d}\,\|A\|}{\mathrm{d}t} = \int_A F \mathrm{d}S. \tag{6.2.1}$$

If one assumes A is transported by a velocity field v, then Gauss' formula for the first variation of area states that

$$\frac{\mathrm{d}\,\|A\|}{\mathrm{d}t} = \int_A (Hv_n + \operatorname{div}_{\partial\Omega} v_t)\mathrm{d}S, \tag{6.2.2}$$

where H is the mean curvature and v_n and v_t are the components of the velocity field v which lie normal, respectively tangent, to the boundary $\partial\Omega$. In the original model, we assumed that $v_t = 0$, however we will not do so now.

In a coordinate chart $U \subset \mathbb{R}^2$ with a map $x : U \mapsto \partial\Omega$, the tangential vector field v_t is expressed as $v_t = v_1\partial_1 x + v_2\partial_2 x$ and the divergence on the manifold $\partial\Omega$ is given by

$$\operatorname{div}_{\partial\Omega} v_t = \frac{1}{\sqrt{g}}\left(\partial_1(\sqrt{g}v_1) + \partial_2(\sqrt{g}v_2)\right), \tag{6.2.3}$$

where g is the determinant of the metric tensor $g_{ij} = \partial_i x \cdot \partial_j x$.

Since A was chosen arbitrarily, the terms in the integrals must be equal and

$$F = v_n H + \operatorname{div}_{\partial\Omega} v_t. \tag{6.2.4}$$

To determine the evolution of the cell wall we wish to solve this for v_n, however this cannot be done without additional requirements on the tangential velocity.

6.3 Minimization of kinetic energy

To determine v_t we impose the modelling assumption that the cell minimizes the total kinetic energy of the cell wall. If we assume the cell wall has a constant surface density, then this kinetic energy is proportional to E, where

$$E = \frac{1}{2}\int_{\partial\Omega}(v_t^2 + v_n^2)\mathrm{d}S. \tag{6.3.1}$$

Solving (6.2.4) for v_n and substituting we see this energy can be expressed solely in terms of the tangential velocity v_t,

$$E[v_t] = \frac{1}{2}\int_{\partial\Omega} v_t^2 + \left(\frac{F - \mathrm{div}_{\partial\Omega}\, v_t}{H}\right)^2 \mathrm{d}A, \tag{6.3.2}$$

we wish to find a vector field v_t which minimizes the above expression.

The Euler-Lagrange equation for v_t is

$$v_t = -\nabla\left(\frac{F - \mathrm{div}_{\partial\Omega}\, v_t}{H^2}\right), \tag{6.3.3}$$

setting $u = \frac{F - \mathrm{div}_{\partial\Omega}\, v_t}{H^2}$ we see that $v_t = -\nabla u$ and u satisfies

$$-\Delta_{LB}u + H^2 u = F \tag{6.3.4}$$

where the Laplace-Beltrami operator Δ_{LB} is the divergence on $\partial\Omega$ of the gradient,

$$\Delta_{LB}u = \frac{1}{\sqrt{g}}\left(\partial_1(\sqrt{g}\partial_1 u) + \partial_2(\sqrt{g}\partial_2 u)\right). \tag{6.3.5}$$

The normal velocity can then be expressed as,

$$v_n = \frac{F - \mathrm{div}_{\partial\Omega}\, v_t}{H} = \frac{F + \Delta_{LB}u}{H} = uH. \tag{6.3.6}$$

There are two advantages to this model. The assumption that $v_t = 0$ was based solely on observations, and no physical mechanism (other than some hand waving and shouting 'pressure!') exists to justify it, this model removes it although one might expect that v_t remains small due to the minimization (although this remains to be proven.) Furthermore, $-\Delta_{LB} + H^2$ is a positive operator and (6.3.4) can be solved even when the mean curvature H is zero on parts of the cell wall. At these points the previous model with the assumption of orthogonal growth ($v_n = F/H$) is not defined. Basically, when the curvature is zero the area cannot be increased by normal growth, allowing any arriving material to flow away tangentially removes this problem.

6.4 Travelling waves

The proof, based on a Schauder fixed point argument, of the existence of travelling waves for the original Diffusive VSC model could probably be modified for this model.

The Schauder map is constructed as follows: given an initial shape $\tilde{r}(s), \tilde{z}(s)$ we solve the Dirichlet problem to calculate a family of fluxes F_ξ in the same manner as for the original model. Given these fluxes, for each ξ we solve (6.3.4) to obtain u_ξ, using maximum principles it should be possible to show that u_ξ is monotone in ξ. To obtain the next shape we then solve

$$r'(s) = \sqrt{1 - \left(\frac{\tilde{G}_\xi(s)}{r(s)}\right)^2}, \tag{6.4.1}$$

where

$$\tilde{G}_\xi(s) = \int_0^s (F_\xi(\sigma) + \Delta_{LB} u)\tilde{r}(\sigma)\mathrm{d}s = \int_0^s u_\xi H^2 \tilde{r}\mathrm{d}s. \tag{6.4.2}$$

Similar to the diffusive model we find a value of ξ such that $r_\xi(s) \to 2$ as $s \to \infty$, this will give the next shape. This sets up a map from tip shapes to tip shapes (described by the function r_ξ), under the right conditions we can then use Schauder's fixed point theorem to prove the existence of a travelling wave.

The difficulty in this approach most likely lies in finding suitable estimates on F, u_ξ and G_ξ and choosing the right subset of some (probably $C^{1,\alpha}$ or $C^{2,\alpha}$ Hölder continuous) function space such that we can set up the Schauder fixed point argument.

Bibliography

[1] S. Bartnicki-Garcia, C. E. Bracker, G. Gierz, R. López-Franco, and H. Lu, *Mapping the growth of fungal hyphae: orthogonal cell wall expansion during tip growth and the role of turgor*, Biophysical Journal, 79 (2000), pp. 2382–2390.

[2] S. Bartnicki-Garcia, F. Hergert, and G. Gierz, *Computer simulation of fungal morphogenesis and the mathematical basis for hyphal (tip) growth*, Protoplasma, 153 (1989), pp. 46–57.

[3] N. Bessonov, F. Crauste, and V. Volpert, *Modelling of plant growth with apical or basal meristem*, Mathematical Modelling of Natural Phenomena, 6 (2011), pp. 107–132.

[4] N. G. De Bruijn, *Asymptotic methods in analysis*, vol. 4, Courier Corporation, 1970.

[5] M. De Keijzer, A. Emons, and B. Mulder, *Modeling tip growth: pushing ahead*, (2008).

[6] E. Eggen, *Self-regulating tip growth, modelling cell wall ageing*, Master's thesis, University of Utrecht, 2006.

[7] E. Eggen, M. N. de Keijzer, and B. M. Mulder, *Self-regulation in tip-growth: The role of cell wall ageing*, Journal of theoretical biology, 283 (2011), pp. 113–121.

[8] B. Ferguson, T. Dreisbach, C. Parks, G. Filip, and C. Schmitt, *Coarse-scale population structure of pathogenic Armillaria species in a mixed-conifer forest in the Blue Mountains of northeast Oregon*, Canadian Journal of Forest Research, 33 (2003), pp. 612–623.

[9] T. Frankel, *The Geometry of Physics: An Introduction*, Cambridge University Press, 1997.

[10] C. Gerhardt, *Flow of nonconvex hypersurfaces into spheres*, in J. Diff Geom, Citeseer, 1990.

[11] G. Gierz and S. Bartnicki-Garcia, *A three-dimensional model of fungal morphogenesis based on the vesicle supply center concept*, Journal of Theoretical Biology, 208 (2001), pp. 151–164.

[12] D. Gilbarg and N. S. Trudinger, *Elliptic partial differential equations of second order*, Springer, 1983.

[13] A. Goriely, G. Károlyi, and M. Tabor, *Growth induced curve dynamics for filamentary micro-organisms*, Journal of mathematical biology, 51 (2005), pp. 355–366.

[14] G. Huisken and T. Ilmanen, *A note on inverse mean curvature flow*, in Proc. of the Workshop on Nonlinear Part. Diff. Equ.(Saitama Univ, 1997.

[15] G. Huisken and T. Ilmanen, *Higher regularity of the inverse mean curvature flow*, J. Differential Geom., 80 (2008), pp. 433–451.

[16] J. Hulshof, R. Nolet, and G. Prokert, *Existence of solutions to the diffusive VSC model*, SIAM Journal on Mathematical Analysis, 45 (2013), pp. 700–727.

[17] J. Hulshof, R. Nolet, and G. Prokert, *Existence and linear stability of solutions of the ballistic VSC model*, Discrete Contin. Dyn. Syst. Ser. S, (2014).

[18] E. Javierre, F. Vermolen, C. Vuik, and S. Van der Zwaag, *A mathematical analysis of physiological and morphological aspects of wound closure*, Journal of mathematical biology, 59 (2009), pp. 605–630.

[19] A. L. Koch, *The problem of hyphal growth in streptomycetes and fungi*, Journal of theoretical biology, 171 (1994), pp. 137–150.

[20] J. Ortega and S. Welch, *Mathematical models for expansive growth of cells with walls*, Mathematical Modelling of Natural Phenomena, 8 (2013), pp. 35–61.

[21] M. Smith, J. Bruhn, and J. Anderson, *The fungus Armillaria bulbosa is among the largest and oldest living organisms*, Nature, 356 (1992), pp. 428–431.

[22] S. Tindemans, *Modeling tip growth in fungal hyphae*, Master's thesis, University of Amsterdam, 2004.

[23] S. H. Tindemans, N. Kern, and B. M. Mulder, *The diffusive vesicle supply center model for tip growth in fungal hyphae*, Journal of theoretical biology, 238 (2006), pp. 937–948.

[24] H. Triebel, *Higher analysis*, vol. 93, Huthig Pub Limited, 1992.

[25] J. I. Urbas, *On the expansion of starshaped hypersurfaces by symmetric functions of their principal curvatures*, Mathematische Zeitschrift, 205 (1990), pp. 355–372.

[26] F. Vermolen, *Simplified finite-element model for tissue regeneration with angiogenesis*, Journal of engineering mechanics, 135 (2009), pp. 450–460.

[27] F. Vermolen and E. Javierre, *Computer simulations from a finite-element model for wound contraction and closure*, Journal of tissue viability, 19 (2010), pp. 43–53.

[28] G. N. Watson, *A treatise on the theory of Bessel functions*, (1966).

[29] J. Weidmann, *Linear Operators in Hilbert Spaces*, Springer US, New York, NY, 1980.

Summary

Fungal colonies form networks of thread-like hypha in the soil, known as a mycelium. This mycelium absorbs water and nutrients from the surrounding soil and can grow to tremendous size. In 1993 Smith *et al.* discovered a single organism of *Armillaria bulbosa* in a northern Michigan hardwood forest whose mycelium covered a region of 15 hectares and was estimated to be more than 1500 years old [21]. At the time this was reported to be one of the largest and oldest living organisms known to man. Ten years later, this record was broken. In 2003 Ferguson *et al.* reported a single organism of *Armillaria ostoyae* in a mixed-conifer forest in northeast Oregon. This fungus' mycelium was estimated to cover an area of 963 hectare and its age was estimated to be between 1900 and 8650 years old [8].

Microscope observations of these hyphae show that they grow from their tips. Ink markers placed on the cell wall stay roughly in place, moving at right angles to the cell surface, while new cell wall material appears to be created at the tip of the hypha as it moves forward. A cellular body called the *Spitzenkörper* near the tip is suspected to play a role in this growth. This has motivated several models for the growth of fungal hypha, these models assume that

- Cell wall material is created at the *Spitzenkörper* and transported by vesicles to the cell wall. We will often refer to the *Spitzenkörper* as a vesicle supply center (VSC).
- This cell wall material is transported to the cell wall, where the flux F of material arriving at the cell wall results in local expansion of the wall's surface area.
- A curved cell wall can only accommodate this local increase of surface area by expanding outward, the rate of expansion is determined by the mean curvature H of the cell wall.
- The VSC moves at a fixed velocity, possibly because it is attached to the cell wall and is dragged along with it as the cell wall expands.

These model assumptions, when combined with Gauss' law for the variation of area, yield an equation for the normal velocity v_n of the boundary of the cell wall

$$v_n = -\frac{F}{H}.$$

For the flux F two models are examined

- *The ballistic flux* – Vesicles carrying cell wall material emanate from the VSC equally in all directions, and travel in straight lines to the cell wall. In this case
$$F = 4\pi \frac{\cos\theta}{d^2}$$
where d is the distance from a point on the cell wall to the VSC, and θ is the angle between the line between the VSC and this point, and the normal vector to the cell wall surface.

- *The diffusive flux* – Vesicles carrying cell wall material diffuse outward from the VSC, now $F = -\nabla u|_{\partial\Omega}$ where u is the density of vesicles and satisfies the diffusion equation $\Delta u = -4\pi\delta(\vec{x} - \vec{x}_{VSC})$ in the region Ω inside the cell and $u = 0$ on the boundary $\partial\Omega$ of the cell wall.

The main question in this thesis is whether these models allow so called *travelling wave solution*, solutions which remain the same shape and move with a constant velocity along with the VSC. We then obtain the following results:

- In chapters 1 and 2 we prove the existence, uniqueness and stability of travelling wave solutions for the ballistic model, and prove some asymptotic estimates near and away from the tip.

- In chapter 3 and 4 we prove the existence of travelling wave solutions for the diffusive model, and prove some asymptotic estimates near and away from the tip.

- In chapter 5 we do numerical simulations of the growth of a tip starting from initially spherical shape.

- In chapter 6 we briefly look at other modifications to the VSC model.

Acknowledgements

Over the years it took me to complete this thesis a lot of people, family, friends and colleagues have supported, encouraged and helped me. Foremost I would like to thank my father Guust Nolet, and Julia Nolet-Frey for providing a lovely place to work in the south of France, where most of this thesis has been written, and for providing distractions in the form of games of chess, mountain hikes, swims, and good food and wine when the writing got too much. I would like to thank my mother, Wendelien Bos for her support both when things were going good, but especially also when things didn't always look as rose-coloured. I would like to thank the whole Bos family for encouraging me by occasionally reminding me that someone needed to continue in the tradition of my grandfather, that the family needed another mathematics PhD. I would like to thank my colleagues at the Hogeschool van Amsterdam for expressing interest in my thesis, and encouraging me to finish without placing too much pressure, and for providing me with an environment where I continued working with, and thinking about, mathematics. I would like to thank Michelangelo Vargas for his friendship and advice throughout my period as graduate student at the Vrije Universiteit, as well as afterwards when we both worked at the hogeschool, and I would like to thank him for agreeing to be my *paranimf*. I would like to thank Danielle van 't Zand for her friendship, support and for agreeing to be my *paranimf*. I would like to thank Eva Deinum for her support, offering to team up and write our theses together (you beat me by a few years!) and for designing the cover of this thesis.

For help with the mathematical content of this thesis I would like to thank my *promotor*, Joost Hulshof, for always having hundreds of ideas ready whenever I was stuck. One of these ideas would almost always help, and I learned from all of them. I would also like to thank him for his patience, and for providing the necessary kick in the pants I needed to finally plan the defence. I would like to thank my *co-promotor* Georg Prokert for immaculately precise and incredibly detailed feedback on my writing. I'd like to thank Fred Vermolen for the use of his numerical code on which most of chapter 5 is based, and last but not least I would like to thank the entire reading committee Arjen Doelman, Bela Mulder, Fred Vermolen and Mark Peletier for their kind and positive feedback when I turned in this thesis.